Design and Construction of a Double-Octahedral Variable Geometry Truss Manipulator

by

Paul Hickman Tidwell, II

Thesis submitted to the Faculty of the
Virginia Polytechnic Institute and State University
in partial fulfillment of the requirements for the degree of

Master of Science

in

Mechanical Engineering

APPROVED:

Prof. C. F. Reinholtz, Chairman

Prof. H. H. Robertshaw

Prof. N. S. Eiss

June, 1989
Blacksburg, Virginia

Design and Construction of a Double-Octahedral Variable Geometry Truss Manipulator

by

Paul Hickman Tidwell, II

Committee Chairman: Charles, F. Reinholtz
Mechanical Engineering

abstract

This thesis deals with the design and construction of a variable geometry truss (VGT) of the double-octahedral (pyramid-pyramid) geometry. The truss is expected to be the focus of several experimental research projects. In this thesis, a kinematic model is formulated, and the forward and inverse kinematic problems are solved. Issues of motor and instrumentation choices are addressed. Dimensional choices and the important problems of joint design are examined. A computer simulation is performed for force and vibration analysis.

A fully collapsible double-octahedral variable geometry truss with three degrees of freedom was built using NC machining technologies. An improved second generation twenty-one degree-of-freedom truss will be built based on this original test article.

Acknowledgements

I would like to pay special thanks to the chairman of my advisory committee, Dr. Charles F. Reinholtz, known to his graduate students simply as Charlie. He opened up his heart, mind and home to his graduate students. His continued encouragement, friendship, and good humor made this thesis possible.

Also, thanks to the other members of my advisory committee Harry Robertshaw and Norm Eiss for their support.

I should also thank, , for his invaluable engineering advice. He spends countless hours in the machine shop for which he deserves much credit.

I appreciate the students with whom I work and share an office, the "We can do it" team, especially who spent long hours working on preliminary CAD drawings and who has been a great friend.

Thank you to my parents who always encouraged me to set high goals and to work hard for them even when I was struggling. They bore a tremendous financial burden during my education, and never complained even when I worked through vacations.

And finally thanks to my namesake, my grandfather, who instilled in me a love for all things mechanical.

Contents

1 Introduction to Manipulators **1**

1.1 Kinematics 3

1.2 Robotics 5

1.3 Parallel Manipulators 6

1.4 Hybrid Manipulators 8

1.5 High Degree-of-Freedom Manipulators 8

1.6 Literature Review 9

2 Variable Geometry Trusses **14**

2.1 Introduction to VGTs 14

2.2 Possible Truss Geometries 16

2.3 Octahedral Variable Geometry Truss 22

2.3.1 Terminology and Assumptions 22

2.3.2 Forward Kinematic Solution 26

2.3.3 Inverse Kinematic Solution 37

2.3.4 Long-Chain Manipulators 40

3 Design Concepts **42**

3.1 Dimensional Relationships 42

3.2 Actuation 50

3.3 Motor Issues 56
3.4 Instrumentation 58
3.4.1 Control Equipment 58
3.4.2 Position Instrumentation 59
3.4.3 Velocity Feedback 60
3.5 Joint Design 61
3.5.1 Nasa Design 61
3.5.2 VPI & SU Design 64

4 Hardware Design and Selection **68**

4.1 Dimensional Choices 69
4.2 Finite Element Analysis 69
4.3 Motor Choices 72
4.4 Joint Design 74
4.4.1 Purchased Parts 74
4.4.2 Joint Instrument Box 79
4.4.3 Design of C-Bracket 83
4.5 Active Batten Design 84
4.5.1 Lead Screw 84
4.5.2 Lead Screw Nuts 87
4.5.3 Design of the Nut Adapter 87
4.5.4 Tube 88
4.5.5 Fork 88
4.6 Longeron Design 88
4.6.1 Longeron Junction Block 89
4.7 Batten Frame and Joint Design 89

4.7.1 Batten Tube 91
4.8 Summary 91

5 Conclusions **92**
5.1 The VPI&SU Double-Octahedral VGT 92
5.1.1 Problems with the VPI&SU VGT 92
5.1.2 Design Changes and Recommendations 93
5.2 VGT Applications 93
5.3 Future Variable Geometry Truss Work 94

Bibliography **96**

A Shop Drawings **102**

B NC Milling Control Code **122**

List of Figures

1.1 Photograph of Variable Geometry Truss Built at VPI&SU 2

1.2 Parallel and Serial Manipulators 7

1.3 Double-Octahedral Variable Geometry Truss Built by NASA 12

2.1 Various Two Dimensional Trusses 15

2.2 Four Variable Geometry Truss Unit Cells 17

2.3 NASA Space Structures 18

2.4 Cube Formed with Different Unit Cells 19

2.5 Generic Stewart's Platform, Octahedral VGT, and 3-Tetrahedral VGTs 21

2.6 Three Parallel Mechanisms with Six Connecting Links 23

2.7 Double-Octahedral VGT Terminology 25

2.8 Fully Extended and Collapsed VGTs 27

2.9 Equivalence of Longeron Triangle and RS dyad and Symmetry of the Double-Octahedral VGT 28

2.10 Three-RSSR Mechanism 30

2.11 Inverse Kinematic Solution 38

2.12 Long Chain Manipulator to be Built at VPI&SU 41

3.1 Important parameters for sizing a Double-Octahedral VGT 43

3.2 Double-Octahedral VGT with Small B/h Ratio 45

3.3 Relationship between B/h Ratio and Curvature 46

3.4 Double-Octahedral VGT with Large B/h Ratio 48
3.5 Truss-Height and Actuator-Length Relationships 49
3.6 Relationship Between Truss Height and Actuator Length for a Ratio B/h of Two 51
3.7 Standard Lead-Screw Thread Shapes 53
3.8 A Simple Actuator Design 55
3.9 Kinematic Model of Joint Built by NASA 63
3.10 Kinematic Model of VGT Joint Design Developed at VPI&SU 65
3.11 Joint for Double-Octahedral VGT Built at VPI&SU 66

4.1 Helical Nature of the Double-Octahedral VGT 71
4.2 Actuator Joint Assembly 75
4.3 Purchased Parts for Joint Instrument Box 76
4.4 A Photograph of the Joint Instrument Box 81
4.5 Joint Instrument Box Sizing 82
4.6 Actuator Schematic 85
4.7 Batten Joint Limits 90

A.1 Double Octahedral Variable Geometry Truss 103
A.2 Joint Instrument Box 104
A.3 Actuator Tube Adapter 105
A.4 Actuator Fork 106
A.5 Actuator Tube Assembly 107
A.6 Bracket Connecting Universal Joints 108
A.7 C-Bracket, Universal Joint, Pin Assembly 109
A.8 Universal Joint Assembly on Around Joint Instrument Box 110
A.9 Block Connecting Two Longeron Tubes to the Universal Joint 111

A.10 Plug Connecting the Longeron Tube to the Junction Block 112
A.11 Section View of Longeron Tube, Junction Plug and Block 113
A.12 Plug Connecting the Longeron Tube to the Ear Plate 114
A.13 Inboard Ear Plate 115
A.14 Outboard Ear Plate 116
A.15 Longeron Tube Assembly 117
A.16 Block Connecting Pins at the Corners of the Batten Frame 118
A.17 Batten Frame Joint Plug and Batten Frame Joint Pin 119
A.18 Section View of Batten Frame Joint 120
A.19 Batten Frame 121

Chapter 1

Introduction to Manipulators

Many kinematic geometries are possible for manipulators. In the simplest arrangement, the structural members are connected in series by revolute or prismatic joints to form a cantilevered arm (beam). Such devices are called *serial manipulators.* Other joints such as spheric and cylindric joints can be used, but each structural link connects two others in a continuous chain from the ground to the end effector.

More complex geometries are possible where the structural members form one or more closed loops. These closed-loop manipulators are referred to as *parallel manipulators.* This thesis deals with a subset of parallel manipulators called Variable Geometry Truss manipulators (VGTs). The process of designing of a double-octahedral variable geometry truss manipulator is described. One "bay" of this design was built at VPI&SU, and a photograph of it is shown in Fig. 1.1.

A variable geometry truss manipulator containing seven such "bays" is to be built. This new manipulator will serve as the center of several experimental research projects. Furthermore, this VGT will serve as a showpiece to help visualize concepts in VGT research. Therefore, aesthetics are important, in addition to structural integrity, in the truss design.

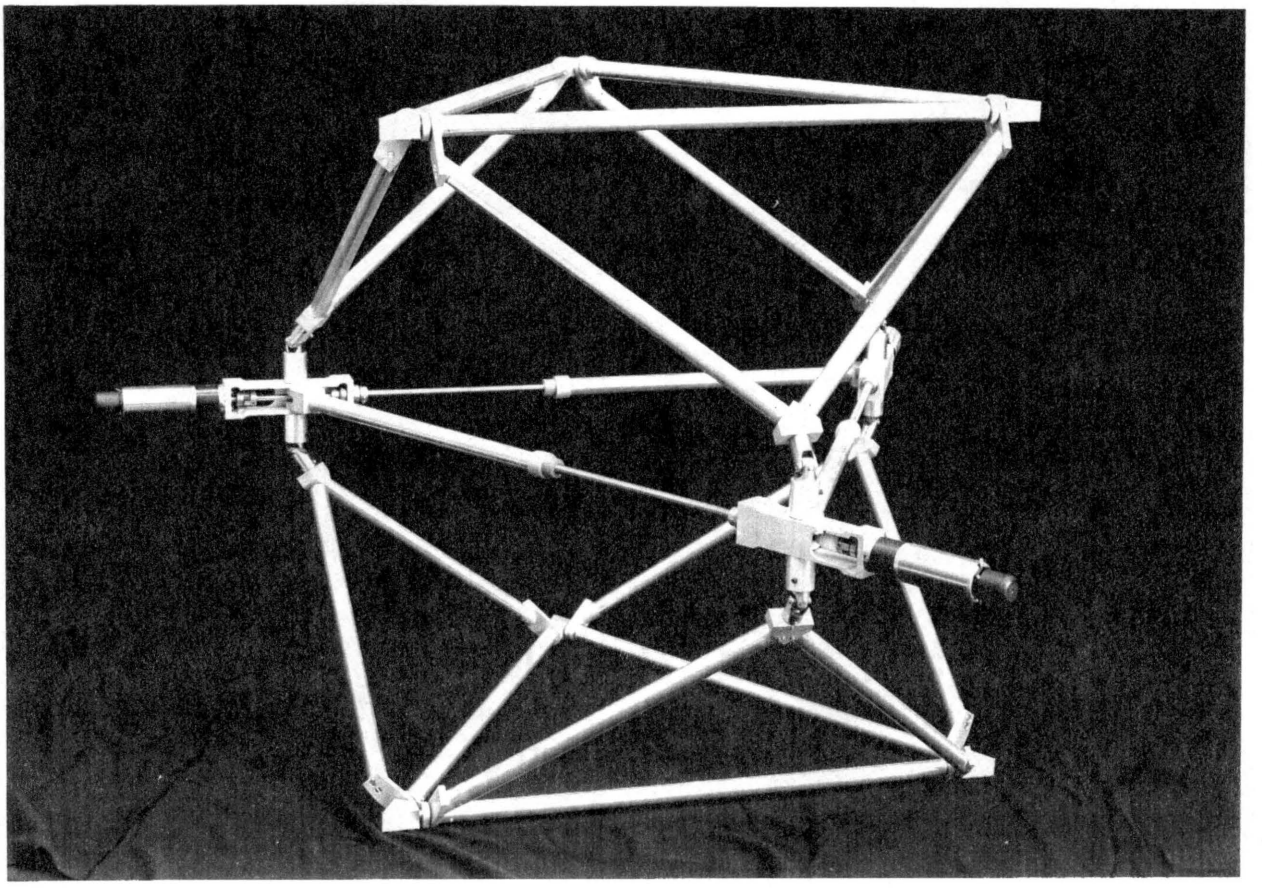

Figure 1.1: Double-Octahedral Variable Geometry Truss Built at Virginia Polytechnic Institute and State University

1.1 Kinematics

The science of kinematics is fundamental to the subject of manipulators. *Kinematics* is the study of pure geometric motion of mechanical devices without regard to forces. In other words, it is a study of the geometric constraints that exist within a machine. Using kinematics, the motion of manipulators can be described mathematically. A number of words in common English use have specific meaning in the context of kinematics. Among these, a few of the more important ones are defined below.

A revolute joint or hinge allows one member to rotate with respect to another. This freedom to rotate can be described by an angle and is called a *degree of freedom.* The *mobility* is the number of degrees of freedom, the number of independent parameters required to specify the location of all of the components of a mechanical system. In three dimensional space, any unconstrained object has a mobility if six or six degrees of freedom.

For spatial mechanisms, the mobility is specified by the Kutzbach equation:

$$M = 6(n-1) - 5f_1 - 4f_2 - 3f_3 - 2f_4 - f_5 \tag{1.1}$$

where
M = mobility, or number of degrees of freedom
n = total number of links, including the ground
f_1 = number of joints that allow one degree of freedom
f_2 = number of joints that allow two degrees of freedom
f_3 = number of joints that allow three degrees of freedom
f_4 = number of joints that allow four degrees of freedom
f_5 = number of joints that allow five degrees of freedom.

For example, revolute and prismatic joints allow one degree of freedom, while spheric joints permit three degrees of freedom [1].

Dexterity is a property of a mechanical device that possesses more degrees of freedom than those needed to specify the end conditions necessary to reach a goal. The number of extra degrees of freedom is sometimes called the *degree of redundancy.*

A *mechanism* is a one degree-of-freedom mechanical device such as a cam and follower, or four-bar linkage. Some mechanisms are much more complex than these, but they all have one output corresponding to one input. The *links* are the mechanical components which, when connected by articulating joints, make up a mechanical linkage. These links are assumed to be rigid.

A *manipulator* is mechanical arm, usually having several degrees of freedom. Manipulators are often designed for a specific task such as a backhoe or milling machine.

The word *robot* comes from the Czech word for serf-worker. In modern use, a robot is a machine (a manipulator) that can be programmed to perform a variety of tasks. An *end effector* is the working tool or "hand" at the free end of a manipulator or robot such as a gripper, welding torch, paint sprayer, ect. Most industrial robots

have interchangeable end effectors. These end effectors often have several degrees of freedom, sometimes as many as six. The *workspace* of a robot is the area or volume which it can reach with an end effector.

In order to use manipulators, their motion must be described mathematically (kinematically). The *forward kinematic problem* is to find the location (position and orientation) of the end-effector given the joint parameters. Usually, joint parameters can be easily and continuously measured, whereas the end-effector location cannot. The solution answers the question "Where is the end-effector is some global frame of reference?"

The *inverse kinematic problem* is the opposite problem, namely finding the joint parameters given the (desired) location (position and orientation) of the end-effector. It answers the question "How should the individual actuators be positioned to achieve a desired end-effector location?"

1.2 Robotics

A variable geometry truss, like any other manipulator, can be used as a robot. Robotics is important for many reasons. The United States needs robotics to effectively compete in the world market. Robots can do many things better and more efficiently than people can. A robot can perform repetitive tasks without growing bored or tired. But, more important than these, robots can to do things people cannot do. For example, robots (if properly designed) can operate in high radiation areas inside nuclear reactors, deep under the ocean, and in the vacuum of outer space. By using robots in dangerous environments, people do not have to risk their lives.

In structured environments, such as a manufacturing operation, the tasks required of a robotic manipulator can be planned and controlled. As a result, it is

usually possible to use a relatively simple serial manipulator having six or fewer degrees of freedom. Unfortunately, these simple manipulators have found little application in unstructured environments, such as emergency repair and exploration, where the required tasks cannot be defined beforehand.

1.3 Parallel Manipulators

Parallel manipulators differ from serial manipulators in the way the links are put together. The joints in serial manipulators are arranged with each link connected to the end of the previous link in an open chain. The movement of one joint moves all others between it and the end effector as shown in Fig. 1.2(a), and all loads are transmitted through every link and joint to the base.

In parallel manipulators, any load applied at the end-effector is transmitted through multiple paths to the ground, see Fig. 1.2(b). The manipulator links form closed loops, in contrast to the serial manipulator. As a result, these parallel manipulators are inherently stiffer than serial manipulators. Therefore, a parallel manipulator can be designed to be lighter in weight for a comparable stiffness.

The problems surrounding parallel manipulators are different from those of serial manipulators. The workspace of parallel manipulators is generally smaller than that of serial manipulators. There are potential problems with link interference that must be overcome with good engineering design. With some designs, there are singularities in the workspace. Unlike serial manipulators, a solution to the forward kinematic problem may not be possible in closed form. Although exceptions are possible, the inverse kinematics problem is also typically much more difficult as well. These problems generally mean that more sophisticated computer control is necessary if the manipulator is to be used as a robotic arm.

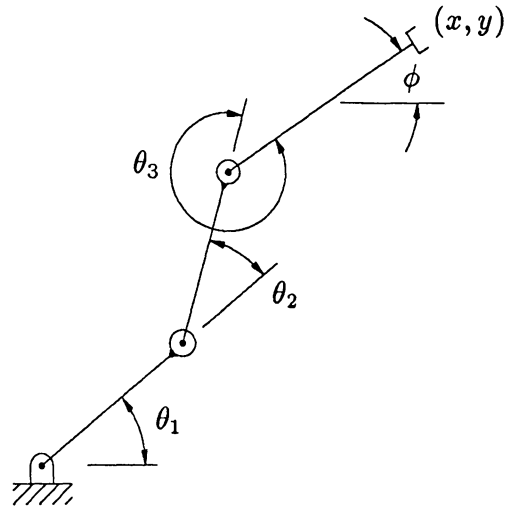

(a) Simple Three Degree-of-Freedom Serial Manipulator

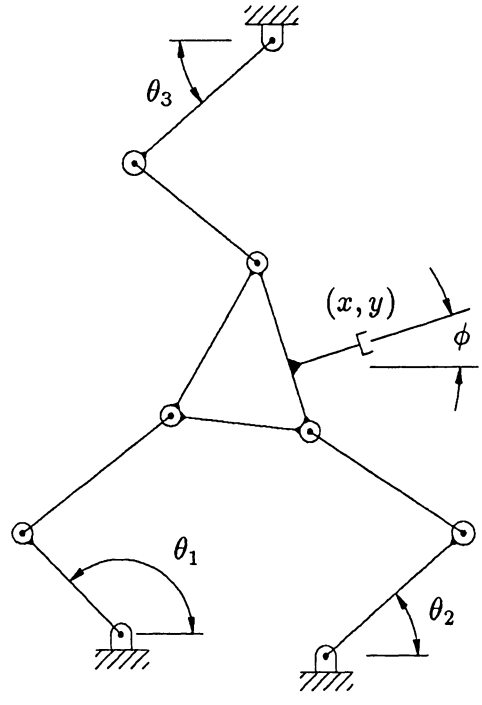

(b) Simple Three Degree-of-Freedom Parallel Manipulator

Figure 1.2: Arrangement of Links in Two-Dimensional Parallel and Serial Manipulators

1.4 Hybrid Manipulators

Parallel manipulators can be connected serially to form hybrid manipulators. These manipulators generally do not have any one link which carries all of the load, but do have complex load paths and many different closed loops. They are composed of parallel devices serially connected. These manipulators are sometimes classified as parallel manipulators, but they are different in fundamental ways.

These manipulators can benefit from the advantages of both serial and parallel devices. They are parallel in some degree and therefore, stiffer, but they can have larger workspaces than purely parallel manipulators. The disadvantages of these manipulators are similar to those of parallel manipulators. The kinematic solution is more difficult than serial manipulators. These problems generally mean that more sophisticated computer control is necessary.

Parallel and hybrid manipulators can be relatively bulky, but they can sometimes be constructed to collapse into a compact package. Although it may be possible for serial manipulators to collapse, this property is more useful for parallel manipulators because they are large compared to their workspace.

1.5 High Degree-of-Freedom Manipulators

High degree-of-freedom manipulators have dexterity and are sometimes called hyper-redundant. They have more degrees of freedom than is necessary to describe the position and orientation of the end effector.

In a general spatial environment, three position variables and three angles are necessary to place the end effector. In other words, six degrees of freedom are necessary for the manipulator to do a positioning task. For a serial manipulator containing six revolute or prismatic joints, there are at most sixteen different solutions to this

problem, but, most of the time, there are fewer than this [2].

For one extra degree of freedom (more than six), there are an infinity of solutions to the inverse kinematic problem. It is, therefore, more difficult to find a distinct solution. Having an infinity of solutions has advantages and disadvantages. Other parameters may be included in the problem. For example, if there is an obstacle in the workspace some of these different solutions may avoid it. These obstacles can be physical things that are "in the way," singularities, or link interference.

Such things as mechanical advantage, stiffness, and strength can be modified using different solutions. Having extra degrees of freedom has other advantages. The redundancy of actuators is a safety feature. It makes the mechanism more reliable; if one actuator fails, others can take over with little loss of performance. However, having many solutions implies (necessitates) sophisticated computer control, and optimal solutions are possible.

1.6 Literature Review

The literature relating to this thesis comes from a number of different fields. Much work on the kinematics of robotic manipulators has been accomplished; however, most of this concerns serial robots which is not discussed here. J. J. Craig is a good source for this information [2]. Work on parallel manipulators especially the Stewart platform is outlined below. Previous work on the double-octahedral VGT and possible space applications is then presented. Design texts and product manuals will not be discussed here, but instead, will be referenced where they are used in the thesis.

Stewart [3] invented the "Stewart platform," a parallel six legged platform manipulator, shown in Fig. 2.5 (a), for use as an aircraft simulator. It was the first three dimensional VGT. Hunt [4] suggested using the Stewart platform as a robotic

manipulator. The transition from the specific requirements of the a simulator to a general mechanical device is an important contribution. Fichter and McDowell [5] examined link sizing, workspace, control algorithms and possible applications for the Stewart platform. Yang and Lee [6] performed a controllability and displacement analysis on this device. They also examined the workspace assuming that the joints of the platform are constructed from ball-and-socket joints. Fichter [7] performed a position, velocity and acceleration analysis. He also and explored the singular configurations (when the end effector gains additional degrees of freedom) and the practical problems of building a working model. Sugimoto [8] used motor algebra to build a kinematic and dynamic model of the Stewart platform.

In addition to the Stewart platform, recently there has been growing interest in other parallel devises. Hunt [9] studied actuator arrangements for parallel manipulators using screw system theory. Sklar and Tesar [10] developed a generic method for kinematic and dynamic analysis of hybrid manipulators. Waldron, Ragahvan, and Roth [11] formulated the kinematics and dynamics for a parallel micro-manipulator. Jain and Kramer [12] designed a variable geometry truss based on the tetrahedron-tetrahedron geometry.

Variable geometry trusses have long been suggested for space applications because of their high strength and light weight. Card and Boyer [13] reviewed large space structure research including those that automatically deploy into the desired configuration and those that are erected in space. Dorsey [14] studied the vibration characteristics of planar VGT's. Mikulas, Davis, and Greene [15] proposed a four degree-of-freedom cubic celled space crane. Utku et al., [16] [17] investigated the control, path planning and vibration characteristics of this manipulator.

Rhodes and Mikulas [18] at NASA's Langley Research Center originally developed the double-octahedral variable geometry truss as a deployable structure for

use in space. This truss was optimized for deployment and analyzed for collapsibility. They also suggested the double-octahedral truss be used as a manipulator and identified how the actuator movement effects the geometry of the truss. This manipulator concept could either be a series of actuated double-octahedrons linked directly together or could have static sections connecting them.

Sincarsin and Huges [19], compared four different possible truss geometries for use as a high degree-of-freedom space manipulator. They recommended the double-octahedral VGT over tetrahedron and cubic-cell based geometries. Based on the design of Rhodes and Mikulas, Sincarsin [20] built and tested a six degree-of-freedom double-octahedral truss. Although it has a very limited range of motion and was designed to test deployment, this device, shown in Fig. 1.3, has had a long and productive life. This truss was loaned to Virginia Polytechnic Institute & State University where it was used by Robertshaw et al., in vibration control [21].

Miura, Furuya and Suzuki [22] developed and studied a single-octahedral deployable truss based on the work of Rhodes and Mikulas. In addition, they studied the double-octahedral truss as a manipulator unit. They present a method for solving the forward kinematic problem and finding the limits of the workspace. Next, Miura and Furuya [23] studied the vibration characteristics of a single-octahedral based adaptive structure and enumerated its possible applications.

There has been important additional work on the double-octahedral VGT. Nayfeh [24] developed an iterative solution to the forward kinematic problem for the double-octahedral VGT for use as a space crane (see Section 2.3.2). Reinholtz and Gokhale [25] develop iterative solutions methods for the forward and inverse kinematic problem for a single double-octahedron. Griffis and Duffy [26] proved the existence of sixteen roots to the forward kinematic problem for a single double-octahedron. Arun, Reinholtz and Watson [27] proved that there is no closed form solution to

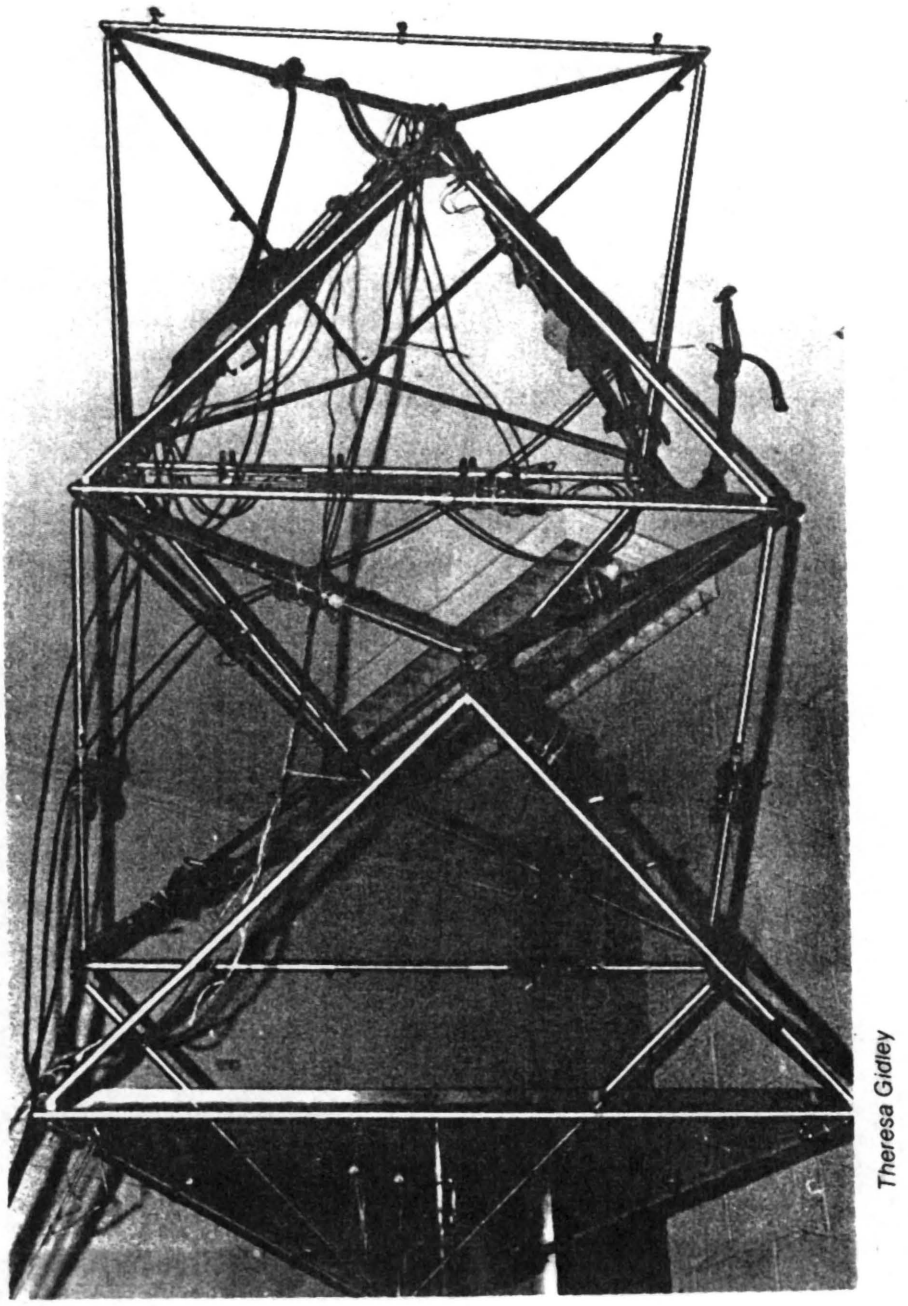

Figure 1.3: Variable Geometry Truss Built by NASA

this problem and enumerated other possible geometries for VGT's. Padmanabhan [28] solved the optimization problem of using the three degree-of-freedom double-octahedral VGT as an improved two degree-of-freedom "gimbal." Arun and Padmanabhan [29] propose using VGT as joints in a conventional manipulator. Padmanabhan, Arun, and Reinholtz [30] solved the inverse kinematic problem in closed form for a single double-octahedron and the hybrid "quadruple-octahedron," which is two double-octahedral VGT connected serially.

Many VGT applications involve using a high degree-of-freedom manipulator. Miura and Matunaga [31] studied the movement of free-floating multi-link manipulators undergoing symmetric and unsymmetric motion. Salerno [32] developed solution methods for precisely controlling these high degree-of-freedom "snake-like" manipulators.

Virginia Polytechnic Institute & State University is working on various issues in robotics, including the design of highly-dexterous VGT manipulators, and the control of compliant manipulators.

This thesis attempts to do for the double-octahedral VGT what Yang, Lee, and Fichter have done for the Stewart platform. No one has yet explored the freedoms needed in the design of the joints. The design of these truss joints is a non-trivial task and is the subject of much of this thesis.

Virginia Polytechnic Institute & State University is working on various issues in robotics, including the design of highly-dexterous VGT manipulators, and the control of compliant manipulators.

This thesis attempts to do for the double-octahedral VGT what Yang, Lee, and Fichter have done for the Stewart platform. No one has yet explored the freedoms needed in the design of the joints. The design of these truss joints is a non-trivial task and is the subject of much of this thesis.

Chapter 2

Variable Geometry Trusses

2.1 Introduction to VGTs

An ideal truss, as shown in Fig. 2.1 (a), is a structure which is designed so that individual members do not carry bending or torsional loads.

These structural linkages need only support tension and compression. Ideally, these links are connected with movable joints so that, even under deformation, they carry no bending moments. As shown in Fig. 2.1 (b), the links remain straight even as the structure deforms. In real truss structures, the joints are often rigid and the members carry small bending loads due to overall deformation of the truss, individual member weight, and compromises in design, fabrication, and construction. These bending loads are usually small, however, compared to the tension and compression loads.

A variable geometry truss (VGT) is a truss containing some number of extensible links. Ideally, its links carry no bending moments. The VGT is movable because some truss elements can change length as exemplified in Fig. 2.1 (c). The VGT is therefore a manipulator. Because of the parallel nature of the VGT, it has the advantages of high stiffness and light weight.

Since the shape of the VGT can change quite dramatically, the joints involved

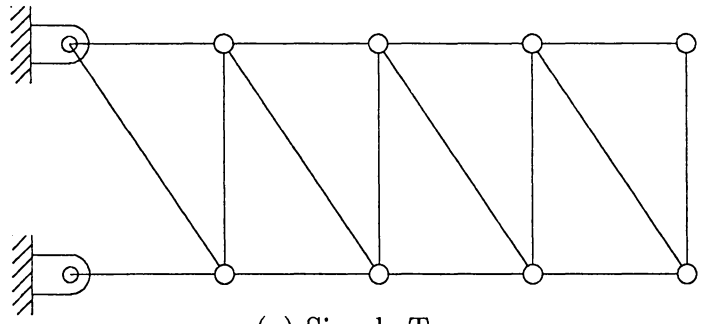

(a) Simple Truss

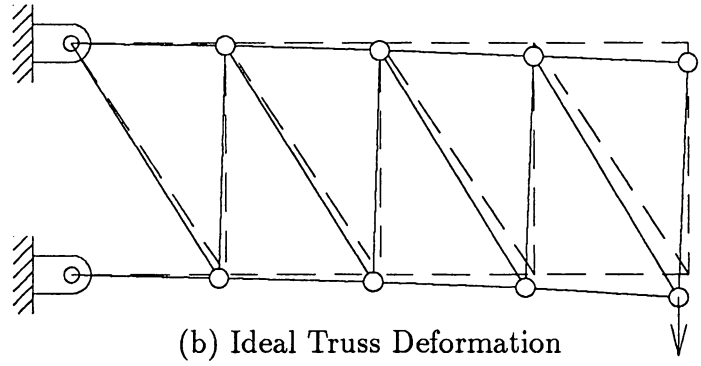

(b) Ideal Truss Deformation

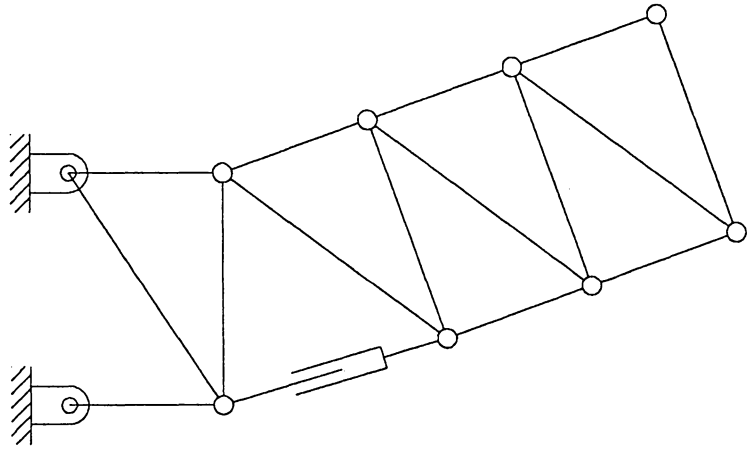

(c) One Degree-of-Freedom Variable Geometry Truss Manipulator

Figure 2.1: Various Two Dimensional Trusses

must not be rigid. The design of these truss joints is a non-trivial task and is the subject of much of this thesis. In some cases where precision and stiffness are not critical, the joints can be flexure joints (such as rubber joints), but flexible joint design will not be addressed in this thesis.

All the truss elements can be made variable in length, but the additional workspace and dexterity gained is small compared to the added complications. Actuating some links leads to more useful designs than actuating others. Choosing which elements to actuate is also very important and greatly affects the performance of the VGT.

2.2 Possible Truss Geometries

There are several different practical VGT geometries *and* different choices for actuating links. Four common truss building blocks have been identified [27]. These are shown in Fig. 2.2.

They are the tetrahedron, octahedron, decahedron, and the dodecahedron. The last two are sometimes called the pentagonal and hexagonal dipyramid, respectively. Several practical choices of actuation are possible for each [19]. Other cells are possible and research in this area is currently being investigated at VPI&SU.

As an example of the many possible variations and subtle combinations of these basic elements, two of NASA's planned space structures will be described. NASA plans to use the cubic truss for building the space station [33]. These cubes are huge, five meters on a side. In construction of the space station, they plan to build a "space crane" out of these truss elements using several one degree-of-freedom joints as shown in Fig. 2.3 (a) [15].

The cubic truss bays can be constructed in four different configurations depending on the orientation of the diagonals: a dodecahedron, a decahedron and a tetrahedron, an octahedron and two tetrahedrons or five tetrahedrons (see Fig. 2.4). The

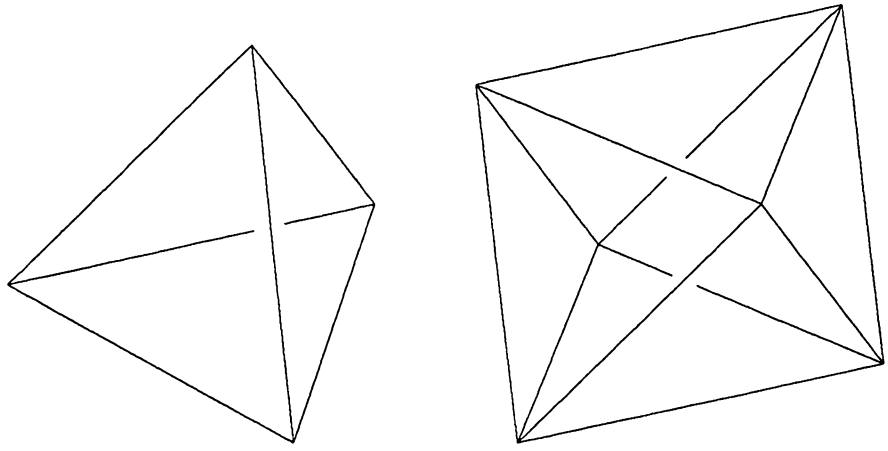

Tetrahedron Octahedron

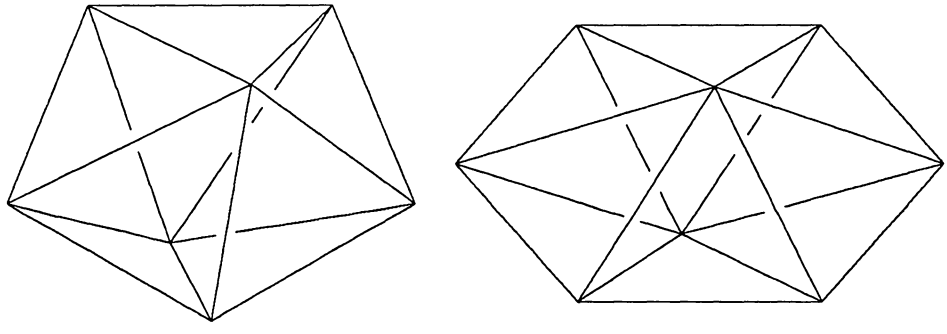

Decahedron Do−Decahedron

Figure 2.2: Four Variable Geometry Truss Unit Cells

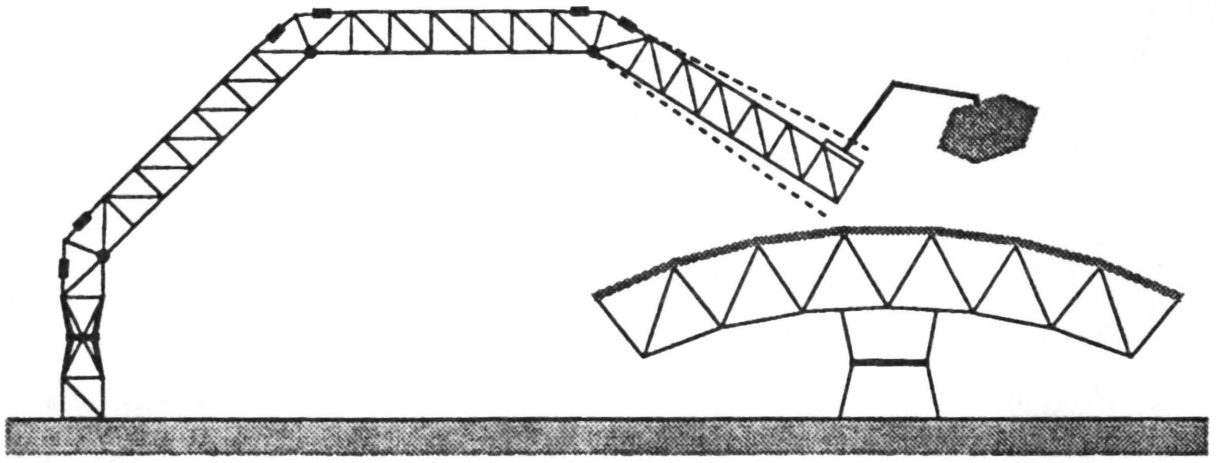

a) NASA's Pathfinder Space crane

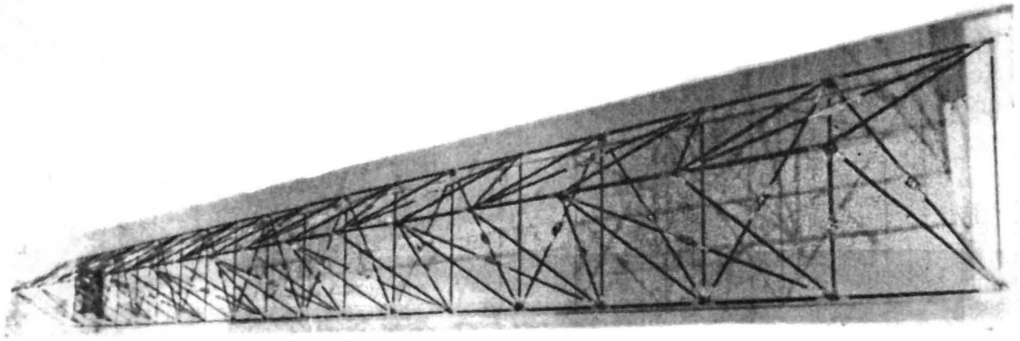

b) NASA's Three Longeron Minimast

Figure 2.3: NASA Space Structures

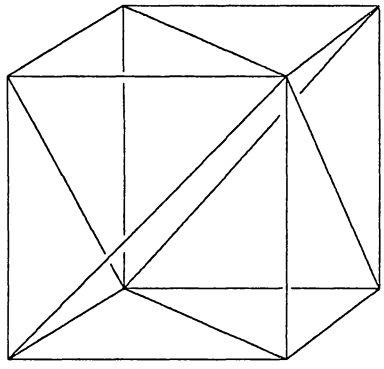

Dodecahedron

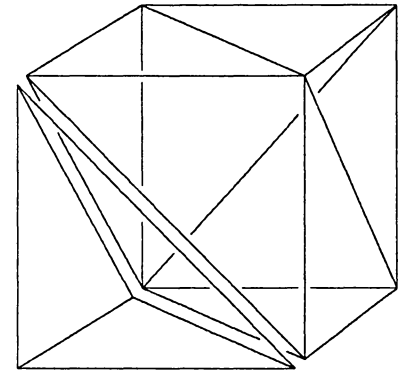

Tetrahedron Decahedron

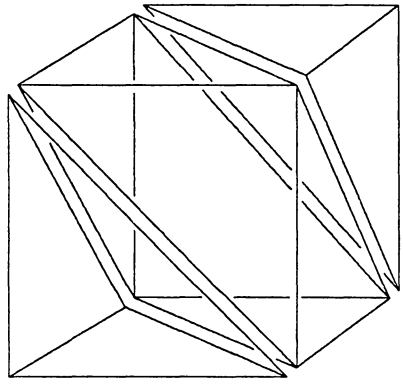

Octahedron and Two Tetrahedrons

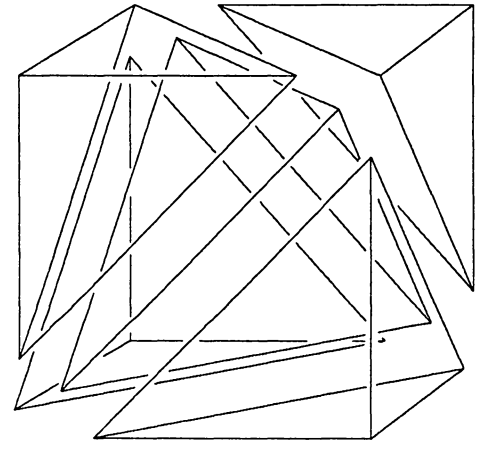

Five Tetrahedrons

Figure 2.4: Cube Formed with Different Unit Cells

cubic truss is statically indeterminate. Single members are redundant and cannot be individually actuated. Therefore, if the truss is to be actuated, multiple links must move in coordination to avoid inducing stresses in the links. NASA plans to avoid this problem by using special one degree-of-freedom actuated bays.

The original variable-geometry-truss concept was for a deployable structure, which would start flat, actuated, and then locked into position. The variable geometry truss is a useful manipulator. One cell of the VGT is a parallel manipulator. These cells can be linked together to form long chains and form a hybrid manipulator.

Another attractive space structure is the three-longeron truss shown in Fig. 2.3 (b). This structure can be composed of either tetrahedrons or octahedrons, again depending on the orientation of the diagonals[34].

The generic Stewart platform manipulator has six degrees of freedom, but it is not a true VGT because it is not a truss. The top and bottom planes are plates which must support complex loads, see Fig. 2.5 (a).

This platform can be a VGT if the spheric joints are in certain locations. If each spheric joint shares its location with one other spheric joint, the Stewart's platform becomes an octahedral variable geometry truss as shown in Fig. 2.5 (b). The Stewart platform can also form a VGT composed of three tetrahedrons. This is accomplished by changing the position of one spheric joint on the top and one spheric joint on the bottom of the octahedron, so that three spheric joints on the top and three spheric joints on the bottom share their centers. This VGT is shown in Fig. 2.5 (c).

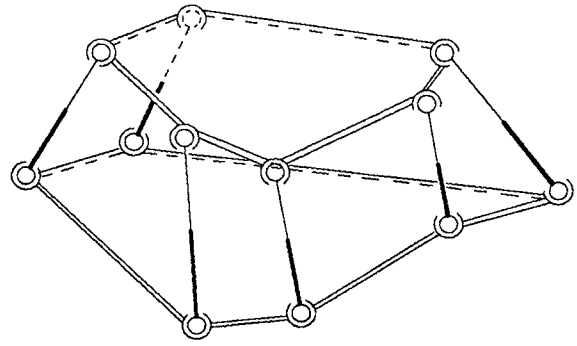

(a) Generic Stewart's Platform Manipulator

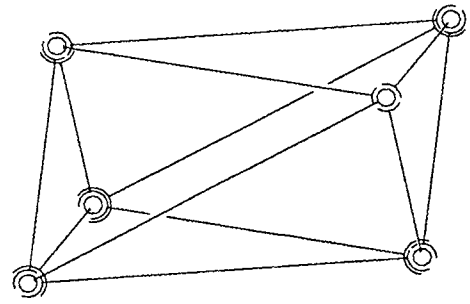

(b) Octahedral VGT

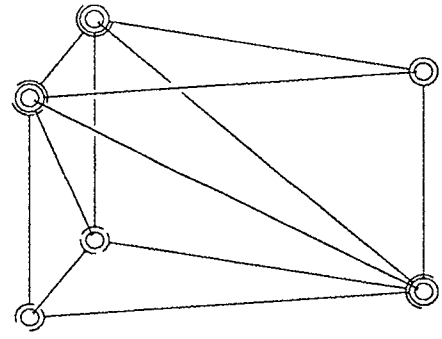

(c) Three-Tetrahedral VGT

Figure 2.5: Generic Stewart's Platform and the Octahedral and Three-Tetrahedral VGTs

2.3 Octahedral Variable Geometry Truss

The octahedral variable geometry truss is composed of twelve links as shown in Fig. 2.6 (a). Six links called *battens* form two triangular frames. Six links called *longerons* connect these two triangular frames. These links form eight triangles around the octahedron. Depending on the length of the individual links (either fixed or actuated), the octahedral truss may take on wildly different physical shapes.

The octahedral variable geometry truss is sometimes referred to as the pyramid-pyramid truss as illustrated in Fig. 2.6 (b), but this is a misleading name. The pyramid is not a basic unit cell because it has one degree of freedom with all link dimensions fixed, so that two such pyramids are always needed to form a structure. Furthermore, once the truss is actuated, i.e. in an arbitrary orientation, the pyramids are hard to identify because their bases are no longer square.

2.3.1 Terminology and Assumptions

There are several ways to actuate the octahedral VGT. The longerons in Fig. 2.5 (a) can all be actuated, in which case a Stewart's platform type VGT results [3]. This differs from the generic Stewart's platform because the frame which form the top and bottom triangular frames are planar trusses. On the other hand, every all the battens can be extensible, but this makes the kinematic problems somewhat difficult to solve. So far, a closed-form solution for the single octahedral has not been derived. On the other hand, the inverse kinematic solution is closed form if one set of three battens are extensible. Two octahedrons can be connected by sharing a set of battens. If these shared battens are actuated, a *double-octahedral* celled truss results. Also, actuating every batten makes designing and building the joints more complicated without much increase in workspace. Although it cannot

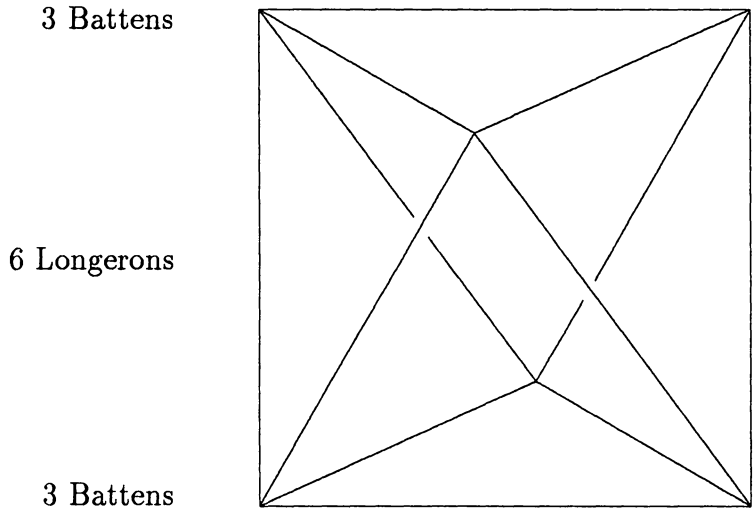

(a) Basic Octahedron

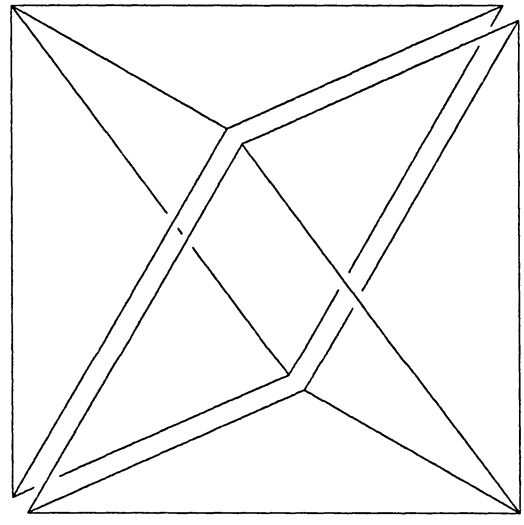

(b) Pyramid-Pyramid Description

Figure 2.6: Three Parallel Mechanisms with Six Connecting Links

be rigorously decided without a specific problem in mind, the general belief is that actuating every batten plane places too many degrees of freedom too close together. These additional degrees of freedom don't add much area to the workspace.

Actuating every other set of battens makes the kinematic problems easier to solve and results in a useful manipulator. Because two octahedrons are needed for this manipulator, it is referred to as the double-octahedral VGT. This actuating scheme is assumed for this thesis.

The three battens in the middle of the double-octahedron can change length and are called *actuators.* The actuators form the *actuated* or *mid-plane.* The *range of motion* is the amount that the actuators can change length. The actuators have length extremes of L_{max}, the maximum length, and L_{min}, the minimum length. Thus, the range of motion is the difference, $(L_{max} - L_{min})$.

To avoid confusion, the name *batten* is reserved for the static members on the top and bottom of the double-octahedron, cannot change length. Three of these form the *batten frame.* It is the batten frame which divides the double-octahedral cell from the connecting structure.

All the battens are assumed to be the same length, represented by the scalar variable B. Likewise, the longerons are assumed to be the same length. Two longerons form the *longeron triangle* with the batten which has base, B, and height, h, as shown later in Fig. 3.1.

A *cell* or *unit cell* is the basic structural unit of the truss. It is composed of one octahedron, which spans from one set of battens or actuators to the next set of battens or actuators. It is independent of the placement of actuators. The other basic unit cells are the tetrahedron, decahedron, and the dodecahedron as shown previously in Fig. 2.2.

A *bay* is a parallel manipulator unit having, in this case, three degrees of freedom.

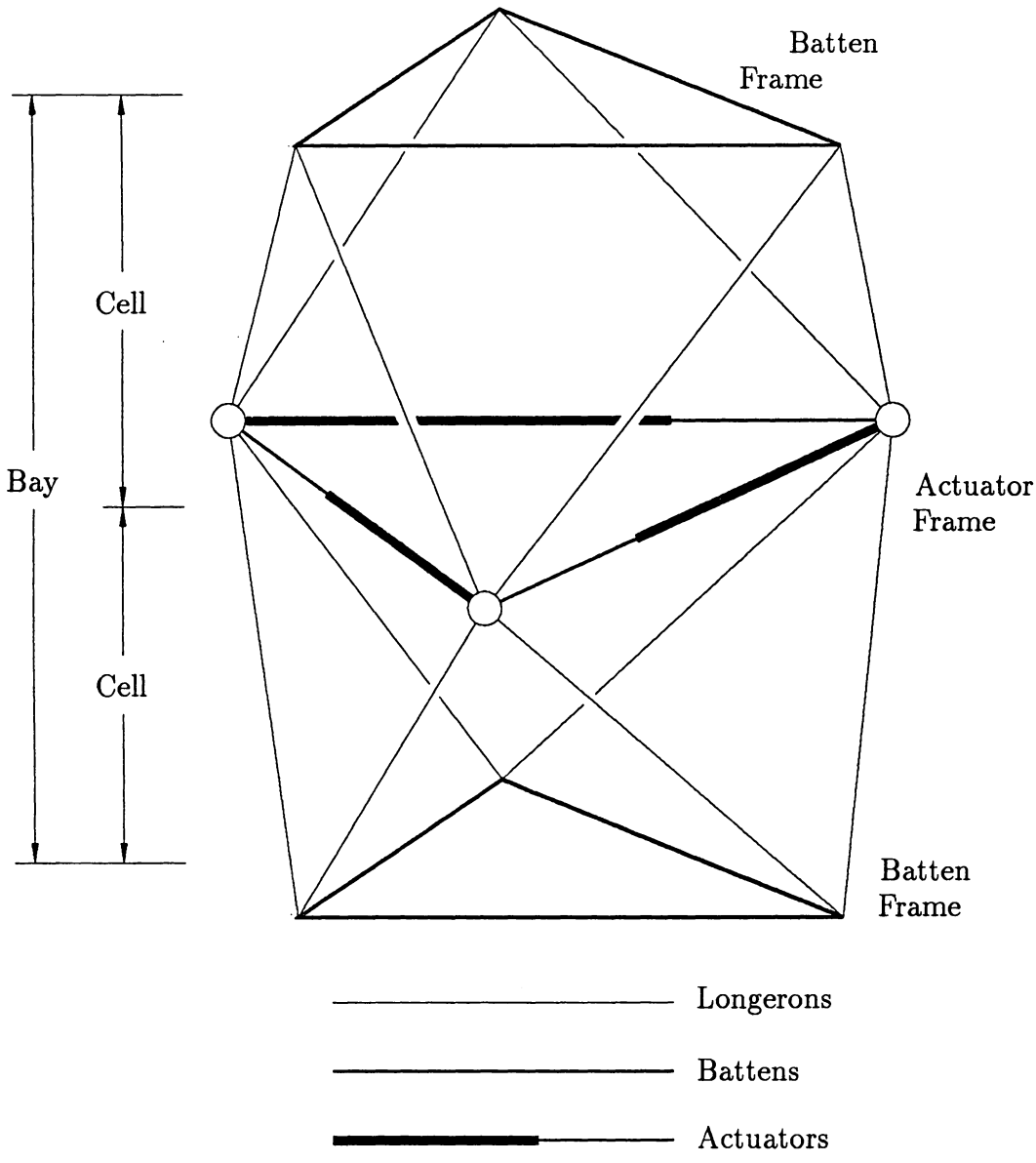

Figure 2.7: Double-Octahedral VGT Terminology

In the general case, the extent of a bay is dependent on the placement of actuators. Bays are connected in series to form a manipulator. Simply, it is the region from one set of battens to the next set of battens. It is the bay that gives the double-octahedral VGT its name. There are six longerons per cell and twelve per bay.

The *collapse* position occurs when the longerons are parallel to the battens as shown in Fig. 2.8 (a). It occurs at *full extension of actuators.* This should not be confused with *full extension of the truss.* Theoretically, the later is the position when the length of the actuators equals half that of the battens as in Fig. 2.8 (b). In many cases, full extension of the truss occurs when the actuators are at their minimum length.

2.3.2 Forward Kinematic Solution

In order to use the VGT as a manipulator, we must be able to calculate the position of a point on the batten frame knowing the fixed and actuated link lengths. This is called the *forward kinematic solution.* Unfortunately, this problem cannot be solved in closed form [27]. Therefore, we will formulate constraint equations and use a numerical solution approach.

It is possible to formulate twelve constraint equations each of which consists of the difference between the location of the ends of each link and the length of that link. Because twelve equations must be solved in twelve unknowns, this method is inefficient and can lead to many extraneous solutions and hence to numerical difficulties. The following method overcomes these difficulties.

As shown in Fig. 2.9 (a),

the two spheric joints at the base of the longeron triangle constrain the point N to move on a circular path where the point N is defined as the end of the actuators, a node. This is the same constraint afforded by a single revolute joint with a link h

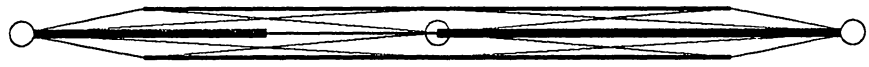

Collapsed Double-Octahedral VGT

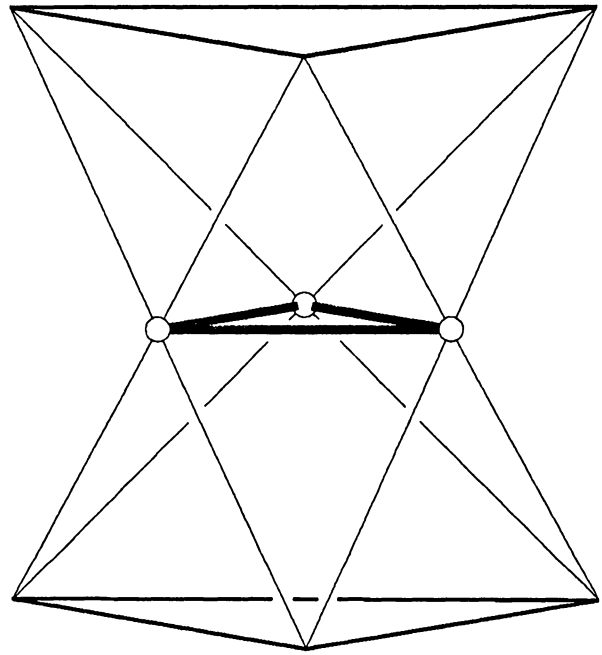

Fully Extended Double-Octahedral VGT

Figure 2.8: Range of Motion of the VGT

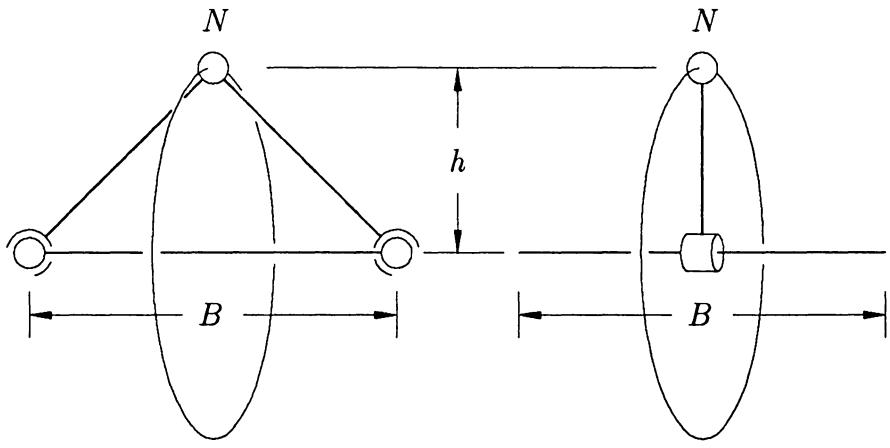

(a) Equivalence of Longeron Triangle and RS dyad

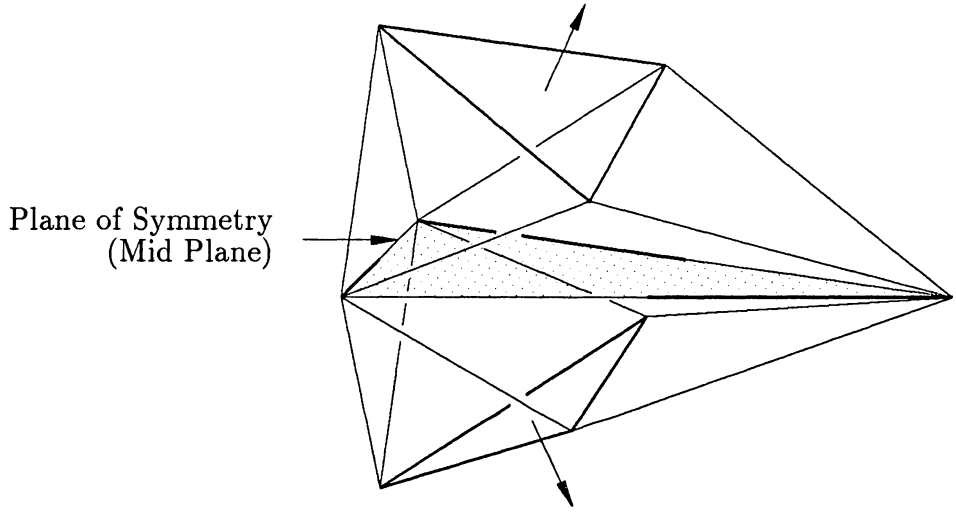

(b) Symmetry of Upper and Lower Cells

Figure 2.9: Equivalence of Longeron Triangle and RS dyad and Symmetry of the Double-Octahedral VGT

units long and a spheric joint on the end. This new pair of links is referred to as an RS (Revolute Spheric) dyad. Although the two devices are kinematically equivalent (i.e. they produce the same motion), they are quite different structurally.

The two octahedrons distort as the actuators move. Because the battens and longerons in each ocahedron are the same length, both octahedrons mirror as they change shape. Therefore, the plane formed by the three actuators, the mid plane, is a plane of symmetry as shown in Fig. 2.9 (b).

Two RS dyads can be combined to form an RSSR mechanism. This spatial mechanism is very similar to the planar four-bar linkage. Therefore, one octahedral VGT cell can be replaced kinematically by three-RSSR mechanisms as shown in Fig. 2.10 (a).

Since a VGT cell can be kinematically represented by three-RSSR mechanisms, we can use this idea to help formulate the constraint equations. Each RSSR mechanism is a single degree-of-freedom device with an input angle and a dependent output angle, see Fig. 2.10 (a). The position of three interconnected mechanisms can be completely described with three angles (θ_1, θ_2, and θ_3). Once these angles have been found, the position of any point on the bay can be calculated *in closed form.*

A set of constraint equations relating L_1, L_2, and L_3, the lengths of the actuators, with θ_1, θ_2, and θ_3 must be formulated. Let the points N_1, N_2, and N_3 be defined as the nodes, the ends of the actuators (corners). These are referred to as *nodes.* The vectors locating these points (N_1, N_2, and N_3) in a local Cartesian co-ordinate frame are:

$$\mathbf{N}_i = \mathbf{a}_i + \mathbf{R}_{\theta_i,\hat{u}_i}\mathbf{h}_i \tag{2.1}$$

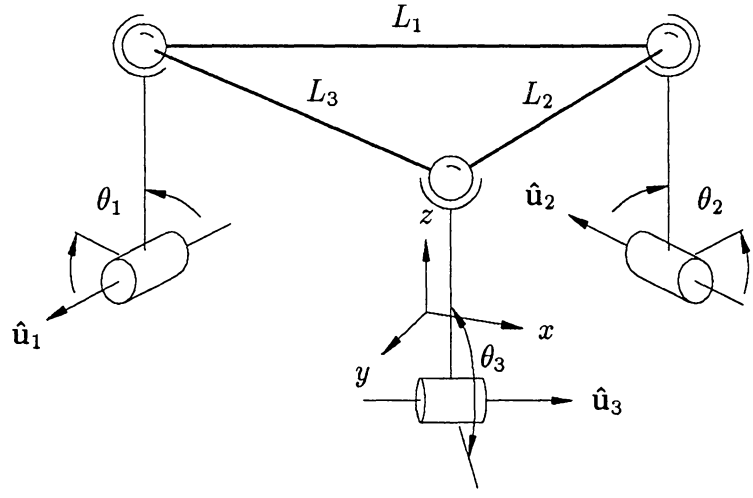

(a) Three-RSSR Model of Octahedral VGT

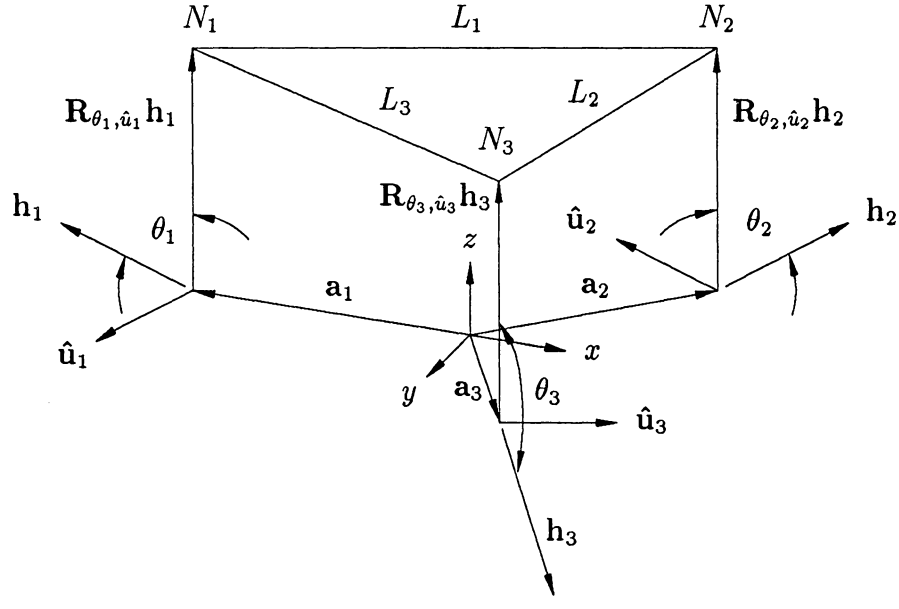

(b) Vector Model of Octahedral VGT

Figure 2.10: Three-RSSR Mechanism

where the vector $\mathbf{a}_i$ locates the revolute joint, and $\mathbf{h}_i$ is the vector describing the RS dyad (longeron triangle) in the reference position in the plane of the battens and pointing away from the origin. $\mathbf{R}_{\theta_i,\hat{u}_i}$ is a rotation matrix which rotates $\mathbf{h}_i$ around the revolute axis represented by the unit vector $\hat{\mathbf{u}}_i$. These vectors are shown in Fig. 2.10 (b).

The global Cartesian coordinate frame is located in the center of the bottom batten plane, the base plane. This position is arbitrary, but it is convenient. The x axis is oriented in the opposite direction from $\mathbf{a}_1$, the z is axis normal to the base plane pointing up toward the actuators, and the y axis is found by the right-hand rule.

Assuming all the battens and longerons are each the same length, ($\mathbf{a}_1 = \mathbf{a}_2 = \mathbf{a}_3$) and ($\mathbf{h}_1 = \mathbf{h}_2 = \mathbf{h}_3$), the battens (base links) are all B long, and the longerons triangles are h high. The vectors $\mathbf{N}, \mathbf{a}$, and $\mathbf{h}$, and the matrix $\mathbf{R}$ can be expressed in terms of the scalar constants B and h and scalar variables θ_1, θ_2, and θ_3, as follows:

$$\mathbf{a}_1 = \begin{bmatrix} -B/4 \\ B/(4\sqrt{3}) \\ 0 \end{bmatrix} \tag{2.2}$$

$$\mathbf{a}_2 = \begin{bmatrix} 0 \\ -B/(2\sqrt{3}) \\ 0 \end{bmatrix} \tag{2.3}$$

$$\mathbf{a}_3 = \begin{bmatrix} B/(4) \\ B/(4\sqrt{3}) \\ 0 \end{bmatrix}, \tag{2.4}$$

and

$$\mathbf{R}_{\theta_1,\hat{u}_1}\mathbf{h}_1 = \begin{bmatrix} -h\sqrt{3/4}\cos\theta_1 \\ (h/2)\cos\theta_1 \\ h\sin\theta_1 \end{bmatrix} \tag{2.5}$$

$$\mathbf{R}_{\theta_2,\hat{u}_2}\mathbf{h}_2 = \begin{bmatrix} 0 \\ h\cos\theta_2 \\ -h\sin\theta_2 \end{bmatrix} \tag{2.6}$$

$$\mathbf{R}_{\theta_3,\hat{u}_3}\mathbf{h}_3 = \begin{bmatrix} h\sqrt{3/4}\cos\theta_3 \\ (h/2)\cos\theta_3 \\ h\sin\theta_3 \end{bmatrix}. \tag{2.7}$$

Therefore, the coordinates of the node points are:

$$\mathbf{N}_1 = \begin{bmatrix} N_{1x} \\ N_{1y} \\ N_{1z} \end{bmatrix} = \begin{bmatrix} -B/4 \\ B/(4\sqrt{3}) \\ 0 \end{bmatrix} + \begin{bmatrix} -h\sqrt{3/4}\cos\theta_1 \\ (h/2)\cos\theta_1 \\ h\sin\theta_1 \end{bmatrix} \tag{2.8}$$

$$\mathbf{N}_2 = \begin{bmatrix} N_{2x} \\ N_{2y} \\ N_{2z} \end{bmatrix} = \begin{bmatrix} 0 \\ -B/(2\sqrt{3}) \\ 0 \end{bmatrix} + \mathbf{N}_3 = \begin{bmatrix} 0 \\ h\cos\theta_2 \\ -h\sin\theta_2 \end{bmatrix} \tag{2.9}$$

$$\begin{bmatrix} N_{3x} \\ N_{3y} \\ N_{3z} \end{bmatrix} = \begin{bmatrix} B/4 \\ B/(4\sqrt{3}) \\ 0 \end{bmatrix} + \begin{bmatrix} h\sqrt{3/4}\cos\theta_3 \\ (h/2)\cos\theta_3 \\ h\sin\theta_3 \end{bmatrix}. \tag{2.10}$$

The link lengths, L_1, L_2, and L_3, are the absolute distances between the node points; therefore,

$$L_1 = |\mathbf{N}_1 - \mathbf{N}_2| \tag{2.11}$$

$$L_2 = |\mathbf{N}_2 - \mathbf{N}_3| \tag{2.12}$$

$$L_3 = |\mathbf{N}_3 - \mathbf{N}_1|. \tag{2.13}$$

Or, in terms of the dot product of vectors

$$(L_1)^2 = (\mathbf{N}_1 - \mathbf{N}_2)\cdot(\mathbf{N}_1 - \mathbf{N}_2) \tag{2.14}$$

$$(L_2)^2 = (\mathbf{N}_2 - \mathbf{N}_3)\cdot(\mathbf{N}_2 - \mathbf{N}_3) \tag{2.15}$$

$$(L_3)^2 = (\mathbf{N}_3 - \mathbf{N}_1)\cdot(\mathbf{N}_3 - \mathbf{N}_1). \tag{2.16}$$

It can be shown that this is a system of degree sixteen in the unknowns, θ_1, θ_2, and θ_3 [26]. In other words, sixteen distinct solutions may result for any given set of link dimensions.

In general, these equations must be solved using a numerical technique. For simplicity the Newton-Raphson iteration technique was used. this technique enables solutions (roots) to the above equations to be found one set at a time from an initial starting estimate. For a single variable problem, an improved solution is obtained from an initial estimate using:

$$x_{n+1} = x_n - \frac{f(x_n)}{f'(x_n)}. \tag{2.17}$$

In our three equation, three variable system we have:

$$\begin{bmatrix} \frac{\partial F_1}{\partial \theta_1} & \frac{\partial F_1}{\partial \theta_2} & \frac{\partial F_1}{\partial \theta_3} \\ \frac{\partial F_2}{\partial \theta_1} & \frac{\partial F_2}{\partial \theta_2} & \frac{\partial F_2}{\partial \theta_3} \\ \frac{\partial F_3}{\partial \theta_1} & \frac{\partial F_3}{\partial \theta_2} & \frac{\partial F_3}{\partial \theta_3} \end{bmatrix} \begin{bmatrix} \Delta\theta_1 \\ \Delta\theta_2 \\ \Delta\theta_3 \end{bmatrix} = \begin{bmatrix} -F_1 \\ -F_2 \\ -F_3 \end{bmatrix} \tag{2.18}$$

where the constraint equations are

$$F_1 = (N_1x - N_2x)^2 + (N_1y - N_2y)^2 + (N_1z - N_2z)^2 - (L_1)^2 \tag{2.19}$$

$$F_2 = (N_2x - N_3x)^2 + (N_2y - N_3y)^2 + (N_2z - N_3z)^2 - (L_2)^2 \tag{2.20}$$

$$F_3 = (N_3x - N_1x)^2 + (N_3y - N_1y)^2 + (N_3z - N_1z)^2 - (L_3)^2. \tag{2.21}$$

Combining the above two sets of equations yields

$$F_1 = \left[(-B/4 - h\sqrt{3/4}\cos\theta_1) - (0)\right]^2$$

$$+ \left[(B/4 + (h/2)\cos\theta_1) + (B/(2\sqrt{3}) - (h/2)\cos\theta_2)\right]^2 \qquad (2.22)$$
$$+ [0 - (-h\sin\theta_2)]^2 - L_1^2,$$

$$F_2 = \left[(0) - (B/4 + h\sqrt{3/4}\cos\theta_3)\right]^2$$
$$+ \left[(-B/(2\sqrt{3}) + h\cos\theta_2) - (B/(4\sqrt{3}) + h/2\cos\theta_3)\right]^2 \qquad (2.23)$$
$$+ [(h\sin\theta_2) - (h\sin\theta_3)]^2 - L_2^2,$$

$$F_3 = \left[(B/4 + h\sqrt{3/4}\cos\theta_3) - (-B/4 - h\sqrt{3/4}\cos\theta_1)\right]^2$$
$$+ \left(B/(4\sqrt{3}) + h/2\cos\theta_3) - (B/(4\sqrt{3}) + h/2\cos\theta_1)\right]^2 \qquad (2.24)$$
$$+ [((h\sin\theta_3) - (h\sin\theta_1)]^2 - L_3^2.$$

Simplifying these produces

$$F_1 = \left[B/4 + h\sqrt{3/4}\cos\theta_1\right]^2$$
$$+ \left[B/4 + (h/2)\cos\theta_1 + B/(2\sqrt{3}) - (h/2)\cos\theta_2\right]^2 \qquad (2.25)$$
$$+ (h\sin\theta_2)^2 - L_1^2,$$

$$F_2 = \left[B/4 + h\sqrt{3/4}\cos\theta_3\right]^2$$
$$+ \left[(-B/(2\sqrt{3}) + h\cos\theta_2) - (B/(4\sqrt{3}) + h/2\cos\theta_3)\right]^2 \qquad (2.26)$$
$$+ (h\sin\theta_2 - h\sin\theta_3)^2 - L_2^2,$$

$$F_3 = \left[B/2 + h\sqrt{3/4}\cos\theta_3 + h\sqrt{3/4}\cos\theta_1\right]^2$$
$$+ [h/2(\cos\theta_3 + \cos\theta_1)]^2 \qquad (2.27)$$

$$+ [h(\sin\theta_3 - \sin\theta_1)]^2 - L_3^2.$$

For an arbitrary initial guess, this method will not always converge to the desired roots, since there are sixteen solutions to this set of nonlinear equations. Some logic must be employed to help in tracking the desired solution. Specifying that θ_1, θ_2, and θ_3 must all lie between zero and ninety degrees will ensure that a correct solution is found.

For a given assembly of the manipulator (set of solutions), this method will always converge to a solution, provided the variation from the previous solution to the new position is small.

Convergence is achieved when $F_1 = F_2 = F_3 = 0$, within some specified tolerance. The values for θ_1, θ_2, and θ_3 are, therefore, approximately correct.

If the values of F_1, F_2, and F_3 are not sufficiently close to zero, an iteration must be performed. The partial derivatives of the functions can be found using a finite difference approximation, but finding the derivatives in closed form is more accurate and faster to evaluate. The derivatives of the constraint equations with respect to the defined angles are

$$\frac{\partial F_1}{\partial \theta_1} = h^2 \sin(2\theta_1) - Bh\left(\frac{\sqrt{3}}{4} + \frac{1}{4} + \frac{1}{2\sqrt{3}}\right)\sin\theta_1 + \frac{h^2}{2}\cos\theta_2 \sin\theta_1 \quad (2.28)$$

$$\frac{\partial F_1}{\partial \theta_2} = Bh\left(\frac{1}{8} + \frac{1}{2\sqrt{3}}\right)\cos\theta_2 + \frac{h^2}{4}\cos\theta_1 \sin\theta_2 + \frac{3}{4}h^2 \sin(2\theta_2) \quad (2.29)$$

$$\frac{\partial F_1}{\partial \theta_3} = 0 \quad (2.30)$$

$$\frac{\partial F_2}{\partial \theta_1} = 0 \quad (2.31)$$

$$\frac{\partial F_2}{\partial \theta_2} = Bh\left(\frac{1}{\sqrt{3}} + \frac{1}{2\sqrt{3}} + \frac{h}{B}\right)\sin\theta_2 - 2h^2 \sin\theta_3 \cos\theta_2 \quad (2.32)$$

$$\frac{\partial F_2}{\partial \theta_3} = \frac{-Bh}{\sqrt{3}} \sin\theta_3 + h^2 \cos\theta_2 \sin\theta_3 - 2h^2 \sin\theta_2 \cos\theta_3 \tag{2.33}$$

$$\frac{\partial F_3}{\partial \theta_1} = \left(\frac{-Bh\sqrt{3}}{2} - h^2 \cos\theta_3\right) \sin\theta_1 - 2h^2 \sin\theta_3 \cos\theta_1 \tag{2.34}$$

$$\frac{\partial F_3}{\partial \theta_2} = 0 \tag{2.35}$$

$$\frac{\partial F_3}{\partial \theta_3} = -h\left(\frac{B\sqrt{3}}{2} + \frac{B}{4\sqrt{3}} + h\cos\theta_1\right) \sin\theta_3 - 2h \sin\theta_1 \cos\theta_3. \tag{2.36}$$

These results are used to find values for $\Delta\theta_1, \Delta\theta_2$, and $\Delta\theta_3$ using Cramer's Rule:

$$\Delta\theta_1 = \det\begin{bmatrix} F_1 & \frac{\partial F_1}{\partial \theta_2} & \frac{\partial F_1}{\partial \theta_3} \\ F_2 & \frac{\partial F_2}{\partial \theta_2} & \frac{\partial F_2}{\partial \theta_3} \\ F_3 & \frac{\partial F_3}{\partial \theta_2} & \frac{\partial F_3}{\partial \theta_3} \end{bmatrix} \div \det\begin{bmatrix} \frac{\partial F_1}{\partial \theta_1} & \frac{\partial F_1}{\partial \theta_2} & \frac{\partial F_1}{\partial \theta_3} \\ \frac{\partial F_2}{\partial \theta_1} & \frac{\partial F_2}{\partial \theta_2} & \frac{\partial F_2}{\partial \theta_3} \\ \frac{\partial F_3}{\partial \theta_1} & \frac{\partial F_3}{\partial \theta_2} & \frac{\partial F_3}{\partial \theta_3} \end{bmatrix}, \tag{2.37}$$

$$\Delta\theta_2 = \det\begin{bmatrix} \frac{\partial F_1}{\partial \theta_1} & F_1 & \frac{\partial F_1}{\partial \theta_3} \\ \frac{\partial F_2}{\partial \theta_1} & F_2 & \frac{\partial F_2}{\partial \theta_3} \\ \frac{\partial F_3}{\partial \theta_1} & F_3 & \frac{\partial F_3}{\partial \theta_3} \end{bmatrix} \div \det\begin{bmatrix} \frac{\partial F_1}{\partial \theta_1} & \frac{\partial F_1}{\partial \theta_2} & \frac{\partial F_1}{\partial \theta_3} \\ \frac{\partial F_2}{\partial \theta_1} & \frac{\partial F_2}{\partial \theta_2} & \frac{\partial F_2}{\partial \theta_3} \\ \frac{\partial F_3}{\partial \theta_1} & \frac{\partial F_3}{\partial \theta_2} & \frac{\partial F_3}{\partial \theta_3} \end{bmatrix}, \tag{2.38}$$

and

$$\Delta\theta_3 = \det\begin{bmatrix} \frac{\partial F_1}{\partial \theta_1} & \frac{\partial F_1}{\partial \theta_2} & F_1 \\ \frac{\partial F_2}{\partial \theta_1} & \frac{\partial F_2}{\partial \theta_2} & F_2 \\ \frac{\partial F_3}{\partial \theta_1} & \frac{\partial F_3}{\partial \theta_2} & F_3 \end{bmatrix} \div \det\begin{bmatrix} \frac{\partial F_1}{\partial \theta_1} & \frac{\partial F_1}{\partial \theta_2} & \frac{\partial F_1}{\partial \theta_3} \\ \frac{\partial F_2}{\partial \theta_1} & \frac{\partial F_2}{\partial \theta_2} & \frac{\partial F_2}{\partial \theta_3} \\ \frac{\partial F_3}{\partial \theta_1} & \frac{\partial F_3}{\partial \theta_2} & \frac{\partial F_3}{\partial \theta_3} \end{bmatrix}. \tag{2.39}$$

With these, new estimates for θ_1, θ_2, and θ_3 are obtained as follows:

$$\theta_1^{new} = \theta_1 + \Delta\theta_1 \tag{2.40}$$

$$\theta_2^{new} = \theta_2 + \Delta\theta_2 \tag{2.41}$$

$$\theta_3^{new} = \theta_3 + \Delta\theta_3 \tag{2.42}$$

Now, new values for F_1, F_2, and F_3 are obtained using these new estimates, $\theta_1^{new}, \theta_2^{new}$,

and θ_3^{new}? Again, convergence is achieved if $F_1 = F_2 = F_3 = 0$, within some specified tolerance. If not, the procedure is repeated until acceptable values for θ_1, θ_2, and θ_3 are found. Experience has shown that this method will converge in three or four iterations unless the desired position is close to full collapse.

The node points can be found using the equations in Eq. 2.10. Now, one octahedron has been solved. The locations of the components of the upper octahedron can be found by symmetry (see Fig. 2.9). Let $\mathbf{g}$ be a vector normal to this plane of symmetry. It can be found from the vectors locating the plane of symmetry,

$$\mathbf{g} = (N_1 - N_2) \times (N_1 - N_3) \tag{2.43}$$

$$\mathbf{a}_{3+i} = 2(\mathbf{R}_{\theta_i, \hat{u}_i} \mathbf{h}_i \cdot \mathbf{g}) \tag{2.44}$$

This solution method can also generate other parameters such as the angles which the upper batten frame makes with the base plane. These parameters could be used in shape control. This method was originally developed by Reinholtz and Gokhale [25].

2.3.3 Inverse Kinematic Solution

Padmanabhan, Arun, and Reinholtz [30] solved the inverse kinematic problem for the single-octahedral cell. To find the necessary actuator lengths to place the end effector at a specificed location, let $\mathbf{P}$, shown in Fig. 2.11, be the vector locating the position in the global Cartesian coordinate frame fixed to the center of the bottom batten plane. This is the same coordinate frame used in the forward kinematic solution described in Section 2.3.2.

Define another moving Cartesian coordinate frame in the center of the top or moving batten frame. The end effector is rigidly connected to this frame. Let the

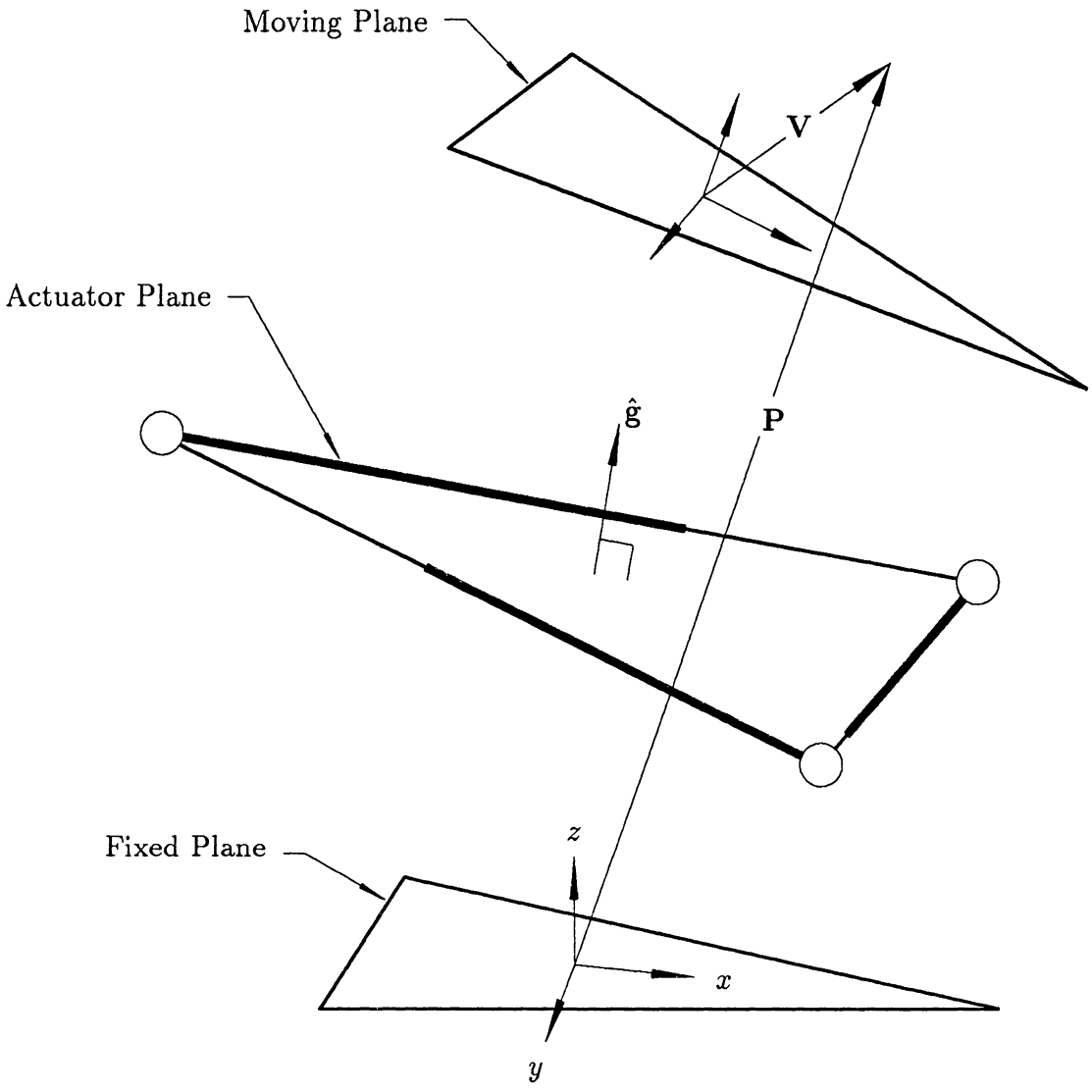

Figure 2.11: Inverse Kinematic Solution

vector $\mathbf{V}$ describe this vector in the moving frame. Because the actuator plane is the plane of symmetry, the line connecting any point with its reflection is normal to the plane of symmetry. Moreover, its midpoint lies on the plane. Thus, the plane can be located by knowing any point and its reflection. The origin of the moving and fixed coordinate frames are the obvious pair to use. The vector locating the origin of the moving coordinate frame in fixed coordinate frame is $(\mathbf{P} - \mathbf{V})$. Thus, the unit vector normal to the plane of symmetry is

$$\hat{g} = \frac{\mathbf{P} - \mathbf{V}}{|\mathbf{P} - \mathbf{V}|} \tag{2.45}$$

The node points (spheric joints of the R-S dyad) are constrained to lie in the plane of symmetry. The constraint equations for finding the node points can be found be noting that $\mathbf{N}_i - (\mathbf{P} - \mathbf{V})/2$ lies in the plane of symmetry. Therefore,

$$\left(\mathbf{N}_i - \frac{\mathbf{P} - \mathbf{V}}{2}\right) \cdot \hat{g} = 0 \tag{2.46}$$

By substuting the eqauation for $\mathbf{N}_i$, Eq. 2.1, into this equation, the angles θ_1, θ_2, and θ_3 can be found:

$$\theta_i = 2\tan^{-1}(t) \tag{2.47}$$

where

$$t = \frac{-k_2 \pm \sqrt{k_1^2 + k_2^2 - k_3^2}}{k_3 - k_1}$$

$$
\begin{aligned}
k_1 &= \left(h_{xi} - \hat{u}_{xi}^2 h_{xi} - \hat{u}_{xi}\hat{u}_{yi}h_{yi}\right)\hat{g}_x + \left(h_{yi} - \hat{u}_{yi}^2 h_{yi} - \hat{u}_{xi}\hat{u}_{yi}h_{yi}\right)\hat{g}_y \\
&\quad + \left(h_{zi} - \hat{u}_{zi}^2 h_{zi} - \hat{u}_{xi}\hat{u}_{zi}h_{zi}\right)\hat{g}_z
\end{aligned}
$$

$$
k_2 = (\hat{u}_{yi}h_{zi} - \hat{u}_{zi}h_{yi})\hat{g}_x + (\hat{u}_{zi}h_{xi} - \hat{u}_{xi}h_{zi})\,\hat{g}_y + (\hat{u}_{xi}h_{yi} - \hat{u}_{yi}h_{xi})\hat{g}_z
$$

$$
\begin{aligned}
k_3 &= \left(\hat{u}_{xi}^2 h_{xi} + \hat{u}_{xi}\hat{u}_{yi}h_{yi} + \hat{u}_{xi}\hat{u}_{zi}h_{zi} + a_{xi}\right)\hat{g}_x \\
&\quad + \left(\hat{u}_{yi}^2 h_{yi} + \hat{u}_{xi}\hat{u}_{yi}h_{xi} + \hat{u}_{yi}\hat{u}_{zi}h_{zi} + a_{yi}\right)\hat{g}_y \\
&\quad + \left(\hat{u}_{zi}^2 h_{zi} - \hat{u}_{xi}\hat{u}_{zi}h_{xi} + \hat{u}_{yi}\hat{u}_{zi}h_{yi} + a_{zi}\right)\hat{g}_z - |\mathbf{P}|
\end{aligned}
$$

The node points $\mathbf{N}_1, \mathbf{N}_2$, and $\mathbf{N}_3$ can be found by substituting these values for θ_1, θ_2, and θ_3 back into Eq. 2.1. The actuator lengths can them be found using Eq. 2.12.

2.3.4 Long-Chain Manipulators

Because of the high stiffness and low weight of these VGTs, the double-octahedral VGT offers some interesting possibilities as a manipulator. Double-octahedral bays can be connected together by sharing sets of battens. This is the basis for the idea of a long "snake-like" manipulator. A seven bay double-octahedral VGT manipulator shown in Fig. 2.12 is planned to be built at VPI&SU. A control methods for this high DOF device is presented in Bob Salerno's Thesis [[32]].

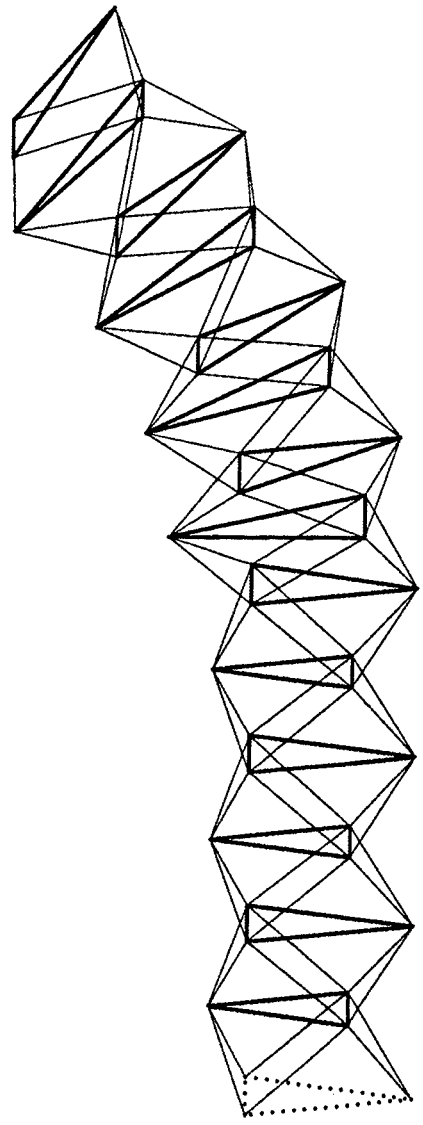

Figure 2.12: Long Chain Manipulator to be Built at VPI&SU

Chapter 3

Design Concepts

This thesis documents the design and construction of a variable geometry truss. As with any design, this process iterative and many ideas had to be pursued in parallel. Many issues discussed in this chapter are interrelated with issues addressed further on in the thesis.

3.1 Dimensional Relationships

One of the first things to consider in building a truss is how big it needs to be. This, of course, depends on the intended uses and the work environment of the VGT.

If we assume that the longerons and battens are each the same length respectively, the size of the truss can be described with a minimum number parameters. For purposes of kinematic design and analysis, the absolute size of the truss is not as important as the relative size of the members with respect to each other.

As shown in Fig. 3.1 (a), two longerons and one batten form a triangle, hereafter referred to as the *longeron triangle*. One important design parameter is the ratio of the height of the longeron triangle, h, to the length of the batten or base of this triangle, B. The length of the longerons and the angle between the longerons and batten could be used, but using the longeron triangle height instead gives a better

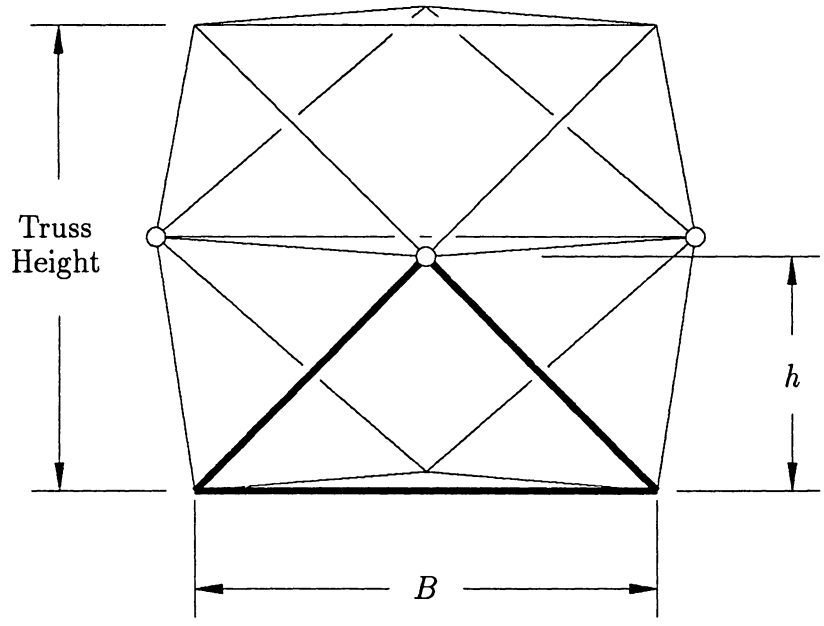

(a) Longeron Triangle with Base, B, and Height, h

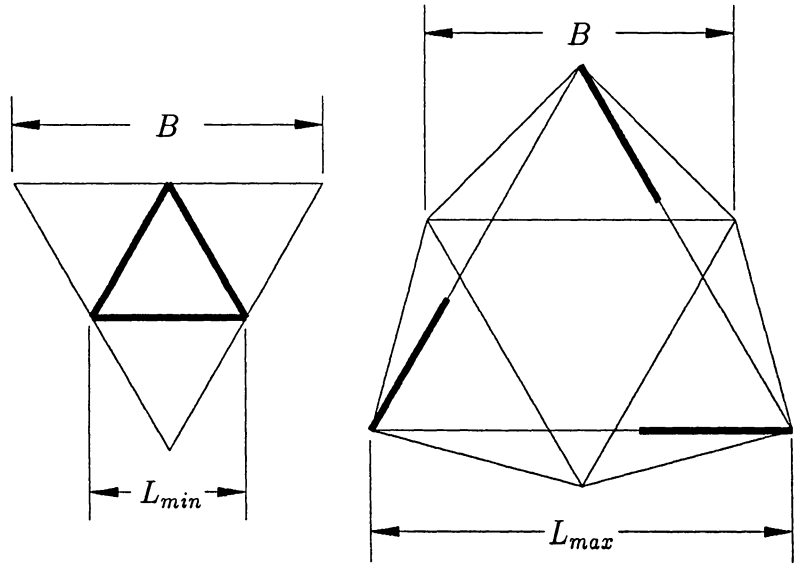

(b) Top View of VGT Showing Maximum and Minimum Actuator Lengths

Figure 3.1: Important parameters for sizing a Double-Octahedral VGT

intuitive feel. The range of motion of the actuators is also important. The actuators can extend to L_{max} and contract to L_{min} as demonstrated in Fig. 3.1 (b).

Changing the ratio of base, B, to height, h, has a dramatic effect on the way the truss works. When the batten is short compared to the height, the truss is tall and slender as shown in Fig. 3.2 (a). The actuators must have a large range of motion for the truss have a large workspace. To reach full extension, L_{min} must be less than or equal to $B/2$, but to collapse fully, L_{max} must be several times larger (see Fig. 3.2 c). If an actuator can be built to do this, the resulting truss will be able to bend through large angles with one bay. This angle is defined as the angle between the normal of one batten frame and the normal of the next batten frame.

There are two actuation schemes which result in a bend in the truss. One is with two longeron sets up and one down (forming planes perpendicular to the plane of the un-actuated battens) as shown in Fig. 3.2 (b). This configuration is strong in the direction of the curvature but weaker perpendicular to it. Unfortunately, this configuration can not bend through large angles. The maximum angle is dependent on the ratio B/h. For small ratios (large h), the maximum angle approaches 90°. For larger ratios it is less, as shown in Fig. 3.3. The figure assumes $L_{min} = B/2$ and makes no limitations on L_{max}.

The other bending option is with one longeron pair up and two down. It is very weak in the direction of the bend and stronger perpendicular to it. It can bend with angles greater than 90°, but is limited by link interference and high stresses. Theoretically, this type of bend is limited by a singularity which existed when the sum of the two shorter links equals the longer link. Consequently, the triangle formed by the three actuators is no longer a triangle and, the VGT is no longer a structure.

When the ratio of B/h is large, on the other hand, the truss is short (short h)

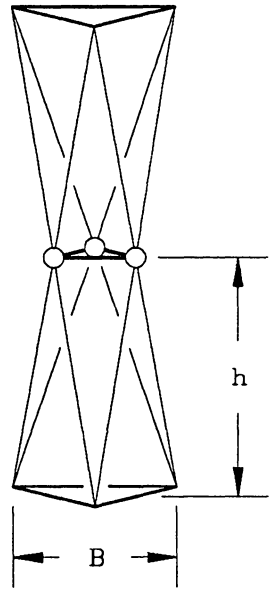

(a) Full Extension

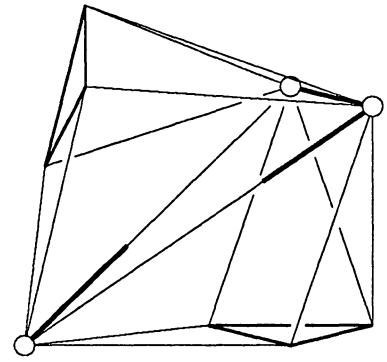

(b) Bending

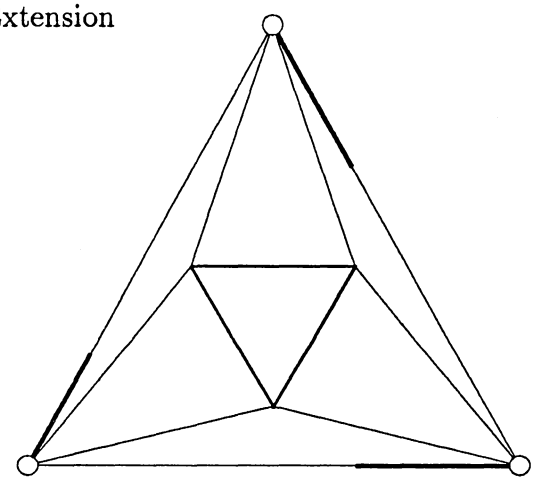

(c) Top View of Fully-Collapsed Truss

Figure 3.2: Double-Octahedral VGT with Small B/h Ratio

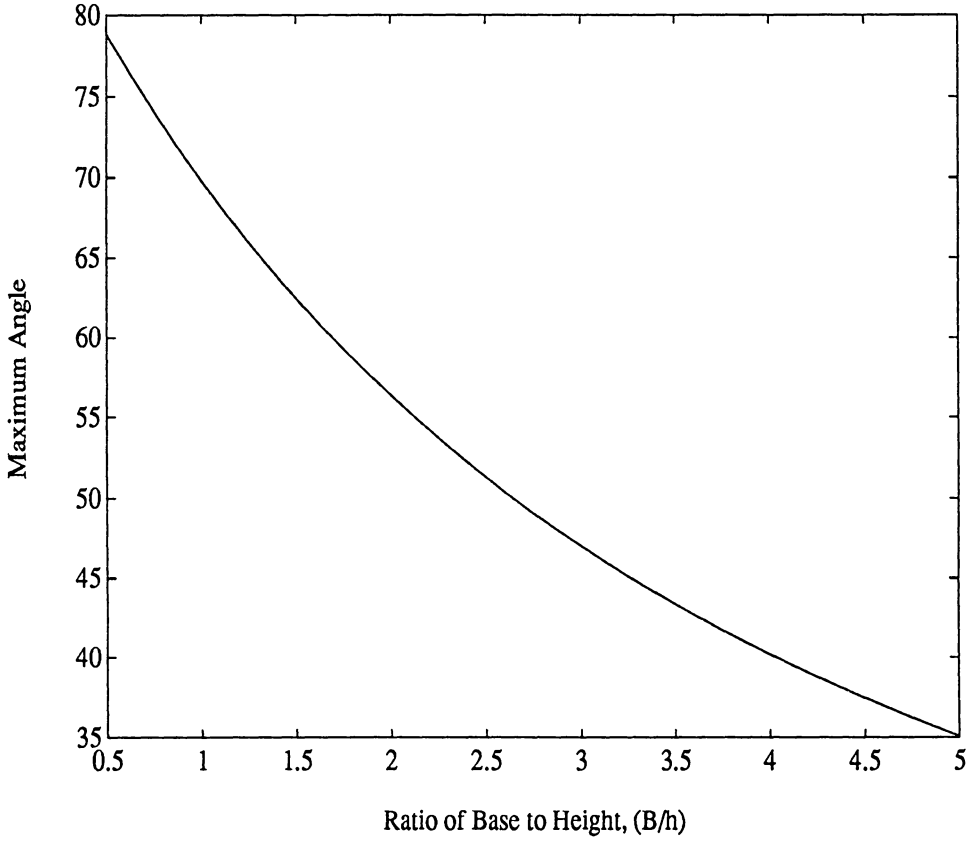

Figure 3.3: Relationship between B/h Ratio and Curvature

and wide (a long B), as shown in Fig. 3.4. The range of motion of the actuators (the difference between L_{max} and L_{min}) is small. Therefore, the range of angles which the actuated plane can move through with respect to the batten frame is severely limited. This range can be extended slightly by having values of θ greater than 90°, but it is still limited. The advantage of having a small B/h ratio is that the full workspace of the truss can be reached with a small range of motion in the actuators.

Almost all trusses will have ratios between these two extremes. A good first step in choosing a value for B/h is 2. Another is to have the largest possible ratio and still have sufficient range of motion in the actuators to reach full extension and complete collapse. Using extreme ratios of B/h can lead to trusses with strength problems.

The relationship between truss height and actuator length for various B/h ratios is plotted in Fig. 3.5. This represents a line through the workspace where the VGT is always straight, ie. the top and bottom batten frames remain parallel. An actuator length of 0.5 is full extension (L_{min}) and zero truss height is full collapse (actuator length of L_{max}).

The choice of B/h is dependent on actuator range and design. To reach full extension $L_{min} \leq B/2$. Likewise, to reach full collapse $L_{max} = B/2 + \sqrt{3}h$. Therefore, if a VGT is to reach both extremes, the range of the actuators is $L_{max} - L_{min} = \sqrt{3}h$. For an ideal actuator where the inner member "telescopes" out of the outer member, the longest link length can be no more than twice the shortest ($L_{max} \leq 2L_{min}$). Real actuators will probably have less range than this. Therefore, the best actuator range ($L_{max} - L_{min}$). that can be achieved is L_{min}. The smallest ratio B/h that can be achieved while still maintaining the ability to extend and collapse fully is $B/h = 2\sqrt{3} = 3.46$.

For the truss built at VPI&SU, a ratio of B/H of 2 was chosen. Although this

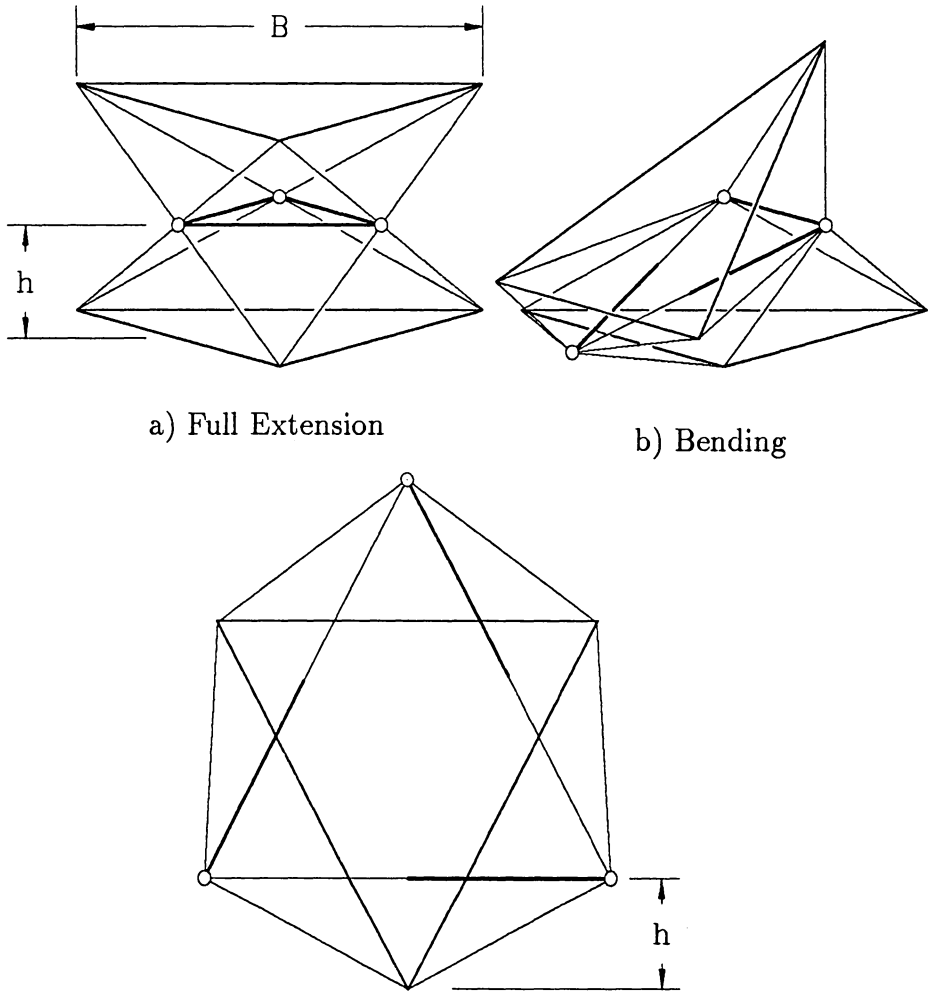

a) Full Extension

b) Bending

c) Top View of Fully Collapsed VGT

Figure 3.4: Double-Octahedral VGT with Large B/h Ratio

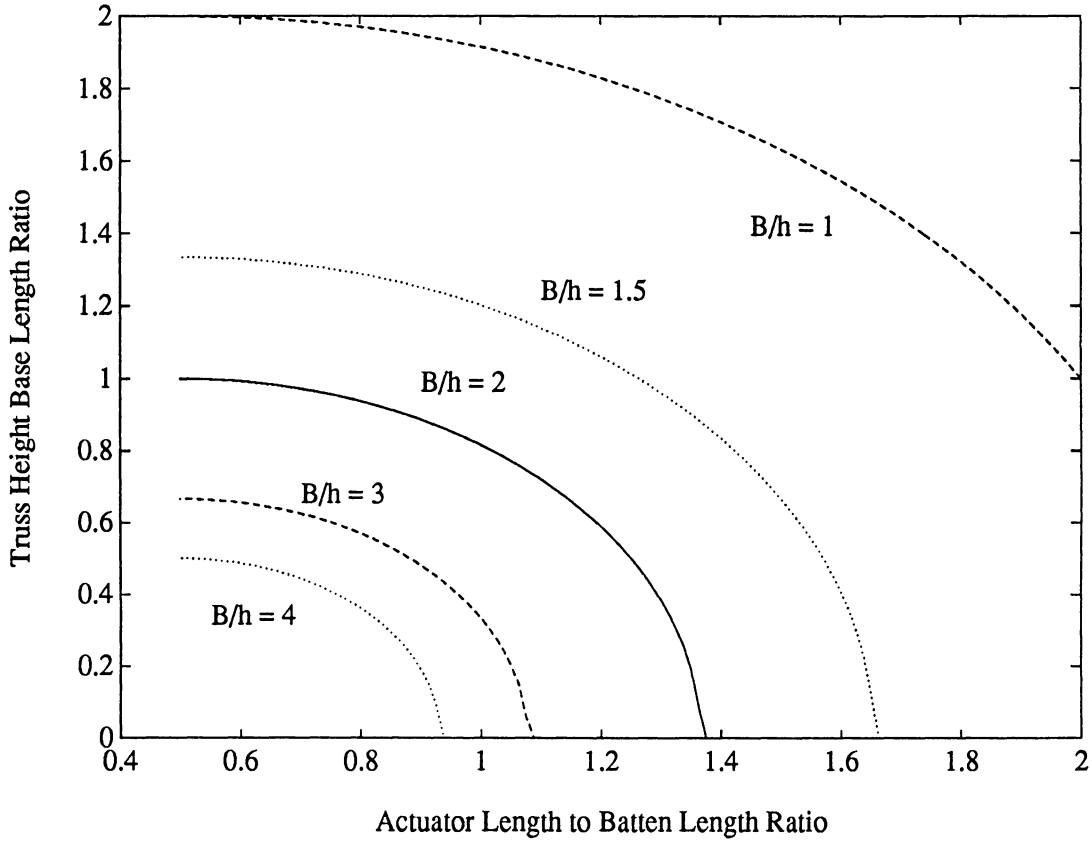

Figure 3.5: Relationship Between Truss Height and Actuator Length for Various Ratios of B/h

limits the range of motion, the limitation is not as severe as might appear at first. A plot of the relationship between truss height and actuator length for this ratio is shown in Fig. 3.6. This plot shows that the loss of workspace is relatively small. The region of actuation close to full extension was removed because much actuator stroke is needed for a small movement in the end of the truss. Losses in the range in this area will also limit bending.

The region close to collapse was also removed. This part of the actuator range is only used for collapsing and radical bending. Although link interference will, in most cases, keep the truss from reaching it, the fully-collapsed position is, in fact, a dead-center (kinematically indeterminate) position. Because of the low mechanical advantage near the dead-center position, there are extremely high forces in the links, and high torques are necessary to move the truss. This should be avoided unless compact storage of the VGT is an overriding consideration. More work in dimensional optimization could be done in this area. Such issues will be addressed in Section 5.1.2.

Once the ratio of base to height is chosen, the overall dimensions of the VGT can be chosen based on spatial constraints. Detailed geometric design and other questions such as maximum reach of a VGT manipulator will be addressed in Chapter 4.

3.2 Actuation

In order to move the truss, some form of mechanical actuator is needed in the actuated links. This actuator could be a hydraulic or pneumatic cylinder. These types of actuators are fast and simple to build, but they require some fluid supply system and a relatively complex control systems. Although there are some applications for which hydraulic actuators would be preferred, this thesis does not address these actuators.

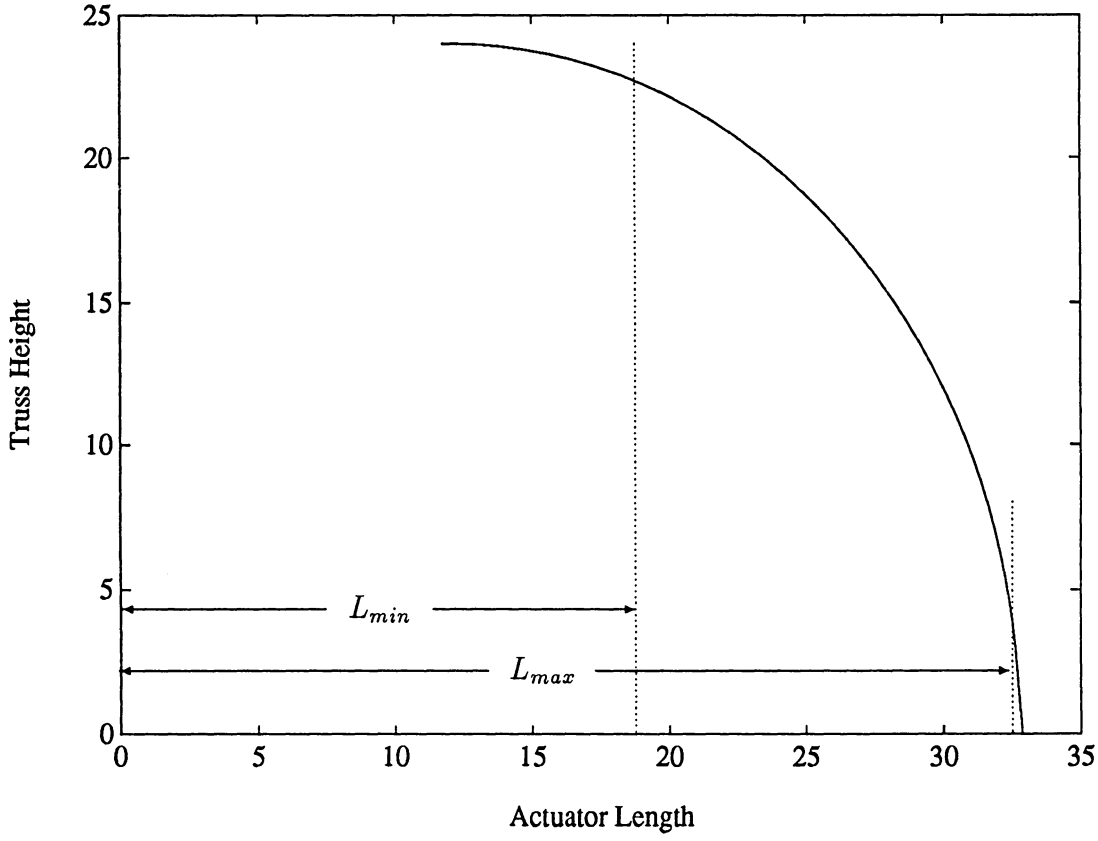

Figure 3.6: Relationship Between Truss Height and Actuator Length for a Ratio B/h of Two

Another possible actuator choice is a screw mechanism driven by a motor. The screw mechanism could use ball screws or conventional threaded screws. Ball screws use ball bearings between the screw and the nut to minimize friction. As a result, they are typically back drivable. If there was not sufficient friction in the motor and gearhead, the axial forces in the actuator could cause the screws to turn. Although desirable for vibration control, such a situation may be undesirable in a manipulator because the motors would have to constantly resist motion, otherwise the truss could move to or beyond its limit positions. Furthermore, the motors could not be removed while the truss was under load (gravity) unless some other locking system was employed. These screws are heavy and expensive. They are also bulky which compromises the ability of the truss to collapse into a compact shape.

Conventional lead screws (power screws) can do the same job but have higher friction. These screws are smaller, lighter, and less expensive. A number of thread shapes are available. These include standard, square, and Acme threads, all of which are shown in Fig. 3.7.

Standard threads (the same threads available for fastening screws) are available in a wide variety of sizes. These were used successfully on the NASA truss. For a more information on this design, see Section 3.5.1. Their low cost and wide availability are advantages, but high frictional forces must be overcome for their use as actuators. Part of this friction is due to the wedging action of the triangular threads.

Square threads have lower friction because of the elimination of the wedging action. They are used in vices and jacks and can be rather large (diameters of several inches). Square threads have stress concentrations at the base and therefore have lower fatigue strength. They are also costly.

Acme threads are similar to square threads but have a thread angle of 14.5°.

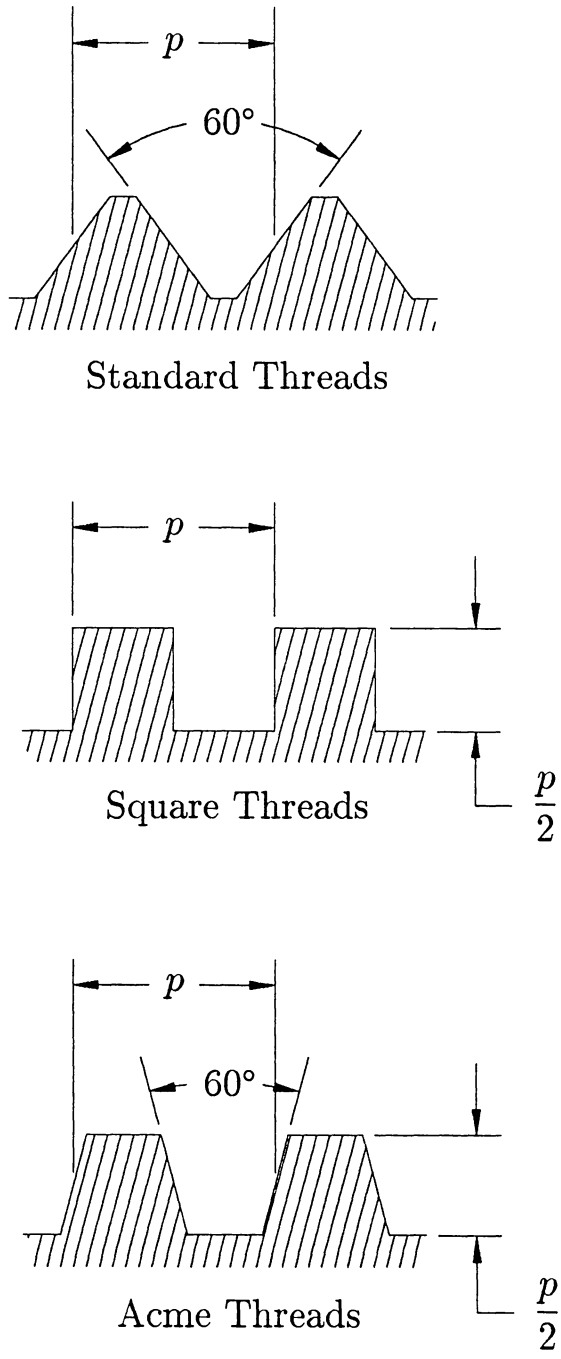

Figure 3.7: Standard Lead-Screw Thread Shapes

This slight angle helps reduce the stress concentrations and lowers the production cost [35]. These threads were chosen for the truss. More on the design of the lead screws is given in Section 4.5.1.

Once a motor/lead-screw combination has been picked, the issue of how to arrange them must be addressed. The first and most obvious choice is to connect the motor to the lead screw and screw this assembly in to a nut mounted in a hollow tube as shown in Fig. 3.8. The whole system is mounted "ideally" between the two spheric joints. This design is used on the NASA truss (see Section 3.5.1). The disadvantage of this system is that the motor and associated parts take up too much room. The shortest length that the actuated link can attain is much more than half the longest link length, ($L_{max} < 2L_{min}$). The NASA truss has an actuator range if 42 to 54 in (1.07 to 1.37 m).

A small actuator range limits the ability of the truss to reach full extension *and* full collapse. To get around this, the height of the cross-longeron triangles, h, must be shortened relative to B. This modification decreases maximum angle through which one bay can bend which, in turn, decreases the range of motion and workspace of the device.

Two methods were devised to improve on this arrangement of the motors and lead screws. One is to let the lead screw stick through the joint. The nut could be in the joint itself. The advantages are simple construction on the nut side, and large range of motion, ($L_{max} > 2L_{min}$). This allows for a much larger ratio of h/B. A disadvantage is that the lead screw sticks out and could interfere with (hit) something. If the motors have a large diameter, this increases the joint offset, a problem which is addressed more fully in Section 3.5.1. Also, it is not aesthetically pleasing or convenient to have greasy screws protruding from the truss. These could detract from the elegance of the truss, although the design has many kinematic

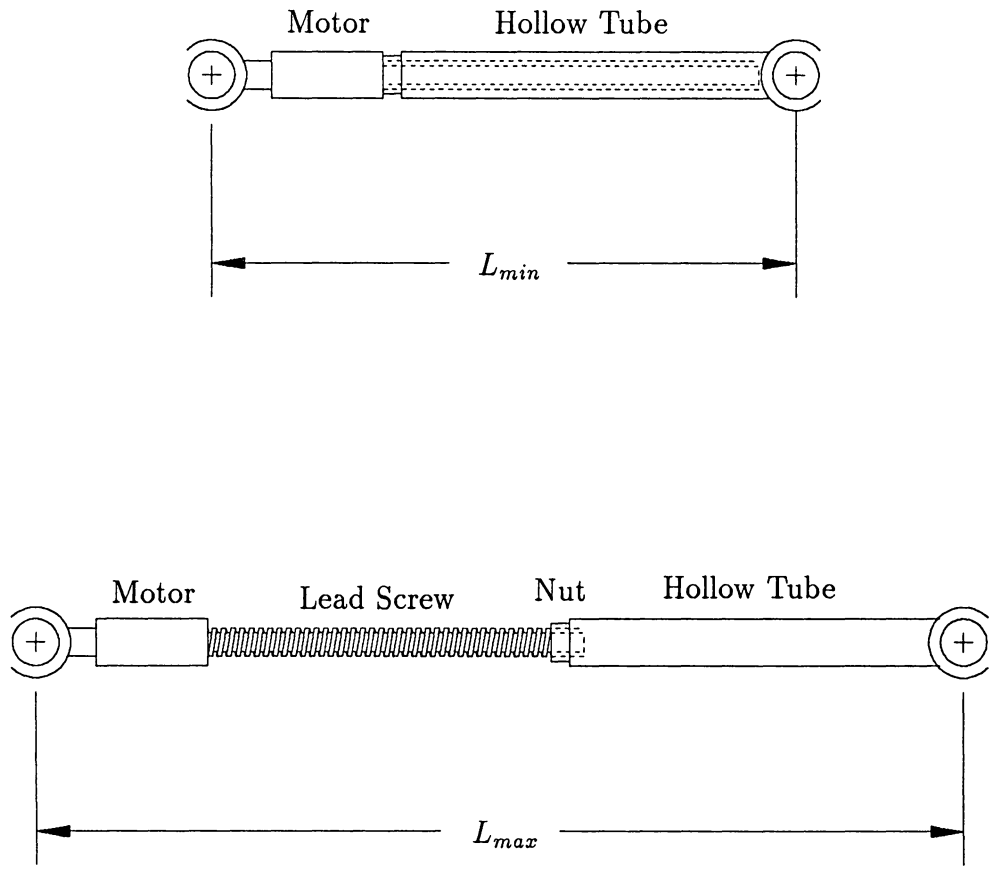

Figure 3.8: A Simple Actuator Design

advantages.

The other proposed actuator design is to have the motor outside of the joint. The lead screw goes through the joint to a nut in the batten, as in the original design. The advantages are a smaller joint offset, more elegant design, and easy access to the motor. But, unfortunately the nut must be at the midpoint of the actuated batten, thus limiting the range of motion somewhat. Since it is inherent in this design that $L_{max} \leq 2L_{min}$, the range of motion is less than or equal to L_{min}. Nevertheless, this design has many advantages that make it an attractive choice. The motors are readily accessible and the screws remain fully within the truss. This is the design which was used for the new VGT.

3.3 Motor Issues

In order to drive the screw actuators, some form of motor is needed. For simplicity of control, portability and potential use in space, we will assume the only choice for this motor is an electric powered one.

These motors must be able to provide intermittent and reversible torque over a variable speed range. They also need to be powerful and light in weight, since the motors support their own weight and the weight of all motors further out in the truss. These motors must readily lend themselves to control by a digital computer. AC motors were ruled out because they are difficult to control and do not readily permit variable speed.

Eliminating AC motors leaves a wide variety of DC motors with many options. The type of DC motor will be addressed here and the power and torque requirements will be addressed in Section 4.3. Permanent-magnet, shunt-wound and series-wound DC motors are available. Direct-drive and gear motors will be addressed. DC motors can have commutators (brushes), or they can be brushless, relying on solid-state

commutation.

In space applications, brushless motors are a necessity because the brushes quickly wear out in a vacuum, but brushless motors are expensive. Regular commutator DC motors were chosen for the VGT.

Permanent magnet field motors have provided a comparatively simple and reliable DC drive where high efficiency, high starting torque, and a linear speed-torque curve were desirable [36]. These motors are also smaller and lighter than comparable torque motors with windings, either shunt or series wound motors.

Motors can operate directly, or they can drive through a series of gears. Gearheads enable the system to generate higher torque at a lower speed, and the VGT needs high torque because of high actuator forces. Unfortunately, almost all gear trains introduce backlash into the drive system. A direct drive system would have no backlash. Although backlash is not a serious problem from a kinematic viewpoint, it can be from a controls standpoint. Since the motion of the power screw must be measured, the position instrumentation can be located on it eliminating the position uncertainty of instrumenting rotation at the motor. Choosing the gear ratio is addressed in Section 4.3.

Once a motor has been selected, power must be transferred from rotation to translation. This is accomplished with a lead screw. The pitch and the number of threads of the lead screw determines the relationship between rotation and translation. They are just as important as the gear ratio because they determine how much force is developed for a given torque. Leas screw design is discussed in Section 4.5.1.

3.4 Instrumentation

3.4.1 Control Equipment

For any manipulator to be used as a robot, some automatic control system is needed. An IBM PC clone computer was chosen as the core of the control system for the VGT. The voltage from the position and velocity instrumentation devices are fed back to A/D boards in the computer. This information tells the computer where the VGT is and what it is doing.

The computer can also be equipped with transputers. Transputers are microprocessors built to work in parallel with each other. A transputer parallel network has faster computing speeds and lower costs compared to conventional microprocessors [37]. It is hoped that these transputers will allow faster and more complex control algorithms to be implemented on the VGT.

The computer can solve the forward/inverse kinematic problems to control the movement of the VGT. The A/D boards also have the capacity for output. These boards output a voltage which, after amplification, supply the necessary current and power to the motors. Two types of amplifiers were considered, namely, pulse width modulation (PWM) and conventional linear operational amplifiers.

Amplifiers

Amplifiers take a DC reference signal, in this case from the computer, and increase the power by supplying current. Pulse Width Modulation (PWM) is running, in essence, a DC motor with AC current. With no input the PWM system outputs a current which alternates at such a high frequency (usually 5 to 20 kHz) that the motor does not move. To move the motor the PWM system produces a longer wave for the top half phase and a shorter wave for the bottom half phase.

PWM has a very fast rise time, no drift, and is said to help remove the effects of deadband and other nonlinear effects. PWM is also noisy (audio and electrical) because of the high frequency, high current pulses that drive the motors. The continuous AC current supplied to the motor can lead to power dissipation problems and motor overheating. Modeling PWM is also troublesome [38].

Conventional linear amplifiers are readily available, easy to operate and are used in most equipment of this type. For these reasons, this type of a system linear amplifiers were chosen.

3.4.2 Position Instrumentation

In order to control the truss with any degree of accuracy, the variable link lengths must be measured. There are many ways to measure length. Several measurement techniques were considered for possible use in the VGT. Each of the candidates is briefly discussed below.

Linear position transducers (potentiometers or encoders) were not chosen because they would have to be at least as long as the range of motion of the actuated longerons, usually twice as long. They are bulky compared to other transducer designs, and may interfere with truss motion. In addition they are expensive. These are used successfully on some other trusses such as the NASA truss in the Controls-Structures Interaction Lab. However, this truss has a very limited range of motion.

Rotary position transducers (rotary potentiometers or encoders) are less bulky, but if they are driven directly by the lead screw they would have to be able to turn through 200 revolutions. If driven directly by the motor, they would require 4,000 turns and would not indicate any backlash in the gearhead.

Relative encoders were ruled out because of the need for a home position from which to base the measured position. Following a power outage or a shutdown,

the truss could break trying to find the home position. A home position would be unnecessary if we never turned the encoders off, but this is impractical.

Absolute encoders are good, but most rotary encoders are only good for one revolution. One idea addressed was to have two (rotary) absolute encoders. One would measure up to one revolution, and the other would be geared down in such a way that it would measure up to the full stroke. An overlap would be necessary but this may lead to problems when the fine resolution 8-bits do not agree with the low (over overlapping) bits on the coarse measurements. Logic circuits would be needed to avoid this problem, one for each motor. Encoders also have the problem of many wires. If there were two encoders per actuator and 8 bits per encoder for 21 motors that is $2 \times 8 \times 21 = 336$ data wires plus power and ground just for the position transducers.

The final design avoided many of the above-mentioned problems by using a worm/worm-gear pair on the lead screw. This reduced the full stroke of the lead screw to less than ten turns of a shaft. Any backlash in the gearhead or shaft coupling would not be measured and would not introduce error into the measurement. The lead-screw nut will have some backlash, but this part supports large loads that rarely change direction so it would rarely be seen. The backlash in the worm can be eliminated if the worm gear is lightly loaded with a spring. The shaft of the worm gear is connected to a simple ten-turn potentiometer.

3.4.3 Velocity Feedback

Velocity feedback provides another state to measure in addition to position, and this results in more precise control of the truss. Linear velocity transducers are bulky and expensive. Tachometers on the motor (really a low noise generator) work very well and are inexpensive and small. They give good resolution when mounted on

the motor, because voltage is a function of speed. Recall that the motor rotates faster than lead screw because of the gearhead, thus producing more voltage.

3.5 Joint Design

Although mathematically describing the double-octahedral VGT is not very difficult, building one can be. The main problem is joint design. Theoretically, the joints on the VGT are spheric joints so that no moments can be transmitted between links. In the double-octahedral VGT, six links must meet at a single point in space. It is obviously a problem having enough spheric joints to connect these link all centered on the same point. There are several designs to get around this problem. Two of these can be found in NASA's truss and the truss built at VPI&SU. The designers at VPI had the definite advantage of having the NASA truss to improve on.

3.5.1 Nasa Design

In February 1986, the NASA Langly research center loaned a two-bay (four-cell) double-octahedral VGT to Dr. Harry Robertshaw at VPI&SU. This truss had been developed by Mr. Marvin, D. Rhodes and Martin M. Mikulas, Jr. to test space structure deployment concepts. A photo of this truss is shown in Fig. 1.3 in Chapter 1.

NASA solved the joint design problem by noting that not all of the mobility given by six spherical joints is needed if all the links are not actuated and if some moment transmission from link to link can be allowed. Because the three actuators define a plane, we can use revolute joints with axes perpendicular to this plane (the actuator plane) to constrain them.

All the longerons are restricted to be one length, and none may be actuated. As was used in the kinematic solutions in Section 2.3.2, then the two longerons in

one octahedron that meet at the joint can be considered as one link, as shown in Fig. 2.9. One spherical joint (ball and socket) can be used to connect both longerons to the joint itself.

Now, each joint has been simplified into one revolute joint and two spheric joints. If we offset the spheric joints perpendicularly from the longeron plane, the joint can be built, but a strong spheric joint with a large range of motion is hard to find or make. Also, this offset introduces a small bending moment into the component connecting the offset joints. For this reason, the offset should be as small as possible. The offset allows the truss to collapse without link interference.

Again, if only every other set of battens is actuated, then symmetry exists on either side of the actuators, as shown in the inverse kinematics (Section 2.3.3). The sockets for the spheric joints can be one part. Furthermore, if this part can rotate about the axis of the revolute joint (by adding another revolute joint), the spheric joint will not need to revolve about the axis perpendicular to the plane of actuators. If we eliminate this motion in the spheric joint, it can be made much stronger. The kinematic model of this joint is shown in Fig. 3.9.

The joints connecting the battens and longerons are much simpler than the actuator-longeron joints. Since the batten frame is a structure, no joints are needed in it. In the 3-RSSR kinematic model of the VGT, there is a revolute joint along the batten axis connecting each longeron triangle in one octahedron to the batten frame (see Fig. 2.10 (a). In this model, two longerons were considered one kinematic member, see Fig. 2.9 (a). In the NASA truss, each longeron is connected to the batten frame by a similar revolute joint at either end of the batten. The only difficult part is designing the joint for no interference between the twelve longerons and three battens coming together (see Section 4.7).

The NASA truss has served us very well at VPI&SU, but we have noted some

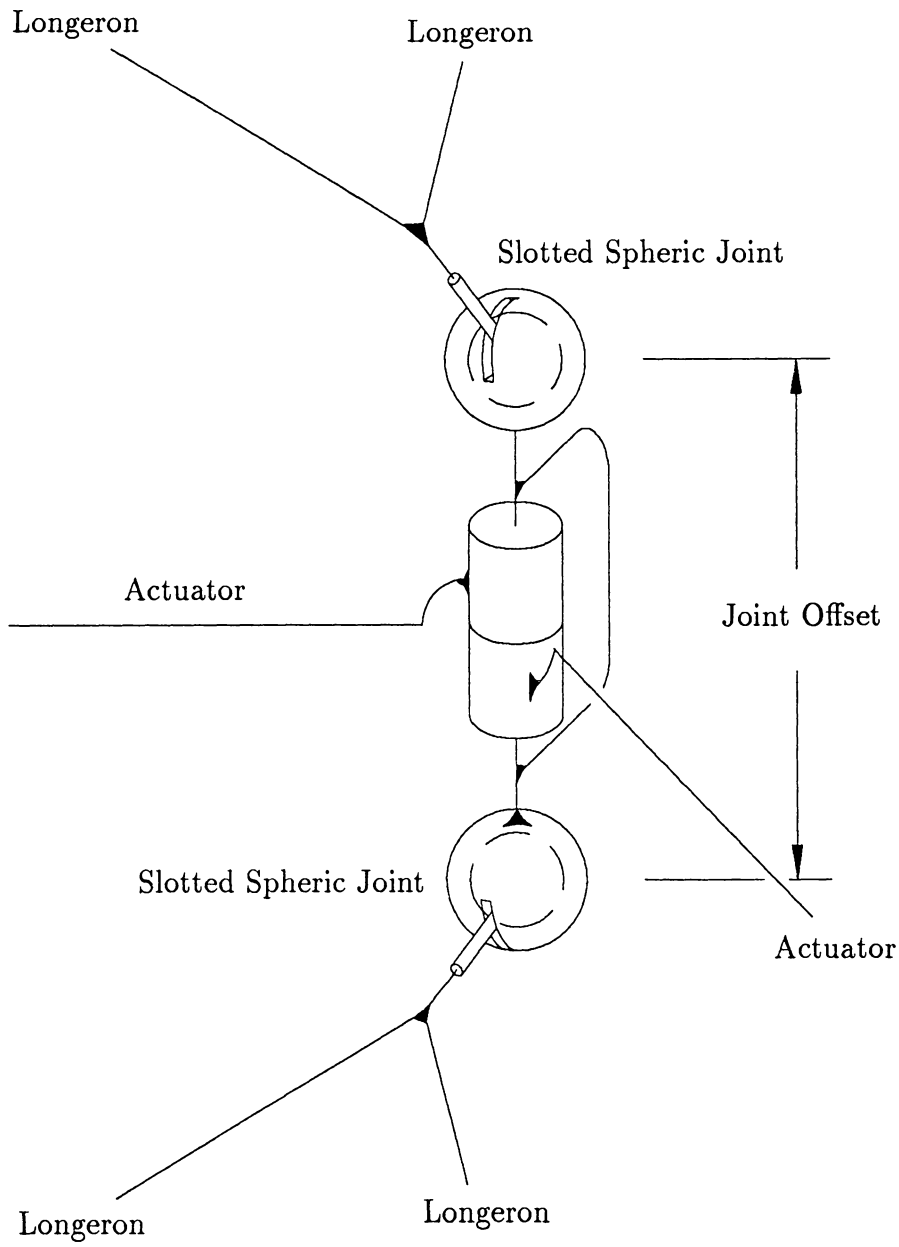

Figure 3.9: Kinematic Model of VGT Joint Built by NASA

problems. There is a singularity at full extension of the truss. The socket in the actuated plane joint can rotate freely when the truss is at full extension. If it rotates, it can break as the truss moves away from the singularity. This problem is moot in the NASA truss because the actuators will not allow the truss to get to full extension. However, if a fully-extending truss is to be built, this becomes critical.

Another problem is that, the truss has a small range of motion. The truss was originally built to test the joints, and the motors were added later. The truss has served well as a vibrational control test article, but has limited utility as a manipulator. Also, after much use controlling vibrations, one of the joints failed due to fatigue.

3.5.2 VPI & SU Design

A different joint design was developed here at VPI&SU as shown in the kinematic model in Fig. 3.10. A photograph of this joint is shown in Fig. 3.11. We retained the joint offsets used in the NASA truss, but changed the spherical joint (which connects the longerons to the actuators) into a universal joint (Hooke's coupling). The actuators are still constrained by revolute joints. Since this design uses only revolute joints, it is stronger, simpler, and less expensive to manufacture.

Motor and instrumentation integration is a fundamental part of the design procedure and is to be considered while designing the joint. As in the NASA truss, only every other set of battens is actuated because actuating every plane causes structural and control problems. Also, the motors are placed on the outside of the actuators to increase their range of motion and for easy motor maintenance.

For revolute joints to behave as spheric joints the axes of the revolute joints must intersect. This prevents the joints from transmitting any moments. The joint offset violates this principle, so to minimize the moment it carries, its length must

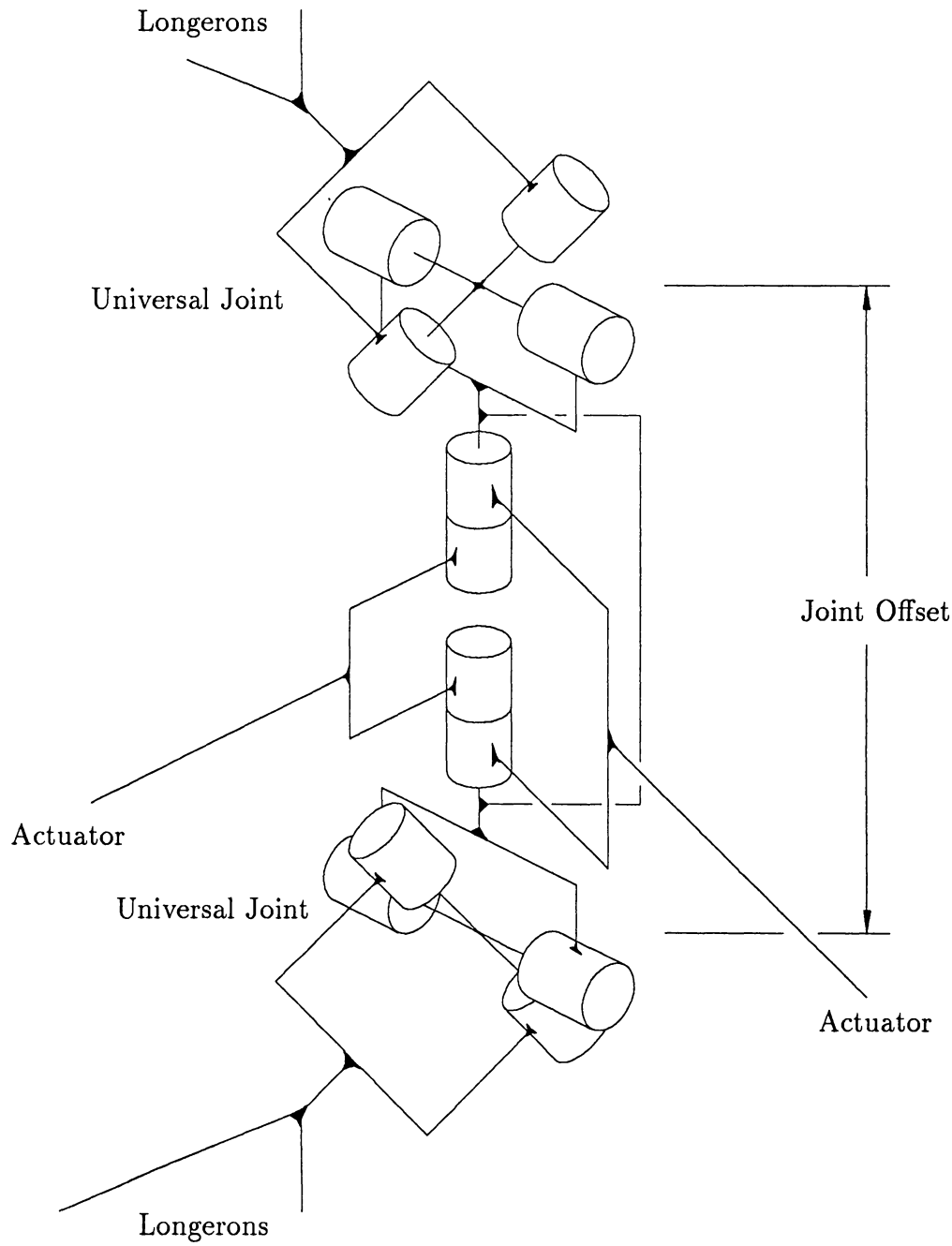

Figure 3.10: Kinematic Model of VGT Joint Design Developed at VPI&SU

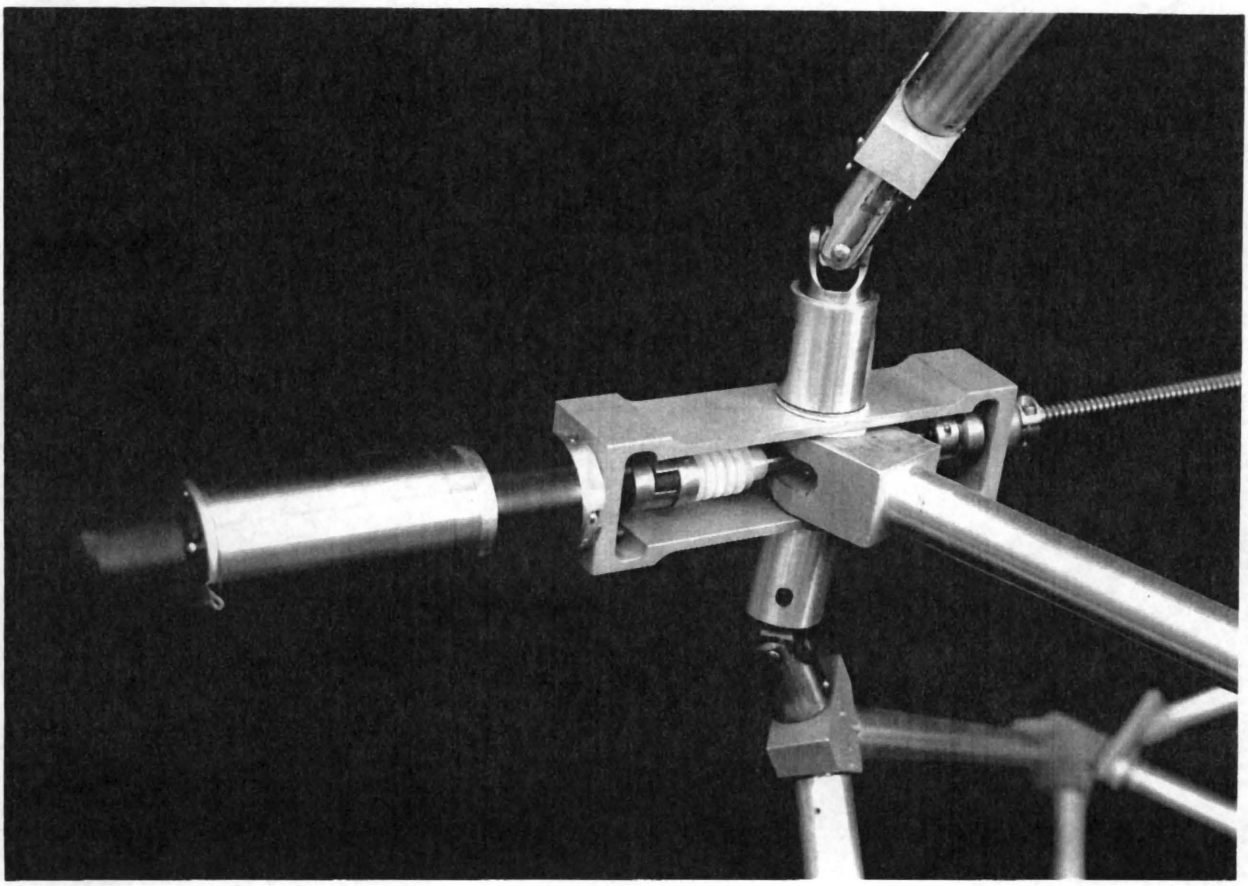

Figure 3.11: Photograph of Joint Design for Double-Octahedral VGT Built at VPI&SU

be minimized.

For strength, and for demonstrating truss concepts, the longeron tubes should be (or appear to be) two-force members. It is hoped that, this VGT will serve our research needs for many years to come.

Chapter 4

Hardware Design and Selection

This chapter discusses the design of the actual machined hardware of the VGT and reasons for choosing certain purchased parts for the VGT. Most of these decisions were based on rational design criteria, but, as with all design processes, some decisions were based on intuition and engineering judgement.

Because this truss is the first prototype of its kind, looks and functionality were both important. Joints or assemblies that looked exceedingly complicated could hinder further research interest in this area.

Although similar in concept, two distinctly different bays have been designed for the seven-bay VGT. The two types will be referred to as the "light" and "heavy" type bays. Four light bays will be supported by three heavy bays. Therefore, the loads in the heavy bays will be substantially higher. These bays are designed with larger cross-section links and more substantial (heavier) joints, and they accommodate larger, more powerful motors. Much design work was completed on light bays first. These design concepts will then transferred to the heavy bays as often as possible. Before construction of the seven bays, one light bay was built to test the design concepts. This thesis deals primarily with this test article.

4.1 Dimensional Choices

In Section 3.1, it was shown that a ratio of B/h of 2 would produce a truss that could nearly reach the full extension and full collapse positions. With this in mind, we proceeded to select the absolute dimensions of the VGT.

The Controls-Structures Lab is over 14 ft (4.3 m)[1] tall and the final truss is to have seven bays. A 1 ft (30.5 cm) per cell height was chosen, permitting the VGT be able to reach full extension. These dimensions were also chosen so that the VGT could be carried around in the back of a station wagon or van.

4.2 Finite Element Analysis

In order to design the elements of the VGT, the forces that these elements must hold needs to be known. These forces are a function of the weight and the orientation of the, as of yet, undesigned parts. To do the analysis, part weights were assumed and forces calculated. Then, with a better idea of the forces, the parts were redesigned and new forces calculated.

In order to do force analysis on the truss, a finite element model of the truss was developed. ANSYS was selected as the finite-element analysis code [39]. The joint offsets were assumed to be zero so that three-dimensional truss elements could be used. These elements can only support axial (tension and compression) loads and no bending loads.

The locations of the nodes in a three dimensional Cartesian coordinate system were generated by a inverse kinematic solving program developed by Robert Salerno [32]. Another program was then written to generate an ANSYS input file from this data. It is important to recognize the complexity of this process and to realize

[1] English units are the primary units used in this thesis because much of the purchased hardware is sized with it. SI units are given in parentheses

that further work is needed in this area. Since the truss changes geometry, each new position and load case dictates a complete reanalysis. The work done to date represents only a small sample of all possible cases.

The position of the VGT has a great impact on the gravitational loads on it. In order for the truss to be useful, it must be able to support itself and a payload over a wide range of orientations. This analysis provided insight on the preferred positions and orientations of the truss.

For this analysis, an operational payload of 50 lbs (220 N) was assumed in addition to the VGT's own weight. A light bay was assumed to weigh 15 lbs (53 N) including motors and gearheads. Thus, a VGT with four light bays and twelve degrees of freedom weighs 60 lbs (260 N).

As a starting point, the VGT was assumed to be positioned with constant bay-to-bay curvature, (ie. the angle between the top and bottom plane of each bay was the same). An analysis for the effect of this curvature of the truss on the forces in the truss was performed. With four bays cantilevered horizontally, a working length was assumed. The radius of curvature was varied, but the truss remained in a plane perpendicular to the gravitational forces. It was found that the forces in the VGT were higher for a configuration straight out than a curved one. This indicates that the double-octahedral VGT supports torsional loads better than it supports bending loads. This makes intuitive sense because the VGT can be viewed as two sets of three helixes. One set rotates clockwise around the truss and the other rotates counter-clockwise as shown in Fig. 4.1.

An analysis was also performed to observe the effect of linear extension and retraction of the VGT on the forces. Again, the VGT was modeled in a horizontally cantilevered position. All actuators were made the same length, and this length was varied. Very high forces due to gravitational loads exist when the truss is close

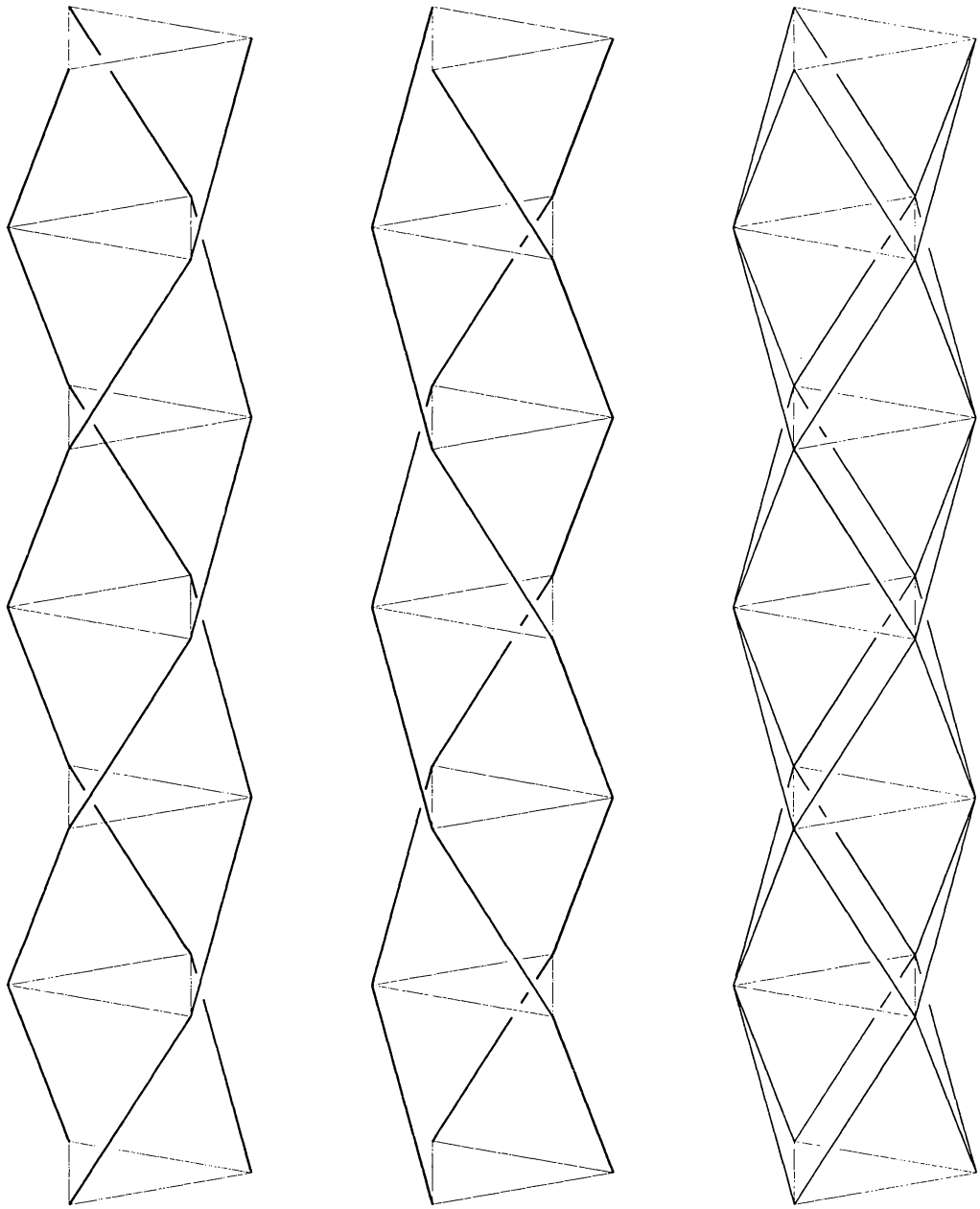

Figure 4.1: Helical Nature of the Double-Octahedral VGT

to its collapsed configuration. Therefore bays carrying high forces should never operate near collapse. If collapse is desired, the outer bays should be collapsed first to minimize the forces on the inner bays before they are collapsed.

The primary result of this investigation was that the highest actuator force in the light bays is 600 lbs (2.67 kN) in the worst case scenario. In most orientations, the highest force was much less than this.

Since vibration control is one of the tasks the VGT will be required to do in the future, a modal analysis was completed on the ANSYS model. The results of this analysis are that the first and second bending and the first torsional modes have frequencies of 6, 40, and 42 hz, respectively. The joints (bushings, backlash) are not modeled so the system frequencies will be different in the actual VGT. Also, the modal frequencies will change with the orientation of the VGT and with the loading. These frequencies will also be different for a VGT with a different number of bays.

4.3 Motor Choices

In order to pick a motor and gearhead, the requirements for torque driving the power screws must be found. The Shigley and Mitchell design text includes a method for doing this [35]. If the lead angle in the lead screw is small, the torque T to raise a load is

$$T = \frac{F d_m}{2} \left(\frac{l + \pi \mu d_m \sec \alpha}{\pi d_m - \mu l \sec \alpha} \right)$$

where

F = force in the lead screw,
d_m = mean diameter of the lead screw,
l = lead,
μ = coefficient of friction,
and α = half thread angle.

For Acme threads $\alpha = \frac{29°}{2} = 14.5°$. For a lead screw diameter of 3/8 in., (0.375 in., 9.5 mm) the mean diameter, $d_m = 0.325$ in. (8.25 mm). The lead, l, is assumed to be 0.1 in (2.54 mm), see Section 4.5.1. The coefficient of friction, μ, was assumed to be 0.3.

The force, F, varies with the choice of motor within the truss and with the truss position and orientation. The worst case force, F, is assumed to be 600 lbs (2.67 kN), based on the previously described finite-element analysis (see Section 4.2). This results in a required torque of 41 in. lbs (4.6 kN m).

A desired actuator rate in the truss would yield a twelve second move from full collapse to fully extension. This is approximately an actuator rate of one inch per second (25 mm/s). To do this the lead screw must turn ten revolutions per second.

Therefore, the worst case power requirements are $T\dot{\theta} = 4.7$ hp (3.5 kW). This indicates that very large motor is needed. Since the first stage of the planned manipulator is to have four bays, a one inch (25.4 mm) motion in the lead screw of the bottom bay produces a large motion in the end of the truss. A more reasonable motion requirement for the bottom bay would be one inch (25.4 mm) per 100 sec. Therefore, a 0.47 horsepower or 35 W motor is needed. This can be supplied by a Maxon RE-Motor (cat # 2434-970-52-225-200). This motor weighs only 1.2 lbs (5.3 N) with a gearhead, but it has a stall torque of 4.1 in. lbs (456 mN m).

Obviously, a gearhead is needed. A 71:1 gear ratio was chosen in order to remain

well below the stall torque. This gearhead will be installed on the lower two bays, while the other two bays which must support lighter forces will use a gearhead with a 27:1 gear ratio.

4.4 Joint Design

Designing the joints for the double-octahedral VGT is definitely the most important part of the design process. After the design for the VGT was completed, a group of undergraduates at VPI&SU developed a CADAM model for a class taught by Dr. Sanjay Dhande [40]. A photograph of a shaded view from this project is shown in Fig. 4.2 (a). A photo of the joint is shown in Fig. 4.2 (b).

4.4.1 Purchased Parts

To save time and cost, most of the parts to build the joints for the VGT were purchased from stock components manufactured by outside sources. The dimensions of these parts are typically limited to a small set, and, once purchased, are fixed. Enough parts were purchased for four bays of this design with some spares.

Shaft Parts

The gearhead shown in yellow in Fig. 4.2 must connect with the lead screw shaft shown in light blue. This is accomplished with a Lovejoy elastomeric coupling, L-035, shown in green and yellow. A flexible coupling was chosen to a allow for minor misalignments. It also enables quick and simple removal of the motor and gearhead because of the jaw type design as shown in Fig. 4.3 (a). Two different jaws were ordered, one with a inside diameter of 1/4 in. (6.35 mm) to fit on the lead screw shaft. The other had a inside diameter of 3/16 in. (4.76 mm) so it could be bored out to five mm (0.197 in.) for the gearhead shaft.

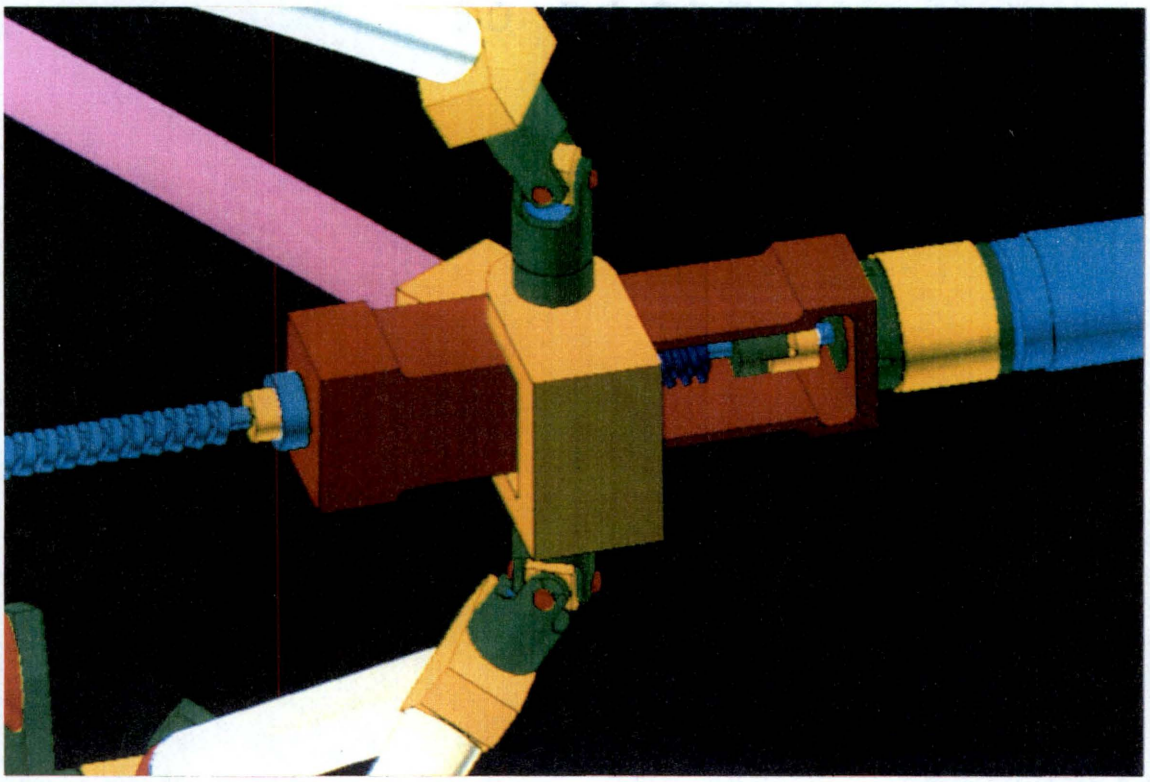

Figure 4.2: Actuator Joint Assembly

a) Flexible Coupling

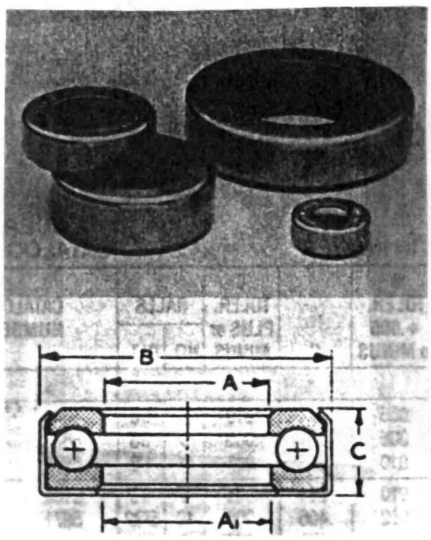

b) Thrust Bearing

c) Clamping Collars

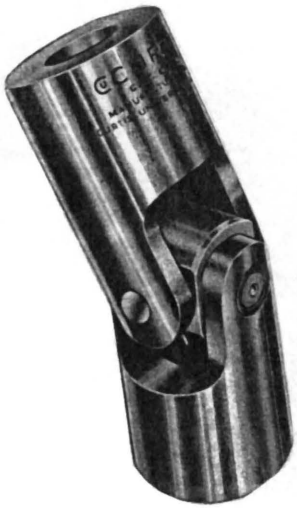

d) Universal Joint

Figure 4.3: Purchased Parts for Joint Instrument Box

The gearheads are not designed to support thrust loads. These loads must be transferred to the structural members of the joint by means of a bearing. Two thrust bearings, shown in light blue in Fig. 4.2, are used per joint; one supports tension, the other supports compression. A ball bearing was chosen over a bearing surface because of the lower friction produced. A Boston 601 (item 50537) thrust ball bearing was chosen to fit on the quarter inch (6.35 mm) lead-screw shaft.

The thrust bearings are held on to the lead-screw shaft with clamping collars shown in yellow in Fig. 4.2. The collars are formed from two C-shaped pieces held together with two screws. The screws are tightened to a recommended torque, and are held in place by friction. If the friction forces prove to be inadequate, the collars can be pinned in place. The collars are stainless steel and were purchased from Boston Gear, cat# 2SSC25 (item 49190) (see Fig. 4.3).

The thrust bearings support no radial forces. A bushing, cat# B46-2 (item 34542), from Boston Gear was chosen to support and guild the shaft. Although this part sees only light loads, it is made of oil-impregnated sintered bronze to provide lubrication. After evaluating the completed prototype truss bay, it was decided that another support may be necessary. This problem will be discussed at greater length in Chapter 5.

Other Joint Parts

One of the main components of the VGT joint is the universal joint as shown in green in Fig. 4.2. The Curtis CJ642 was chosen for its high strength rating and large range of motion. The hubs of these joints were shortened to 3/8 in. (0.375 in., 9.5 mm) to make the joint offset smaller.

Inside the Joint Instrument Box is a fork-shaped piece which connects the next actuator to the joint. A bearing surface is needed between the fork and the joint

box. Since there is a wide bearing area and it supports the weight of the actuators but not any structural loads, a teflon bushing surface was chosen. The teflon is 1/32 in. (0.79 mm) thick and is faced with adhesive on one side.

The bearing surface bushings for pins in the box and in the fork, on the other hand, must withstand much higher forces. Oil-impregnated sintered bronze was chosen for strength.

Instruments

Most of the instrumentation required for controlling the VGT was also purchased. Tachometers were purchased already on the motors. The position instrumentation system uses a worm on the lead-screw shaft which turns a worm gear connected to a ten-turn potentiometer. Finding the proper gears was relatively simple.

The lead screw has a range of 13.75 in. (349 mm) and 10 threads per inch (0.394 threads per mm). Therefore, it has a range of 137.5 revolutions. In order to use the ten-turn pot fully (10 revolutions), a gear ratio of 13.75:1 is needed. In order to buy available parts and be safe and not break the pot, a 20:1 gear ratio was chosen. This ratio will produce 6.875 revolutions on the pot for full range of the actuator. This way, the reference position (zero voltage) can be adjusted over a wide range without danger of breaking the pot by forcing it past its end stops. A 10-turn pot #44F1106 (type 536-2-1-103) from Newark Electronics with a 10 kohm resistance was chosen.

Since the worm and worm gear will have to support very light loads an acetal (plastic) worm was chosen. The worm had a 3/16 in. (0.1875 in., 4.76 mm) diameter hole which was bored out to a 1/4 in (0.25 in., 6.35 mm) diameter hole for the lead-screw shaft. The worm gear was chosen to fit on the pot. The worm and worm gear were purchased from Boston Gear cat# LUHBP (item 54143) and cat# GP1034-1/4

(item 54134), respectively.

As a safety feature, micro-switches will be installed on the actuators. These will disconnect the power to the motor if the lead screw travels beyond a certain point. Ideally, this task could be performed in software on the controlling PC, but it is desirable to have a fail-safe back up system built in. Besides, a software check would slow the computer down.

4.4.2 Joint Instrument Box

Box Concept Design

Integral with the design and selection of the motor, gearhead, lead screws, bearings was the design of a structure to house and support these components. The Joint Instrument Box shown in red in Fig. 4.2 serves these functions. On the screw face of the joint box, a thrust plate is necessary for the thrust bearings to push against. On the motor end, the gearhead needs a mounting plate. The longerons need to rotate on a plate. This gave rise to a box. The back was partially closed to add strength and rigidity. However, a hole was left in the back was for access to the motor mounting screws and for the potentiometer.

Inside the box, the axis of rotation of the fork should be as close as possible to thrust plate for maximum range of motion. Other components can be outboard of this.

Box Designs

Preliminary designs for the box centered on bolting, welding, or silver soldering several plates together. It would be hard to guarantee square corners and high strength with these designs. It was therefore necessary to make the box from one piece of material. The proposed design would be difficult to machine using conventional

methods. As a result, the box was produced on an NC-milling machine. Aluminum 6061-T6 was chosen for the material because of its ease of machining and light weight. The final drawing for the Joint Instrument Box is shown in Appendix A, Fig. A.2. The NC-milling code is shown in Appendix B. A photograph of the box is shown in Fig. 4.4. The width of the Joint Instrument Box was determined by the width of the purchased parts plus clearance necessary for the fork to rotate.

The clearance required by the fork is dependent on the angle it rotates through. As the links move, the fork moves through an angle θ. The maximum angle between two actuators occurs when these are moved to minimum length and the third is at its maximum extension. The other two angles are at minimum θ, as shown in Fig. 4.5 (a). These angles can be found using the Law of Cosines,

$$L_2^2 = L_1^2 + L_3^2 - 2L_1L_3\cos\theta.$$

Assuming $L_1 = L_3 = L_{min}$ and $L_2 = L_{max}$ and that

$$\begin{aligned} L_{max} &= 32.5 \text{ in}, \\ L_{min} &= 18.5 \text{ in}. \end{aligned}$$

Therefore,

$$\theta_{max} = \arccos\left(\frac{1 - L_{max}^2}{2L_{min}^2}\right) = 123°.$$

Because two sides of this triangle are equal, the two corresponding angles are equal. These three angles sum to 180°. Therefore,

$$\theta_{min} = (\theta_{max} - 180)/2 = 28.5°.$$

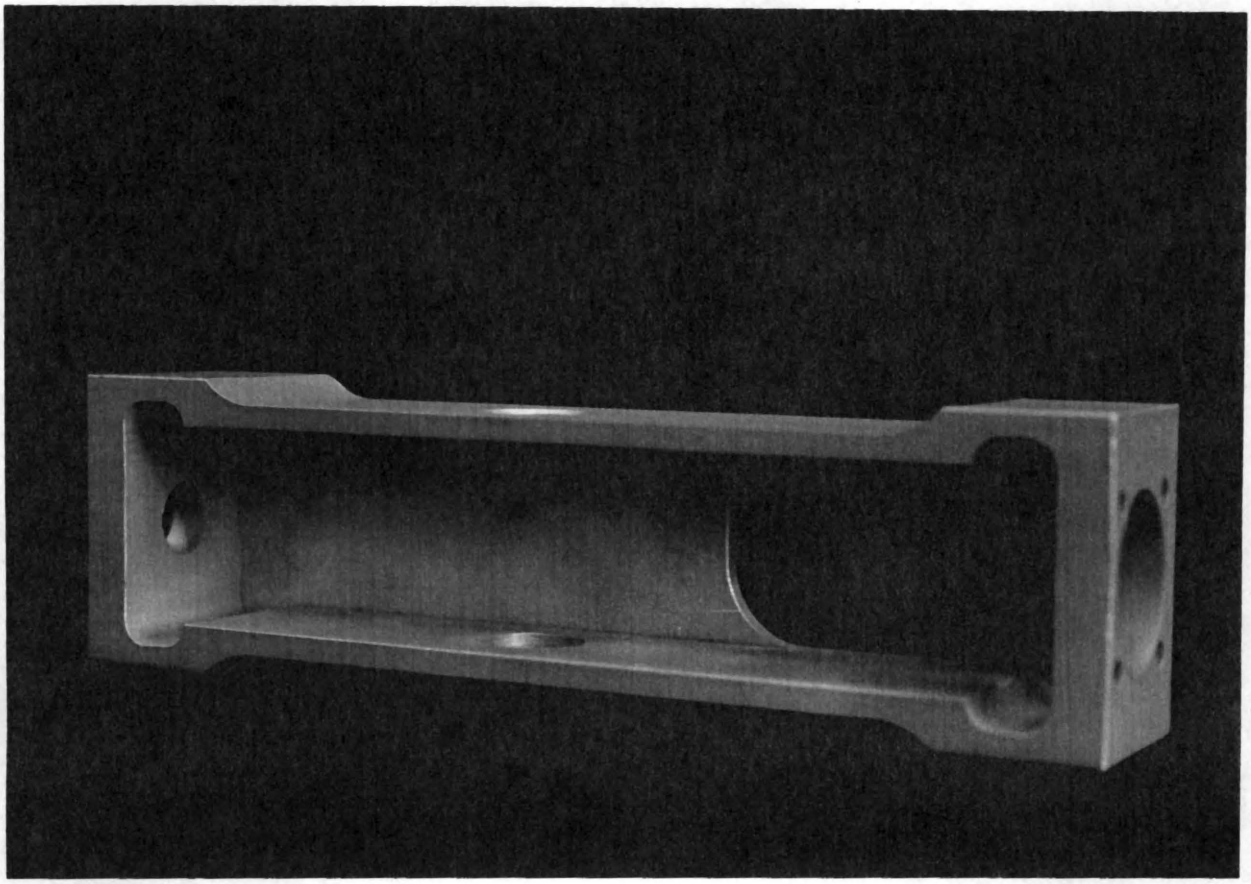

Figure 4.4: A Photograph of the Joint Instrument Box

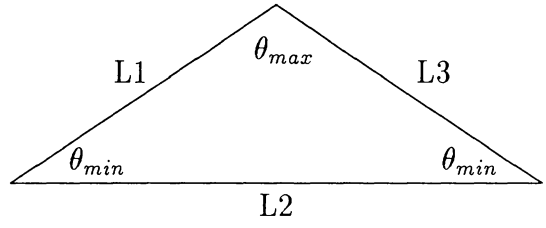

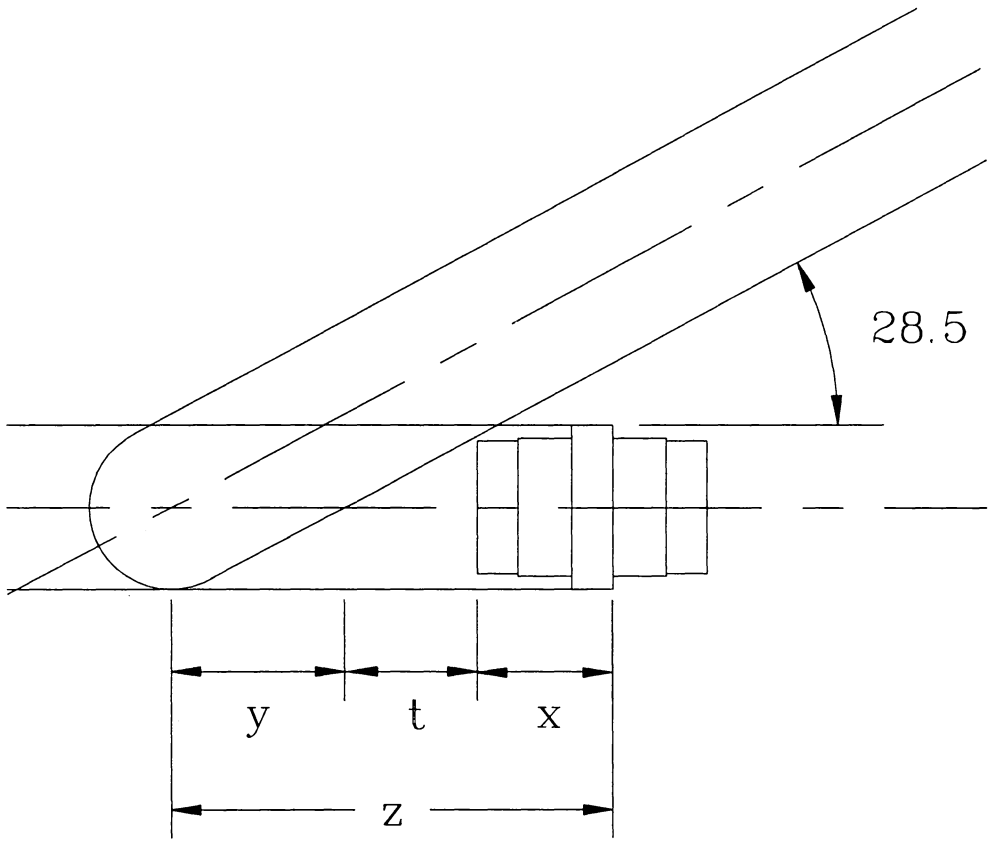

Figure 4.5: Joint Instrument Box Sizing

The fork mounting hole must be far enough from the clamping collar not to interfere. Now, if the fork is assumed to be 1 in. (25 mm) wide, this distance as shown graphically in Fig. 4.5 (b) can be found;

$$z = y + x + t$$

and

$$z = \frac{1}{2\sin\theta_{min}} + \frac{13}{32\tan\theta_{min}} + \frac{61}{64} = 2.75\text{in (70 mm)}$$

Therefore, the hole for the fork must be 2.75 in. (70 mm) from the edge of the trust plate. The fork itself will take up another 0.5 in. (13 mm).

$$t = \frac{3}{8} + \frac{21}{64} + \frac{1}{4} = \frac{61}{64}$$

The fork will not interfere with the worm when $\theta = 123°$ because the hub on the worm is so small. The height of the Joint Instrument Box is determined by the gearhead mount. The other purchased parts of the box are smaller. 1 in. (25 mm) inside leaves barely enough room for the heads of the mounting bolts.

4.4.3 Design of C-Bracket

The C-Bracket is shown in yellow in Fig. 4.2 (a) and in Appendix A, Fig. A.6. It holds the two universal joints together and rotates with them. It rotates as the actuators move. It was designed such that it did not interfere with the Joint Instrument Box.

Teflon bushings are used between the C-Bracket and the joint instrument box.

These are the same as those between the joint instrument box and the Actuator Fork. They are cut to fit and stuck in place.

Two pins extend from inside the U-joint through the Joint Instrument Box into the fork, as shown in Fig. A.17. These allow independent rotation between the C-Bracket, Joint Instrument Box, and the Fork. This rotation occurs on bronze bushings located in the top of the Joint Instrument Box and in the Actuator Fork.

4.5 Active Batten Design

4.5.1 Lead Screw

The workspace of the VGT manipulator is determined by the range of motion of the variable-length members. Ideally, we would like to go from zero length to the maximum (where the truss collapses), but this would be difficult to construct (having two complete joints at the same place).

The lengths of the elements of the actuators as shown in Fig. 4.6 can be considered as variables. At collapse, the actuator is at its maximum length $L = L_{max}$. Summing the parts of the actuator. $L_{max} = A + C + N + G + F$. At $L = L_{min}$, the actuator is at its shortest length. $L_{min} = A + N + G + F$ and to insure that the lead screw does not extend through the Actuator Fork $G + F >= C + E + D$.

Now, from the designed components,

$$A = 3.45 \text{ in. } (88 \text{ mm}) \tag{4.1}$$

$$E = 0.75 \text{ in. } (19 \text{ mm}) \tag{4.2}$$

$$F = 1.375 \text{ in. } (35 \text{ mm}) \tag{4.3}$$

$$N = 1.125 \text{ in. } (29 \text{ mm}), \tag{4.4}$$

$$\tag{4.5}$$

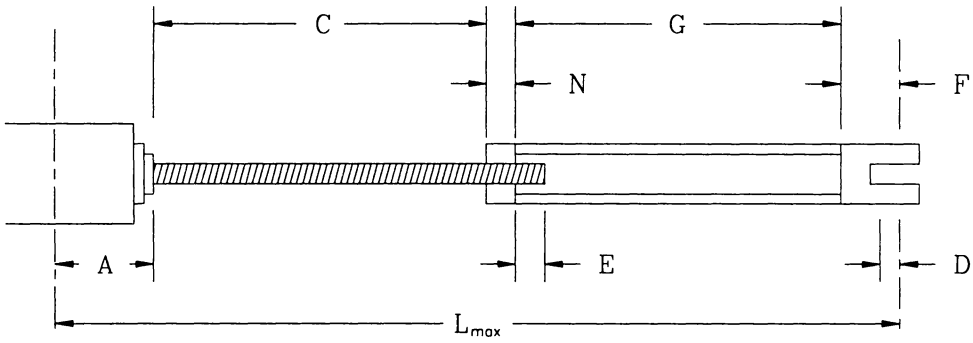

Fully–Extended Actuated Batton

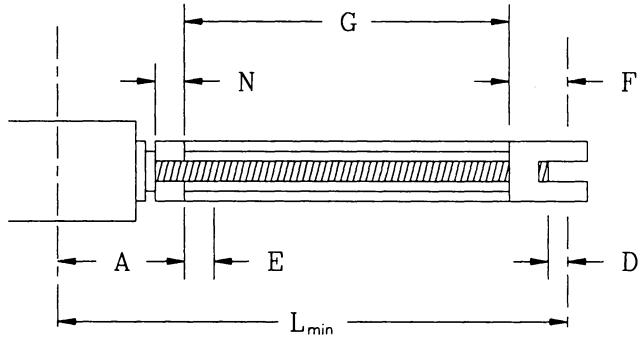

Fully–Retracted Actuated Batton

Where,

A = Offset of joint instrument box
C = Lead-screw stroke length
D = Clearance between lead-screw end and fork pivot
E = Extra lead-screw length
F = Length of actuator end plug (fork)
G = Tube length from nut adapter to actuator end plug (fork)
N = Length of nut and nut adapter
L = Actuator length (variable)

Figure 4.6: Actuator Schematic

and assuming $D = 0.5$ in. (13 mm) $L_{max} = A+C+N+G+F$ therefore $C+G = 26.55$ in. (674 mm).

In order to get to a height of 4 in. (102 mm), $L_{max} = 32.5$ in. (825 mm). In order to get to a height of 18.75 in. (476 mm), $L_{min} = 18.75$ in. (476 mm). Therefore, the tube length $G = 12.8$ in. (325 mm), and the lead-screw stroke length $C = 13.75$ in. (349 mm).

The lead screw must also support high forces. The mode of failure for a long slender member like this is typically buckling in compression. Buckling analysis was performed assuming the lead-screw assembly was one long steel rod with a diameter equal to the inner thread diameter of the lead screw. This is a conservative model except for deformation of the nut and whirling of the screw, which were neglected. The ends of the actuator are ideally spheric so they are modelled as pinned. The length is assumed to be the longest possible for the actuator.

Assume no end moments applied to the ends of the actuator, *Euler's formula* for buckling is

$$P_{cr} = \frac{\pi^2 EI}{L_e^2}$$

where

P_{cr}	=	Load	
E	=	Modulus of Elasticity	10.3×10^6psi
I	=	Moment of inertia	$1/4\pi r^4$
L_e	=	Length	48 in. (1219 mm)
r	=	Radius	

Assuming the radius, r, half the inner diameter of the lead screw, is 0.25 in. (6.3 mm), the load P_{cr} is 2,304 lbs (10.2 kN). This is almost four times the maximum

actuator force of 600 lbs (2.67 kN).

4.5.2 Lead Screw Nuts

The nuts for the lead screws were purchased from a company called Techno. The nuts are threaded on the outside to facilitate connection. They offer two materials Turcite^r X(Actetal - Teflon and Silicone filled) and bronze (SAE 660). Some of both were purchased. The plastic nut (Cat# HB21SN-37101) performed much better than the bronze nuts (Cat# HB20BN-37101) but have a lower strength. The bronze nuts were also of poor quality (tolerances).

4.5.3 Design of the Nut Adapter

These purchased nuts must be connected to a piece of tubing. This is accomplished by the Nut Mounting Adapter, as shown in Fig. A.3. This part threads on to the nuts and is fastened to the tube. Because the lead screw must travel threw the nut and tube, pinning this joint was not an option.

Welding the nut adapter to the tube was tried but the welders experienced great difficulty because the tube is much thinner than the nut adapter. The welded joint also must be heat treated after welding, or it will be much weaker that the surrounding metal. Jerry Lucas suggested using three small screws placed 120° apart to make the connection. This design was tested and deemed satisfactory. It is recommended and will be used on the next four bays.

4.5.4 Tube

The Nut Mounting Adapter and Fork are connected by a length of tube. This tube was sized with a buckling analysis like the one for the lead screw. For reasonably sized tubes, the critical load is much higher than that of the lead screw. For this

reason, the tube dimensions were choosen based on availiblity and cost. A stock diameter of 0.75 in. (19 mm) and a wall thickness of 0.049 in. (1.2 mm) were ordered and cut to length 13.125 in. (333 mm). For cost 6061-T6 was chossen for the material. The tube is shown in Fig. A.5.

4.5.5 Fork

The fork allows the actuator to rotate with respect to the next actuator. The fork also must not interfere with the shaft in the next actuator which connects the gearhead to the lead screw.

The fork is connected to the actuator tube by the same three screws system used with the nut adapter. The Fork width was choosen to be 1 in. wide to support torsional loads on the actuator. The height of the fork is the inside dimension of the joint instrument box less enough space for the teflon bushings. This left 0.9375 in. (23.8 mm) of material.

An inside space of 0.3125 in. (7.9 mm) was cut through the fork to clear the lead-screw shaft. As the actuators move, the shaft rotates. In order that there be no interference, the slot must be cut at an angle. These are the same angles calculated in Sec. 4.4.2 on Fig. 4.5.

4.6 Longeron Design

The longerons connect the universal joint to the battens. The main structural part of the longerons is an aluminum tube. To make the VGT look good and for simplicity, this tube is the same (wall thickness and diameter) as the tube used in the actuator although it carries less load.

These tubes must be connected to the universal joint. Several methods of joining these thin walled tubes to something were examined. Welding was not used for the

same reasons as in Sec. 4.5.3.

4.6.1 Longeron Junction Block

Ideally the longerons should be two force members (at least the tubes). Also, the longerons should appear to be two force members because that is the T part of VGT. Therefore, the center line of the tubes should lie along the line from the corner of the batten frame triangle to the center of the U-joint.

The tubes are plugged to allow connection with two rolled pins (or three screws). These plugs extend into a block shown in Fig. A.9. This is the longeron junction block which has a hole to allow the U-joint to be inserted into it and pinned. The assembly is shown in Fig. A.11.

On the other end of the longeron tube is another plug shown in Fig. A.12. This plug has a diagonal end. This plug is bolted to the batten frame joints on this diagonal face. This is discussed in more depth in the next section.

4.7 Batten Frame and Joint Design

The batten frame joints are much simpler than the actuator plane joints. Twelve longerons come into each plane. These form simple revolute joints with the batten frame. The axes of the revolute joints is along the battens.

The only problem building these joints is eliminating possible interference between the longerons. Interference can occur between longerons from two adjacent bays at full collapse of the truss. This problem is eliminated if the longerons are designed to reside above the plane of the battens frame as shown in Fig. 4.7(a). During sharp bends, longerons can actually go below the batten frame plane, but this interference problem must be dealt with in the control environment. Interference can also occur between neighboring longerons of the same bay at full extension

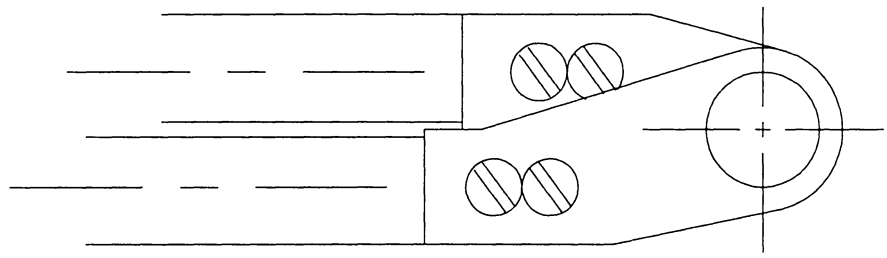

Cross Longerons from Two Adjacent Bays
Viewed Looking Down the Unactuated Batton

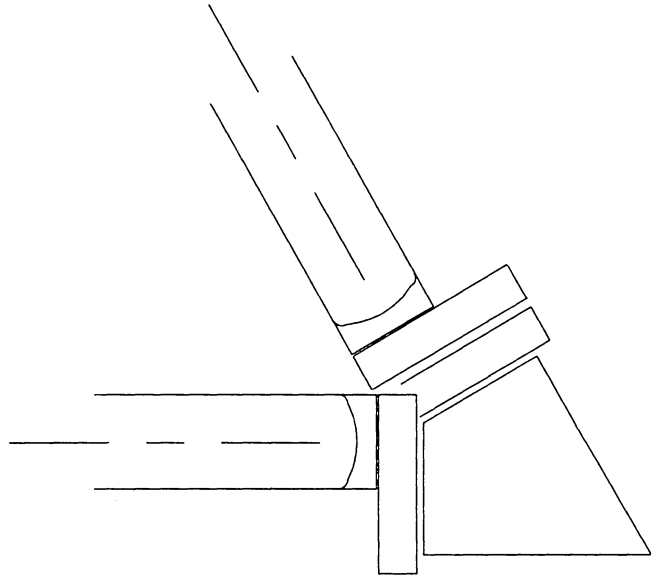

Cross Longerons from the Same Bay
Viewed Normal to the Base Plane

Figure 4.7: Batten Joint Limits

(see Fig. 4.7 (b)).

The longerons connect to these joints by bolting on to ear shaped plates. Two different plates were designed shown in Figs. A.12 and A.13. One plate must be longer than the other because this plate attached to the batten further from the end.

Batten Corner (shown in Fig. A.16) the two battens together. This is accomplished by pinning it to a shaft. The shaft is shown in Fig. A.17. The ear shaped plates rotate on this shaft. Three oil-impregnated sintered bronze bushings enable smooth rotation at this point. Two bushings are flanged type (Boston Gear cat# FB46-2 item 35526) to support axial and radial forces. The third is a flat thrust bushing (Boston Gear cat# TB410 item 35766) used between the two ear shaped plates. The shaft is pinned through a plug and into the batten tube. This assembly is shown in Fig. A.18 and the Batten Frame in Fig. A.19.

4.7.1 Batten Tube

The same tube was used for the battens as the longerons and actuators. The batten will not see as heavy a load and has no mechanical interface in the middle. The same 0.75 in. (19 mm) tube was used to keep the cost of the truss down.

4.8 Summary

After all the parts and manufactured, the truss can be assembled. This takes much care. Then the motors and instrumentation is added. Cables must be run down the longerons to the base. The truss now can function as a manipulator.

Chapter 5

Conclusions

5.1 The VPI&SU Double-Octahedral VGT

5.1.1 Problems with the VPI&SU VGT

The main structural problems with the double-octahedral VGT designed and built at VPI&SU exist when the actuators are in compression. The lead-screw nut must resist buckling. The bronze nuts purchased from Techno are slightly larger than the lead screw itself. Furthermore, the threaded hole is not concentric with the mounting threads. These tolerance problems enable the lead screw to wobble while being run by the motor. The Turcite nuts do not show these symptoms under the light loads. However, the Turcite nuts have neither been tested under heavy loads, nor are rated to hold them. This problem is not helped by the fact that many of the lead screws arrived slightly bent.

When an actuator is in compression, the joint instrument box is also in compression. Buckling between the shaft and box must be resisted by a couple produced by a 1/4 in. (6.3 mm) bushing in the thrust plate and the gearhead. The actuators are in compression when the bay is in tension, torsion or bending. If the truss is loaded in bending such that the truss deforms with a concave upward curvature, then the upper actuators, or battens, is in compression.

Another problem exists with the double-octahedral VGT as designed by VPI&SU. If several bays are connected together to form a long chain manipulator, this manipulator can not twist. Therefore, the angle of rotation about the normal vector on the top batten frame plane cannot be controlled. A two bay double-octahedral VGT has six degrees of freedom, but it can control only five parameters of the end effector, the location of the plane of the last set of battens (three parameters) and a position in this plane (two parameters). The rotation of an object in this plane is fixed. This is not problem because most end effectors have several degrees of freedom and having a rotation in this direction is easy.

5.1.2 Design Changes and Recommendations

Manufacturing longer nuts and/or nuts with tighter tolerances will help the problem at that point. Another shaft support is needed in the joint instrument box. This need could be fulfilled with another 1/4 in. (6.3 mm) bushing mounted between the shaft coupling and the worm.

More possible design changes can be made on the "heavy" bays. The joint design with the screws sticking out could be used here. This would allow a different joint design to be built and tested.

A joint with no offset would eliminate the bending moment placed on the actuators and would resist motor torques much better. If one could be designed, it would greatly enhance the load the truss could manipulate.

5.2 VGT Applications

The truss has many applications which can be divided into two classifications. One is using two bays with one plane of actuators as an improved "gimbal," a two-degree-of-freedom joint. This is an actuated joint which allows motion similar to a universal

joint. It can be used for pointing radio antennas, and solar arrays and anywhere that a two rotations are needed. It has the advantage that it is structurally rigid if the motors lose power or fail. It is high-strength, highly-rigid, and low-weight. The inverse kinematic problem of controlling two degrees of freedom with three has been solved by Babu Padmanabhan [28].

The other application is manipulators with very high degree of dexterity which could retract into a small space. Several bays can be chained together to create a very nimble robot arm. This could be used for reactor maintenance where moving around in tight curved passages is very important. This also could be used as a space crane to move material and people around in space without using propellant.

5.3 Future Variable Geometry Truss Work

Although some work has been completed in this area, more work in the structural analysis of VGT as a function of actuator position needs to be done. Also, a structural analysis as a function of dimensional analysis would be quite helpful in the future.

The assumption of equal longeron lengths is not necessary. An interesting design can be made by lengthening every other longeron until it makes a right angle with the battens and actuators. Therefore the longeron triangle will be a right triangle with short sides formed by the batten and one longeron. The hypotenuse would be the longer longeron.

This configuration in similar to the the longeron truss shown in Fig 2.3 b. Intuitively, it seems stronger in bending than an octahedral VGT with equal longerons. If symmetry of the upper and lower octahedrals is sacrificed, this configuration allows for twist.

Just as serial robots are constructed with different types of joints (revolute and

prismatic), VGT's can be made from different unit cells and combinations of unit cells. These unit cells may be designed with different actuator schemes and with different relative dimensions.

The definitive work on variable geometry trusses needs to be written. All possible unit cells need to be defined and named. Mobility equations specifically for VGT's need to be developed. These could be in terms of links or faces of geometric elements.

Bibliography

[1] Mabie, H. and C.F. Reinholtz, **Mechanisms and Dynamics of Machinery,** J. Wiley and Sons, New York, 1987.

[2] Craig, J.J., **Introduction to Robotics, Mechanics and Control.** Addison-Wesley, Reading, Mass., 1986.

[3] Stewart, D., "A Platform with Six Degrees of Freedom," *Proceedings of the Institute of Mechanical Engineers,* Vol. 180, Part 1, No. 15, 1965-1966, pp. 371-386.

[4] Hunt, K.H., **Kinematic Geometry of Mechanisms,** Oxford, Great Britain, 1978

[5] Fichter, E.F. and E.D. McDowell, "A Novel Design for a Robot Arm" **Advances in Computer Technology,** ASME Publication, 1980 pp. 250-256.

[6] Yang, D.C.H. and T.W. Lee, "Feasibility Study of a Platform Type of Robotic Manipulator from a Kinematic Viewpoint," *Transactions of the ASME Journal of Mechanisms, Transmissions, and Automation in Design,* Vol. 106, No. 2, June 1984, pp. 191-198.

[7] Fichter, E.F., "A Stewart Platform-Based Manipulator: General Theory and Practical Construction," *The International Journal of Robotic Research,* Vol. 5, No. 2, Summer 1985.

[8] Sugimoto, K., "Kinematic and Dynamic Analysis of Parallel Manipulators by Means of Motor Algebra," *Transactions of the ASME Journal of Mechanisms, Transmissions, and Automation in Design,* Vol. 109, No. 1, March 1987, pp. 3-7.

[9] Hunt, K.H., "Structural Kinematics of In-Parallel-Actuated Robot Arms," *Transactions of the ASME Journal of Mechanisms, Transmissions, and Automation in Design,* Vol. 105, No. 4, December 1983, pp. 705-712.

[10] Sklar, M. and D. Tesar, "Dynamic Analysis of Hybrid Serial Manipulator Systems Containing Parallel Modules," *Transactions of the ASME Journal of Mechanisms, Transmissions, and Automation in Design,* Vol. 105, No. 2, June 1988, pp. 109-115.

[11] Waldron, K.J., M. Raghavan and B. Roth, "Kinematics of a Hybrid Series-Parallel Manipulation System," *Journal of Dynamic Systems, Measurement, and Control,* Vol. 111, June 1989, pp. 211-221.

[12] Jain, S. and S. Kramer, "Design of a Variable Geometry Robot Based on an n-Celled Tetrahedron-Tetrahedron Truss," 1988 ASME Design Technology Conference Proceedings, Kissimmee, Florida, DE Vol. 15-3, pp. 119-123. Mechanism or Design March 1988

[13] Card, M.F. and W.J. Boyer, "Large Space Structures - Fantasies and Facts," *Proceedings of AIAA/ASME/ASCE/AHS 21st Structures, Structural Dynamics and Materials Conference,* Part 1, May 1980, Seattle, Washington, AIAA-80-0674-CP.

[14] Dorsey, J.T., "Vibration Characteristics of a Deployable Controllable-Geometry Truss Boom," NASA Technical Paper 2160, June 1983.

[15] Mikulas, M.M. Jr., R.C. Davis and W.H. Greene, "A Space Crane Concpet: Preliminary Design and Static Analysis," NASA Technical Memorandum 101498, November 1988.

[16] Utku, S. et al., "Control of a Slow Moving Space Crane as an Adaptive Structure," *Proceedings of AIAA/ASME/ASCE/AHS/ASC 30th Structures, Structural Dynamics and Materials Conference,* Mobile, Alabama, April 1989. pp. 1119-1126. JPL D-6193

[17] Das, S.K., S. Utku and B.K. Wada, "Inverse Dynamics of Adaptive Structures used as Space Cranes," Jet Propulsion Laboratory report JPL D-6489, June 1989.

[18] Rhodes, M.D. and M.M. Mikulas Jr., "Deployable Controllable Truss Beam," NASA Technical Memorandum 86366, June 1985.

[19] Sincarsin, W.G. and P.C. Hughes, "Trussarm Candidate Geometries," Dynacon Report 28-611/0401, Dynacon Enterprises Limited, 5050 Dufferin Street, Suite 200, Downsview, Ontario, Canada, April 1987.

[20] Sincarsin, W.G., "Trussarm Conceptual Design," Dynacon Report 28-611/0402, Dynacon Enterprises Limited, 5050 Dufferin Street, Suite 200, Downsview, Ontario, Canada, April 1987.

[21] Robertshaw, H.H. et al., "Dynamics and Control of a Spatial Active Truss Actuator," *Proceedings of AIAA/ASME/ASCE/AHS/ASC 30th Structures, Structural Dynamics and Materials Conference,* Mobile, Alabama, April 1989. pp. 1473-1479.

[22] Miura, K., H. Furuya and K. Suzuki, "Variable Geometry Truss and its Application to Deployable Truss and Space Crane Arm," *35th Congress of the International Astronautical Federation,* IAF-84-394, Lausanne, Switzerland, October 1984.

[23] Miura, K. and H. Furuya, "An Adaptive Structure Concept for Future Space Applications," 36th Congress of the International Astronautical Federation, IAF-85-211 Stockholm, Sweden, October 1985.

[24] Nayfeh, A.H., "Kinematics of Foldable Discrete Space Cranes," publication of the Department of Aerospace Engineering and Engineering Mechanics, University of Cincinnati, Cincinnati, Ohio, 1985.

[25] Rienholtz, C.F. and D. Gokhale, "Design and Analysis of Variable Geometry Truss Robots," *Proceedings of 10th Applied Mechanisms Conference*, Vol. 1, New Orleans, Louisiana, December 1987.

[26] Griffis, M. and J. Duffy, "A Forward Displacement Analysis of a Class of Stewart Platforms," publication of the Center for Intelligent Machines and Robotics, University of Florida, Gainesville, Florida, January 1989.

[27] Arun, V. C.F. Reinholtz, and L.T. Watson, "Enumeration and Analysis of Variable-Geometry Truss Manipulators," Accepted for presentation at the *21st ASME Mechanisms Conference,* Chicago 1990,

[28] Padmanabhan, Babu, "Design of a Robotic Manipulator using Variable Geometry Trusses as Joints," Masters Thesis, Virginia Polytechnic Institute and State University, Blacksburg, Virginia 1989.

[29] Arun, V. and B. Padmanabhan, "VGT's - A New Concept for Manipulator Joints," Design Project, Student Mechanism Design Contest (Graduate), ASME Desugn Automation Conference, October 1988, Orlando, Florida.

[30] Padmanabhan, B., V. Arun and C.F. Reinholtz, "Closed-Form Inverse Kinematic Analysis of Variable Geometry Trusses Manipulators," Accepted for publication in *Journal of Mechanical Design.*

[31] Miura, K. and S. Matunaga, "An Attempt to Introduce Intelligence in Structures," *Proceedings of AIAA/ASME/ASCE/AHS/ASC 30th Structures, Structural Dynamics and Materials Conference,* Mobile, Alabama, April 1989. pp. 1145-1153

[32] Salerno, R.H., "Shape Control of High Degree-of-freedom Variable Geometry Truss Manipulators," Masters Thesis, Virginia Polytechnic Institute and State University, Blacksburg, Virginia 1989.

[33] Mikulas, M.M., et al., "A manned-Machine Space Station Construction Concept" NASA Technical Memorandum 85762, 1984.

[34] Pappa, R.S., "Results of 20 Meter Mini-Mast Ground Test Program," *Structural Dynamics Division Research and Technology Accomplishments for FY 1988 and Plans for FY 1989,* NASA Technical Memorandum 101543, 1989.

[35] Shigley, Joseph E. and Larry D. Mitchell, **Mechanical Engineering Design**, 4th ed., McGraw-Hill, New York, 1983. p. 365.

[36] Bodine, Clay ed., **Small Motor, Gearmotor and Control Handbook** Bodine Electric Company, Chicago, Il.?1978.

[37] Ellis, G.K., "Transputers Advance Parallel Processing," *Research & Development*, March 1989. pp. 50-54

[38] **DC Motors Speed Controls Servo Systems, Third Edition,** An Engineering Handbook by Electro-Craft Corporation, (October, 1975)

[39] ANSYS, Swanson Analysis Systems Inc., Houson, Pa. (1986)

[40] Dr. Sanjay Dhande, *Introduction to Cad Cam,* class at Virginia Tech, (1986)

Appendix A

Shop Drawings

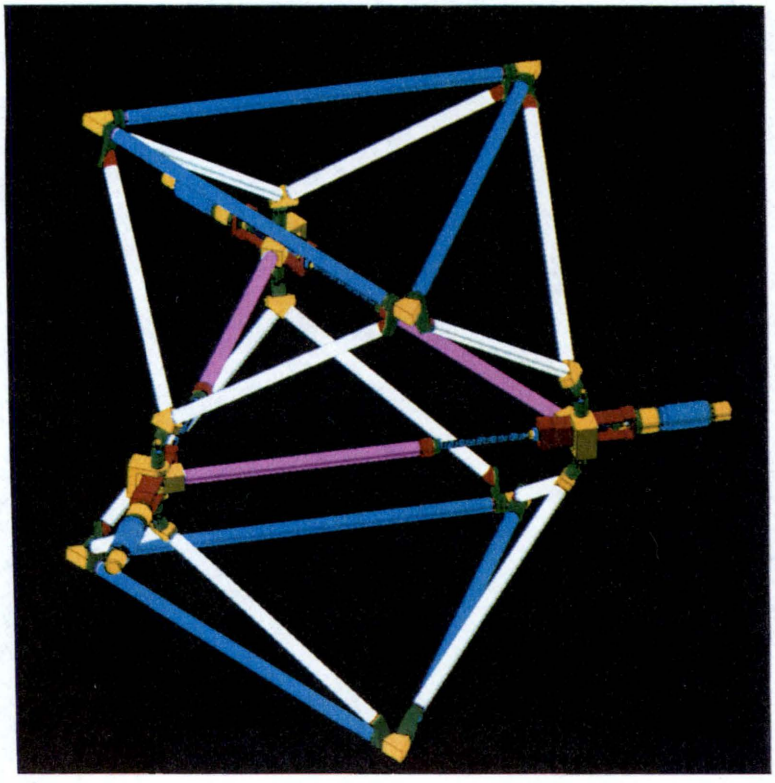

Figure A.1 Double Octahedral Variable Geometry Truss

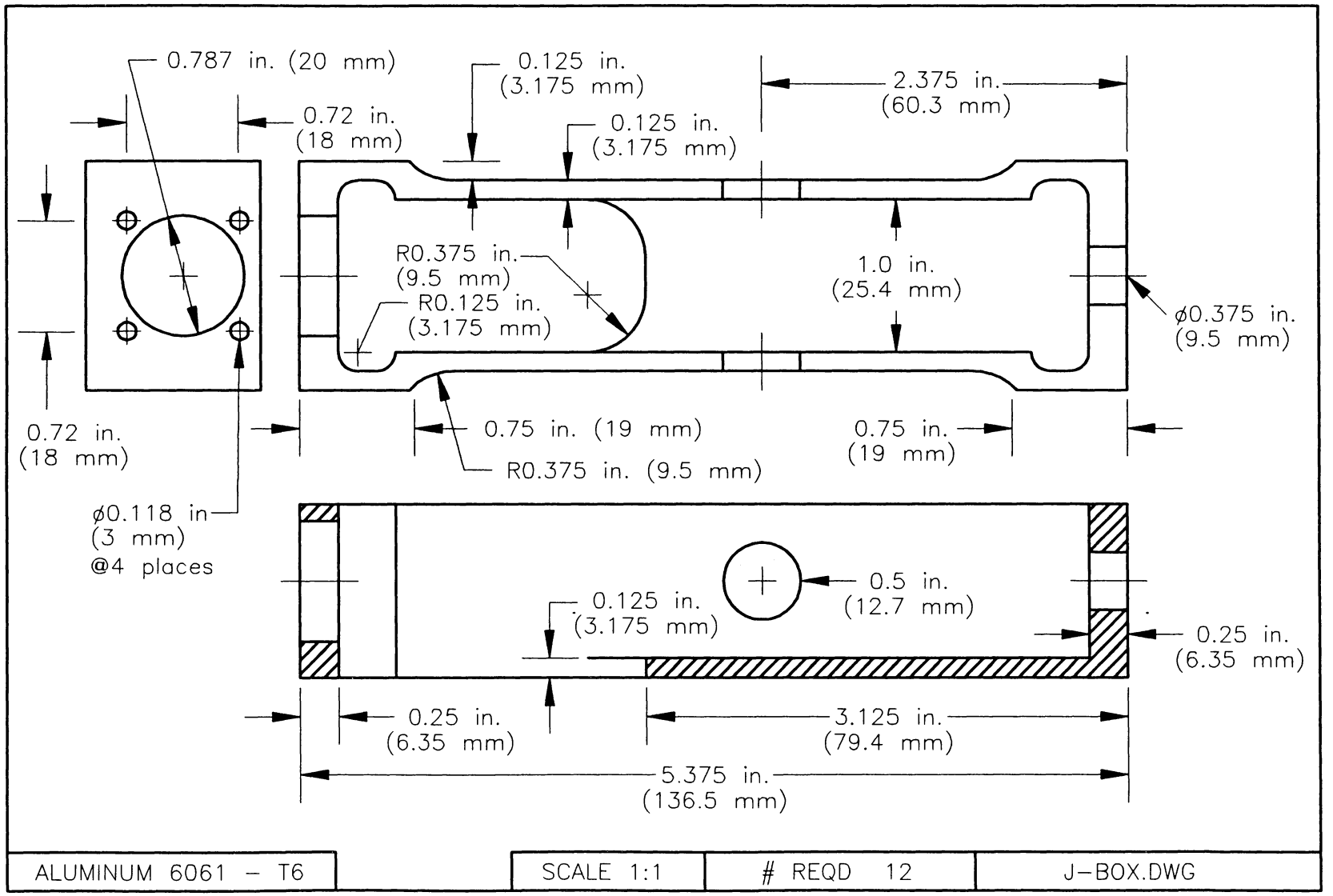

Figure A.2: Joint Instrument Box – Connecting the Motor to the Lead Screw

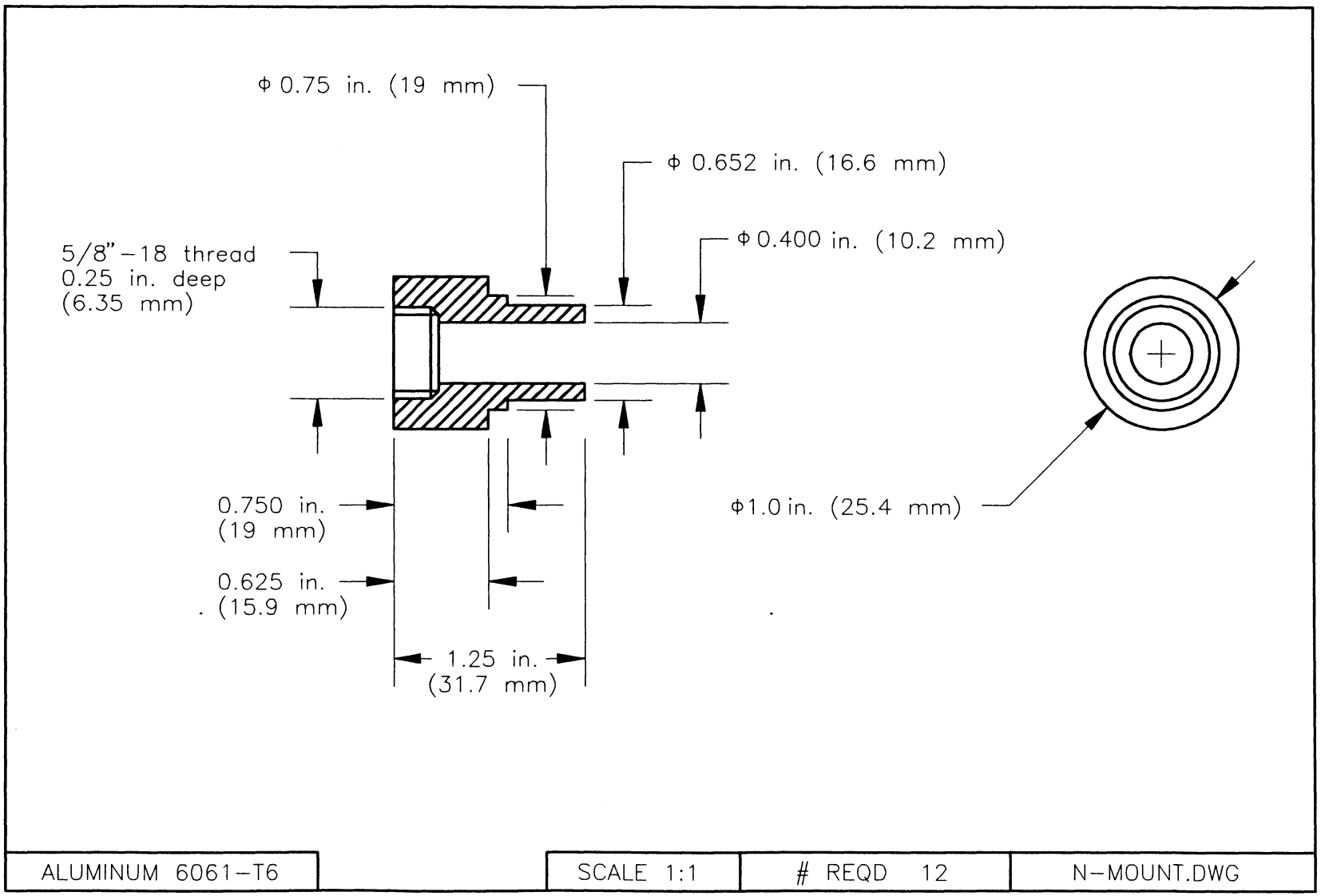

Figure A.3 Nut Mounting Adapter – To Connect Lead Screw to Actuator Tube

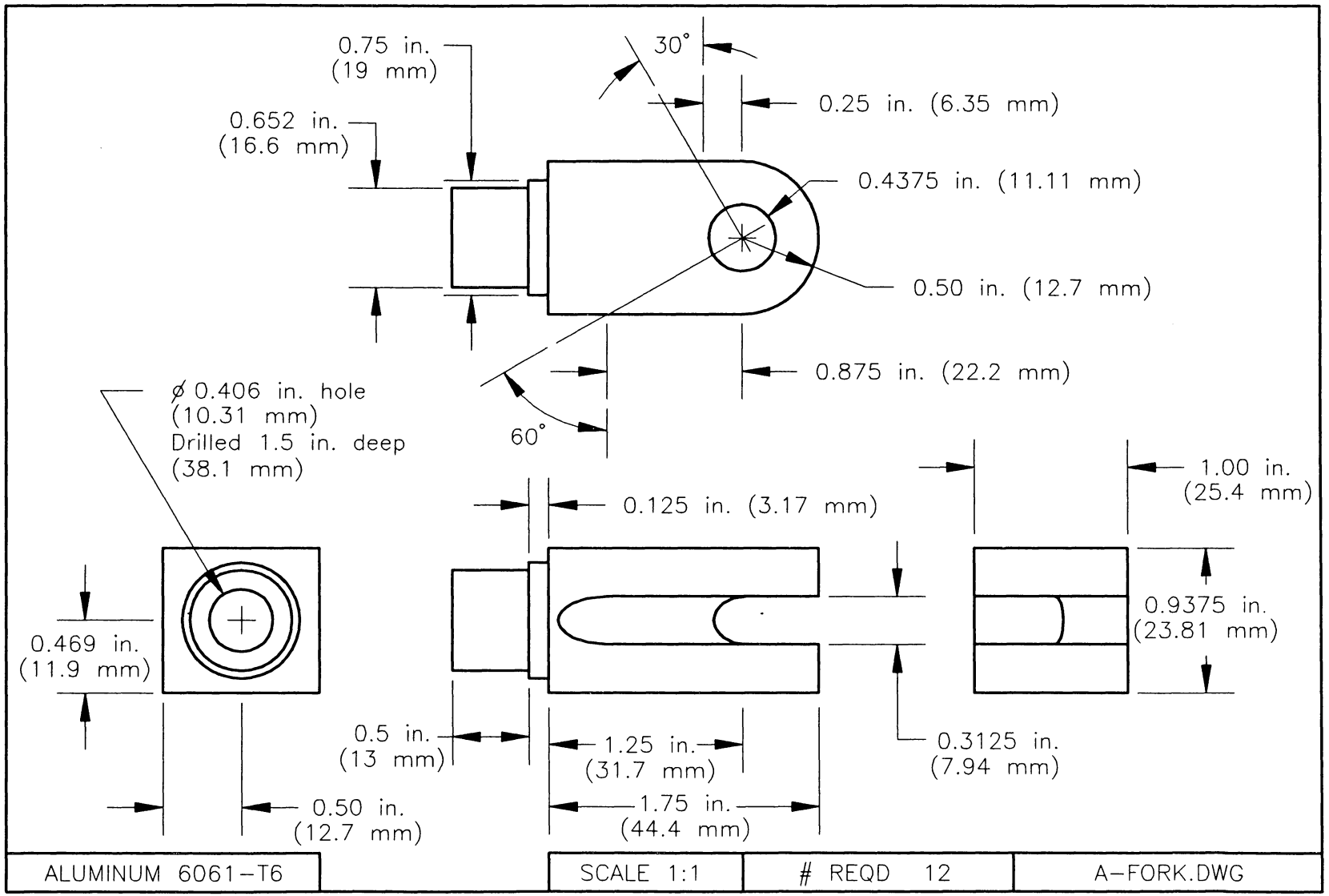

Figure A.4: Actuator Fork – Connecting Actuator Tube to Joint Instrument Box

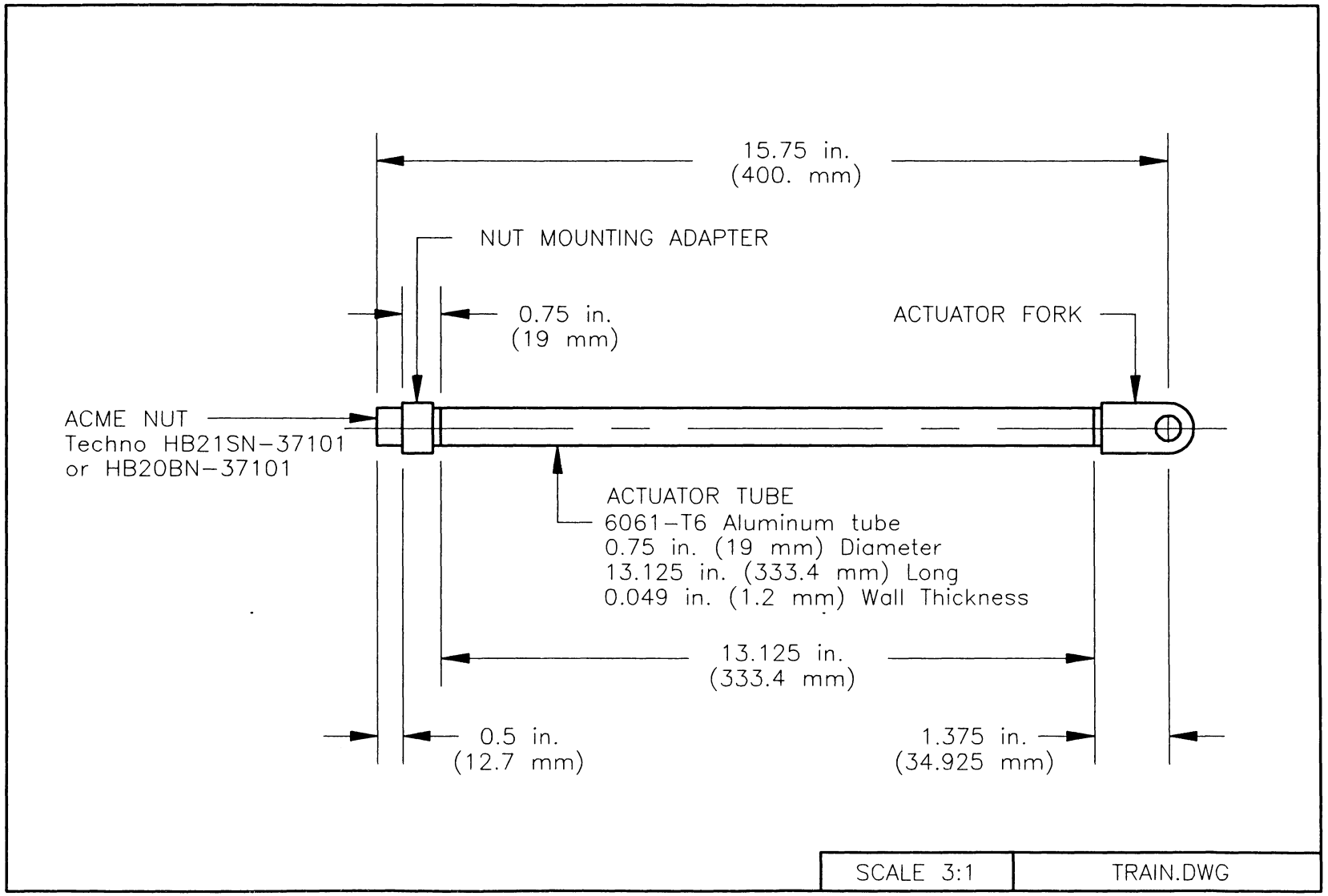

Figure A.5: Actuator Tube Assembly

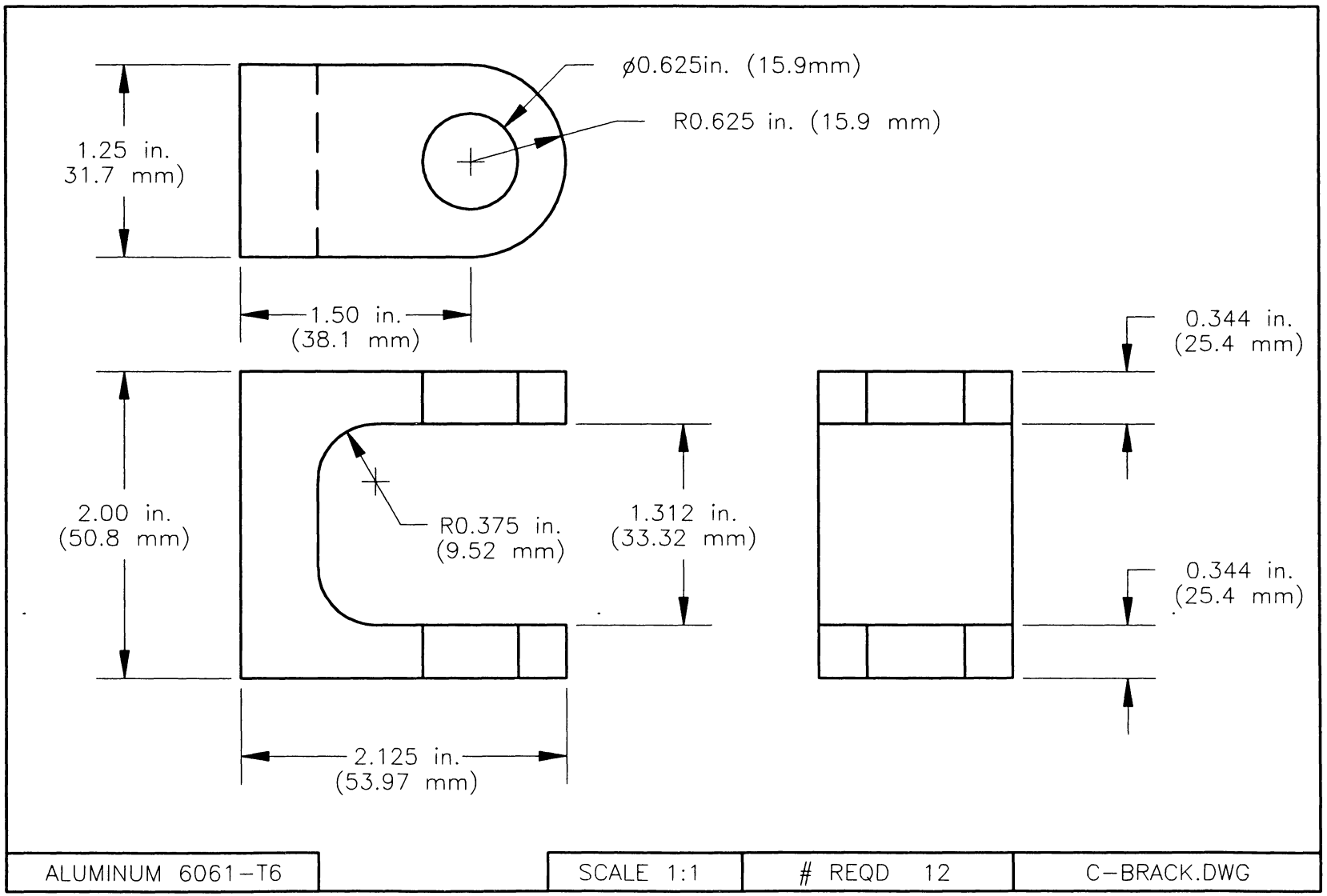

Figure A.6: Bracket Connecting Universal Joints

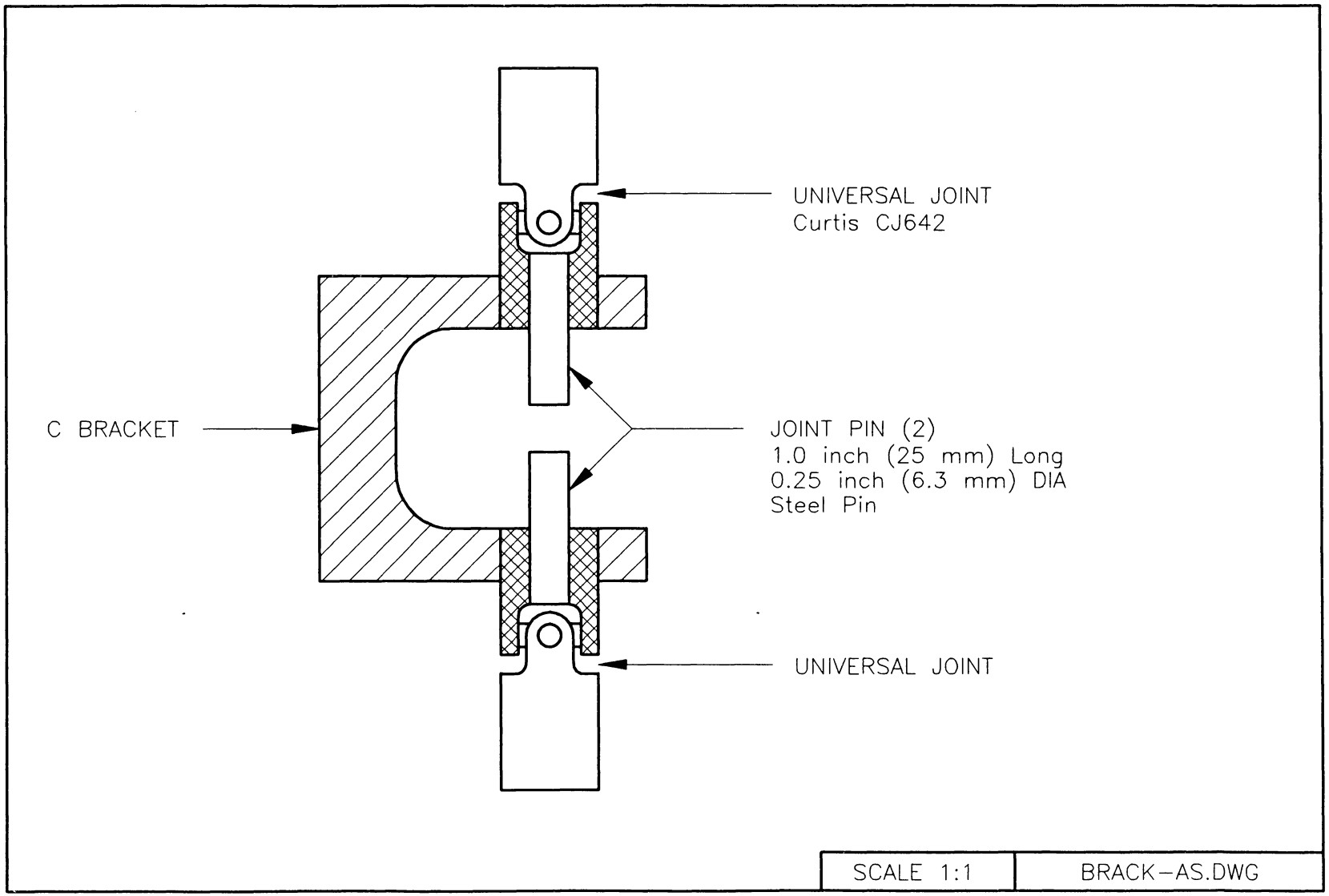

Figure A.7: C Bracket Assembly Section – Connecting Longeron Assemblies to Actuator Joint

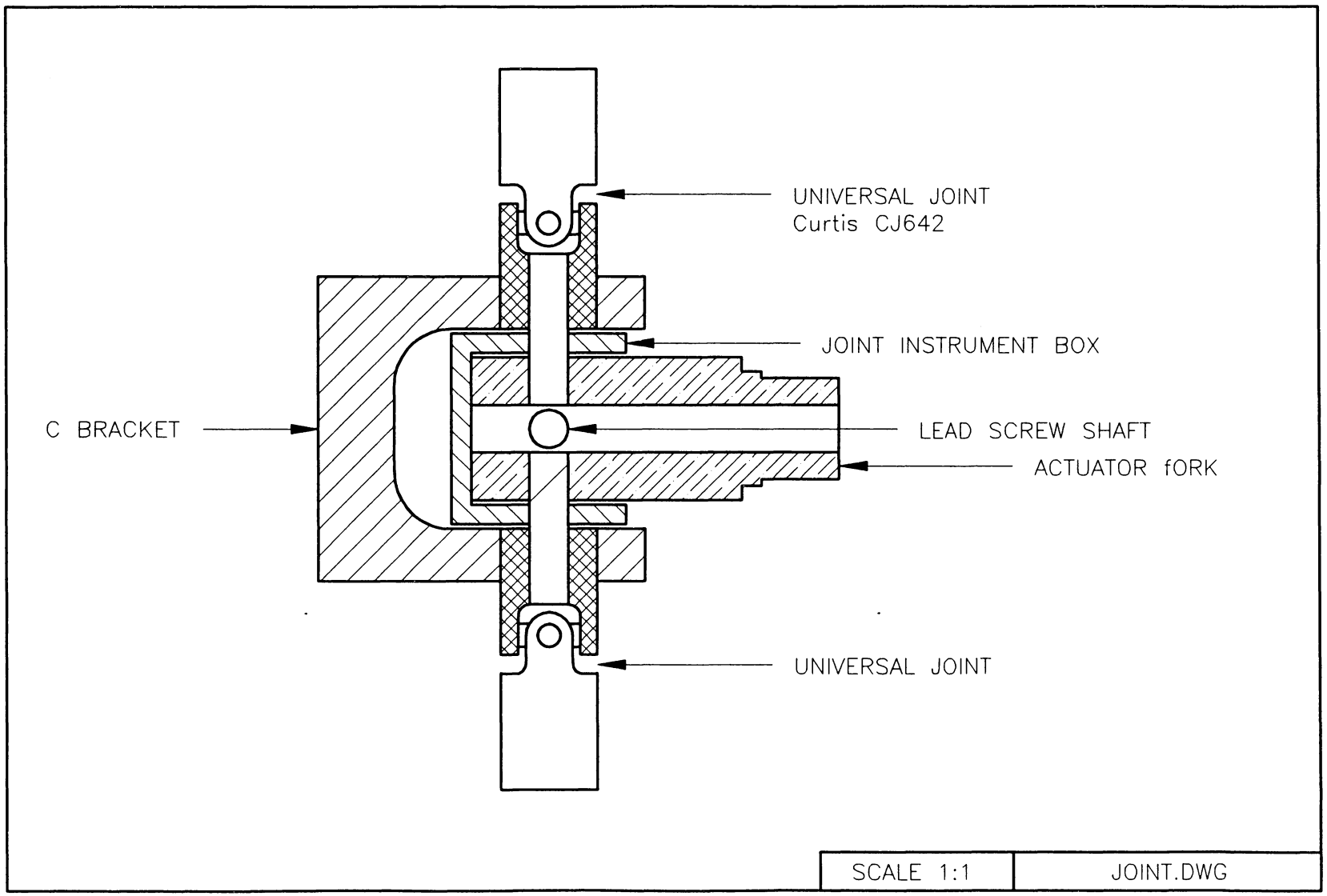

Figure A.8 Joint Assembly Section – Connecting Atuators and Longerons

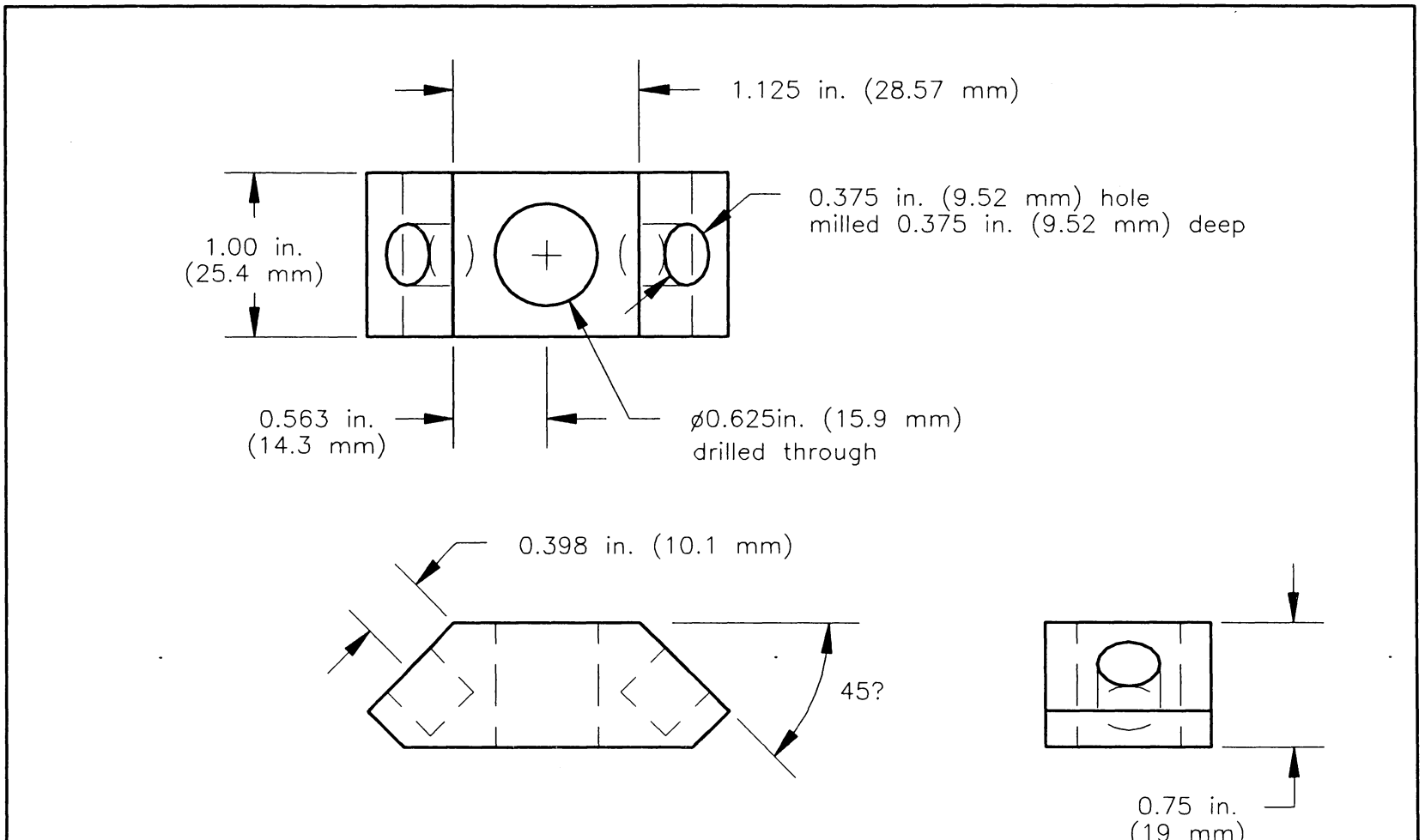

Figure A.9: Longeron Junction Block – Connecting Two Longerons to the Universal Joint

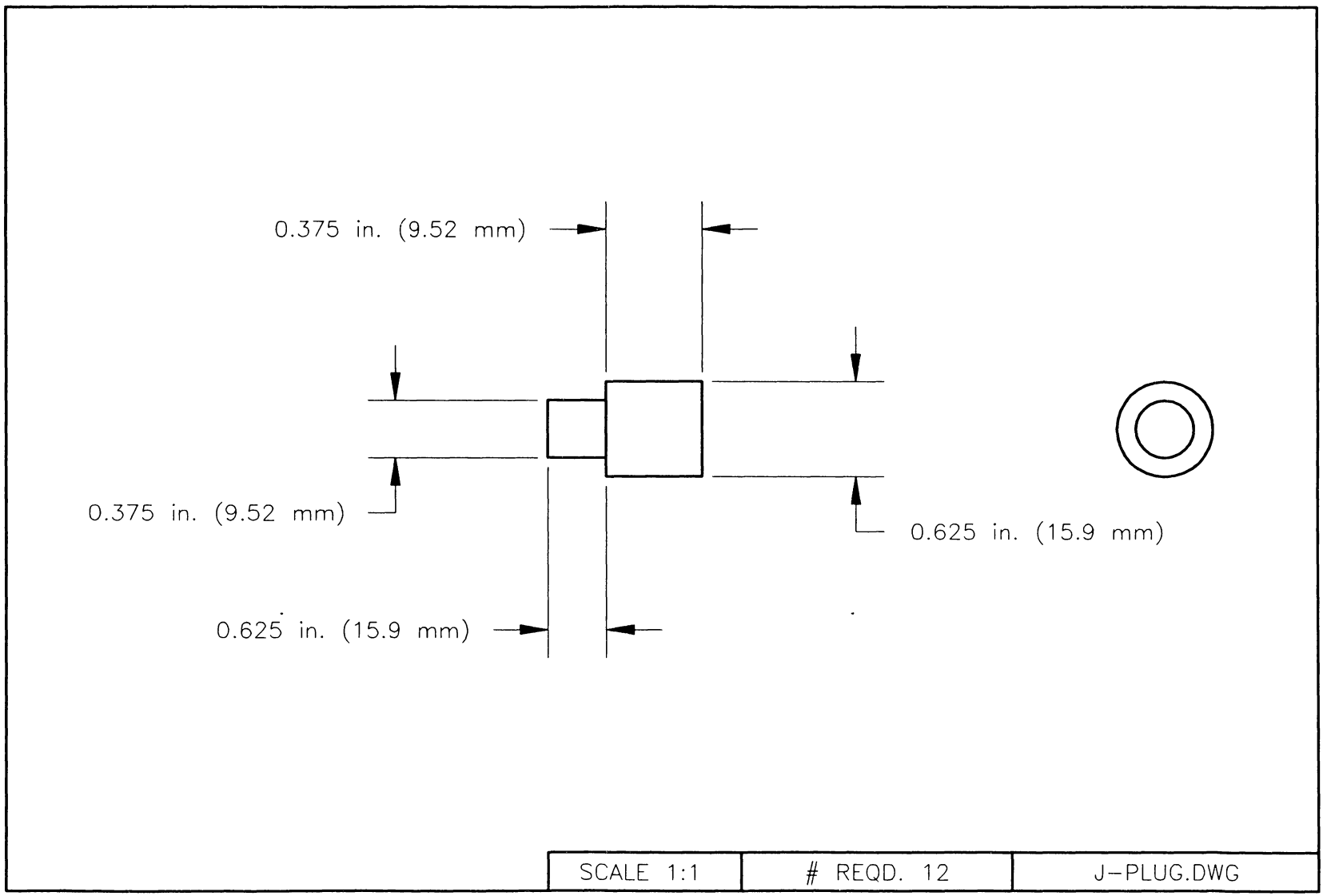

Figure A.10: Longeron Plug – Connecting Longeron Tube with Junction Block

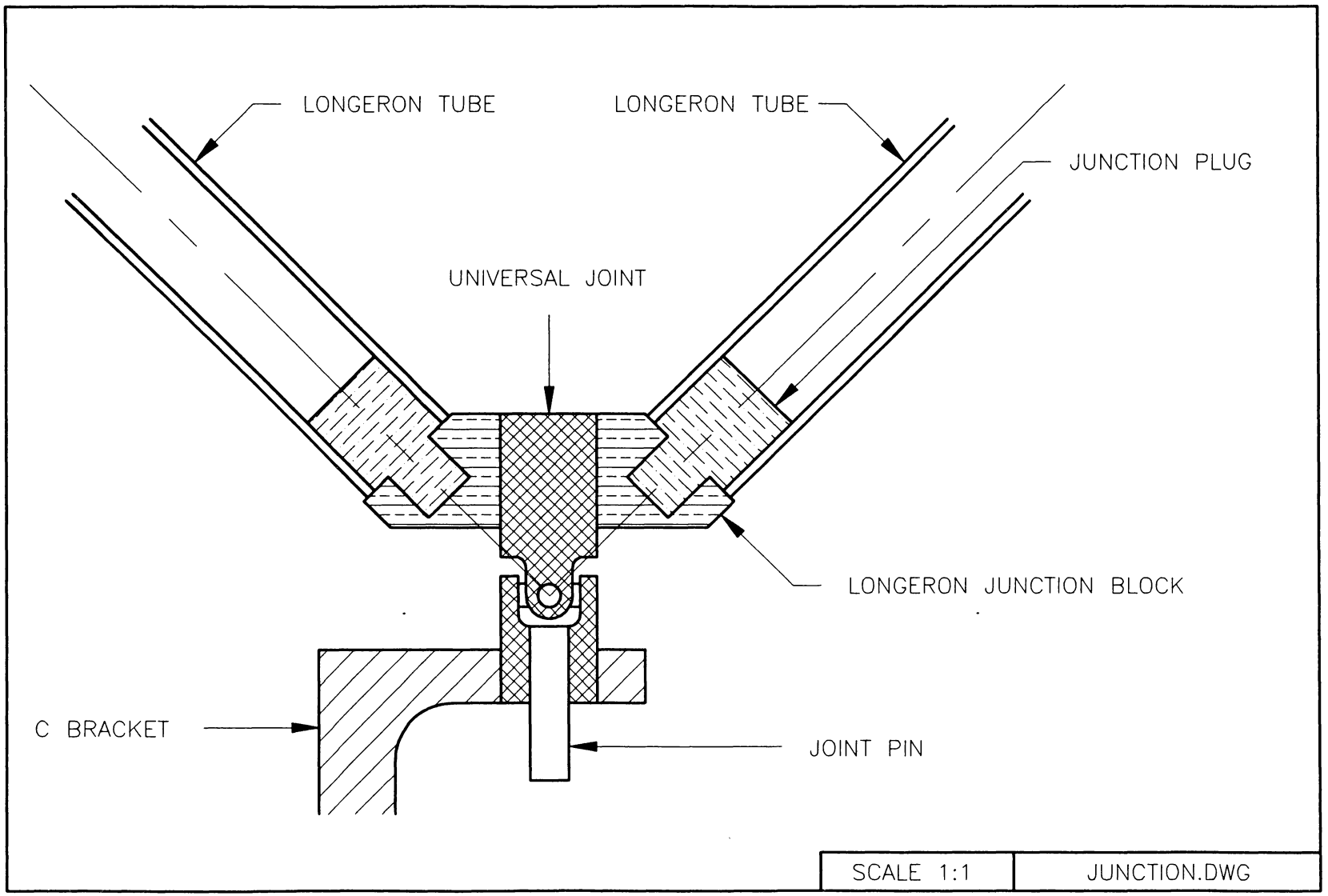

Figure A.11: Longeron Assembly Section

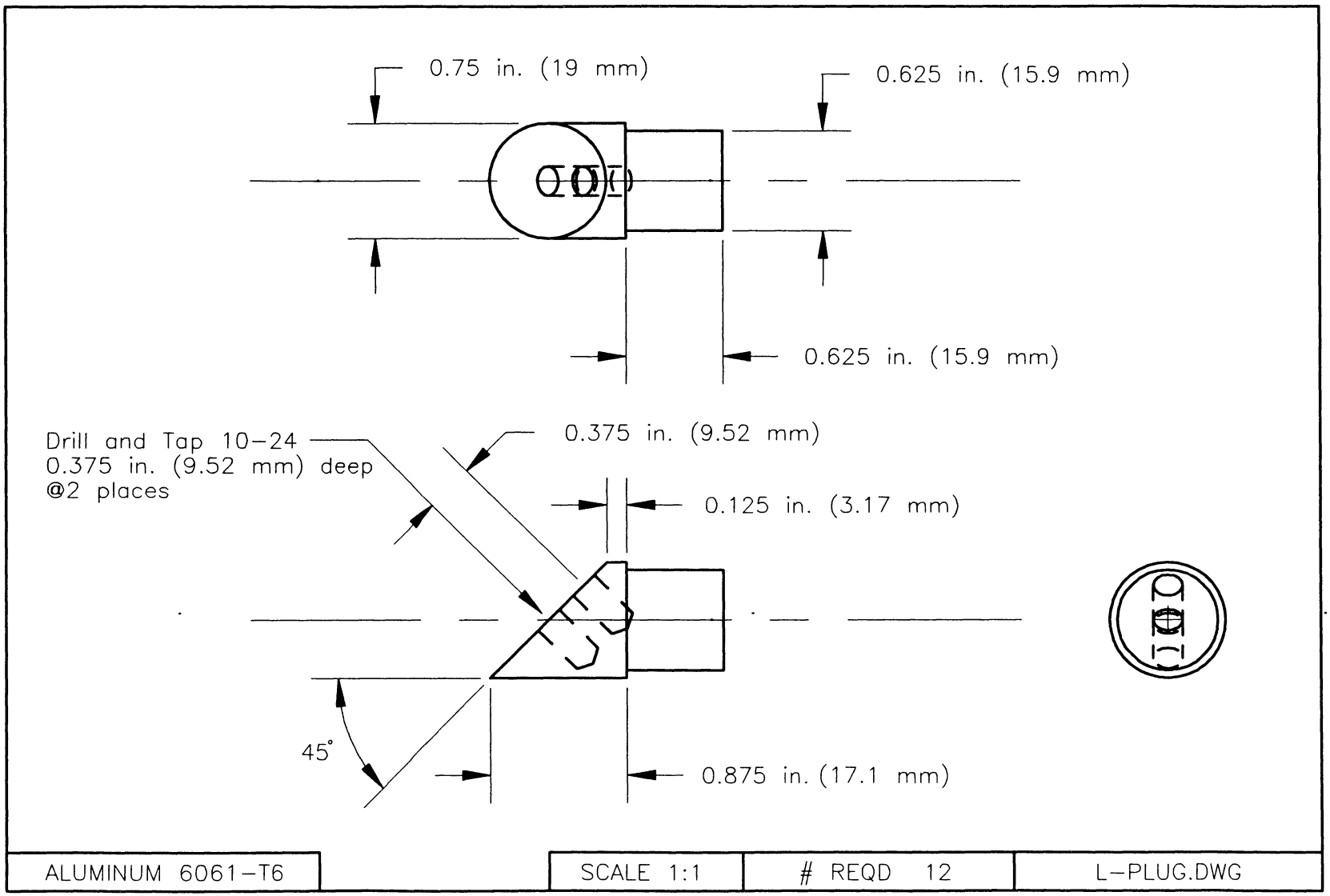

Figure A.12: Longeron Plug - Connecting Longeron Tube to Ear Plate

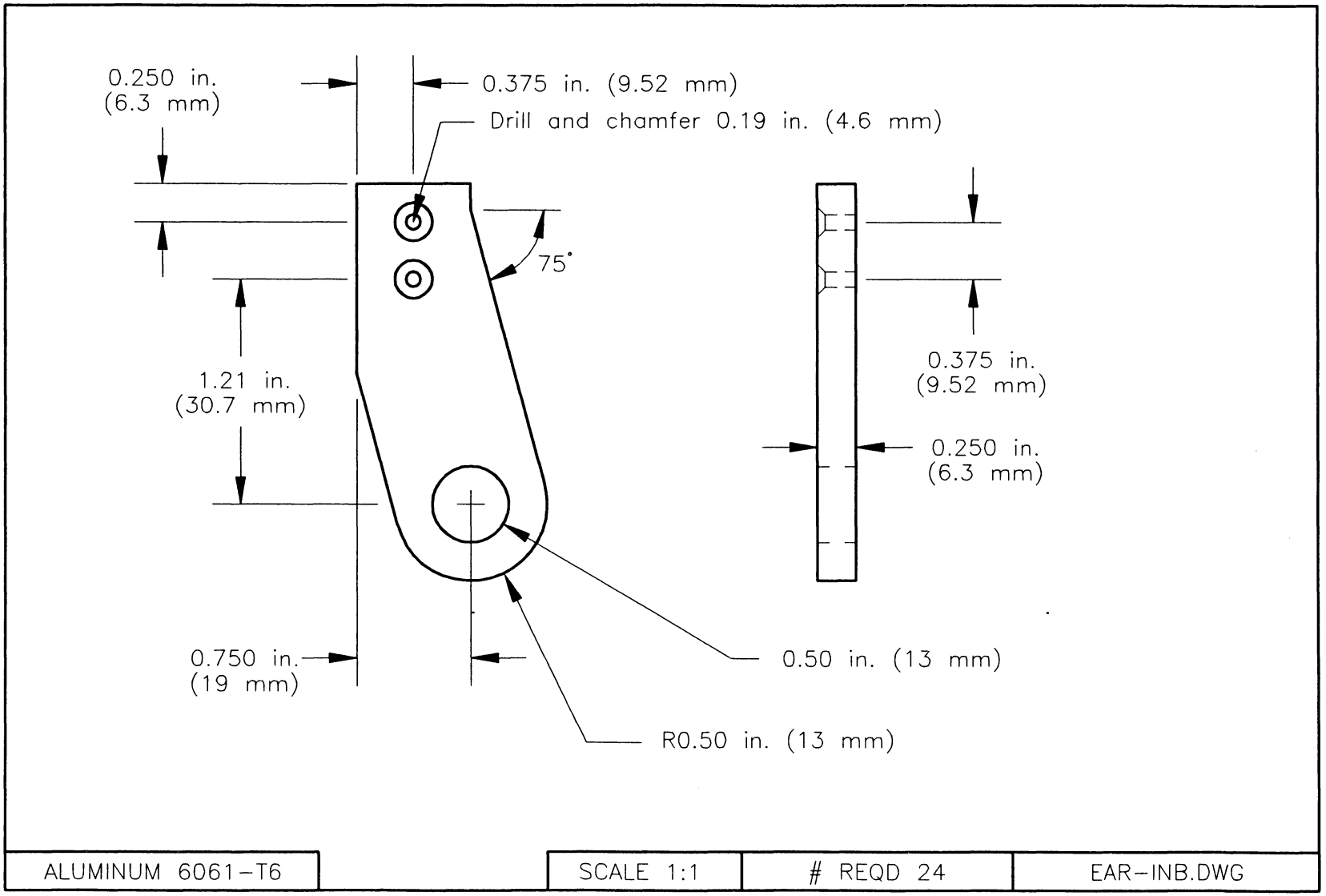

Figure A.14: Inboard Ear Plate – Connecting Short Longeron to the Batten Frame Joint

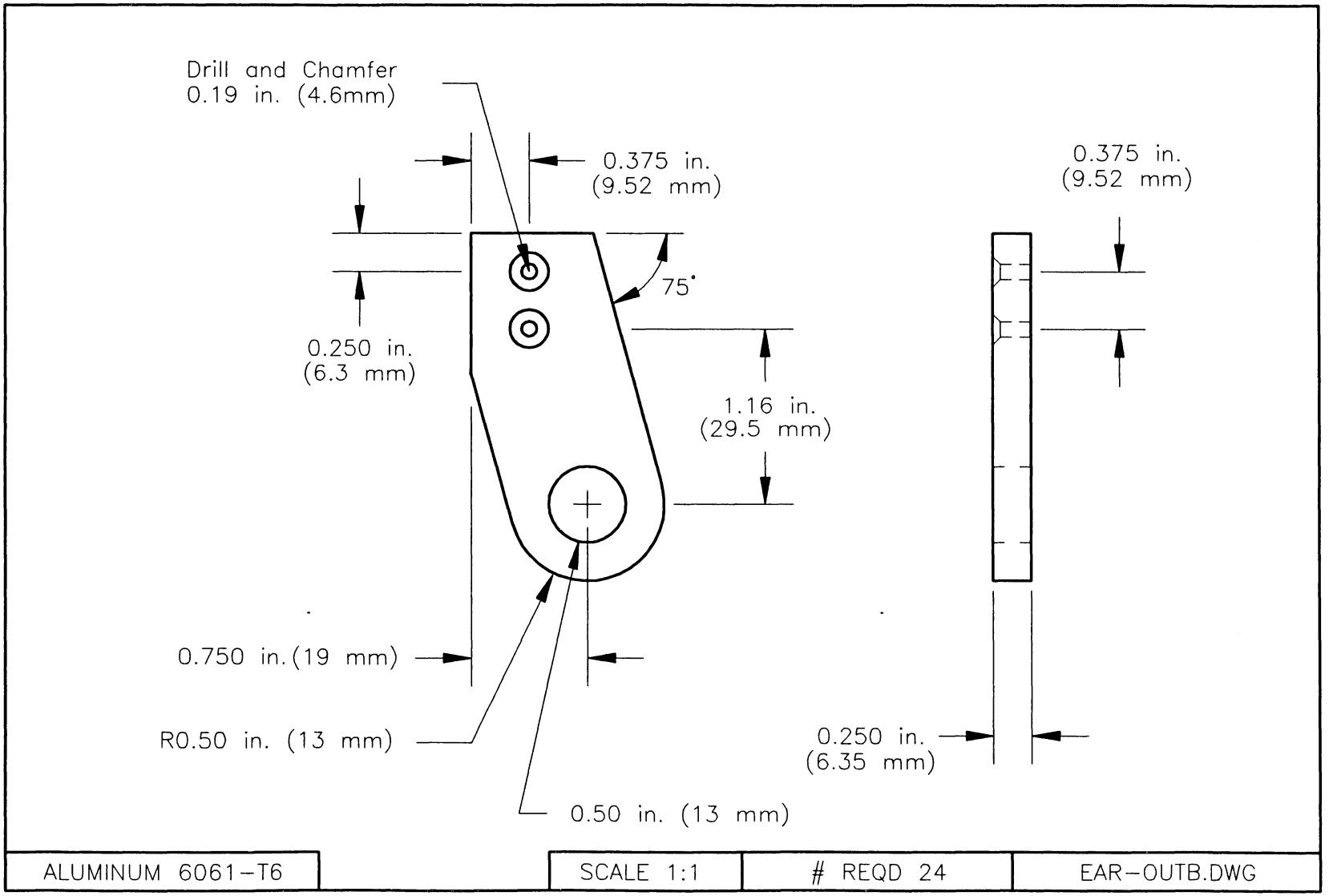

Figure A.13: Outboard Ear Plate – Connecting Long Longeron to the Batten Frame Joint

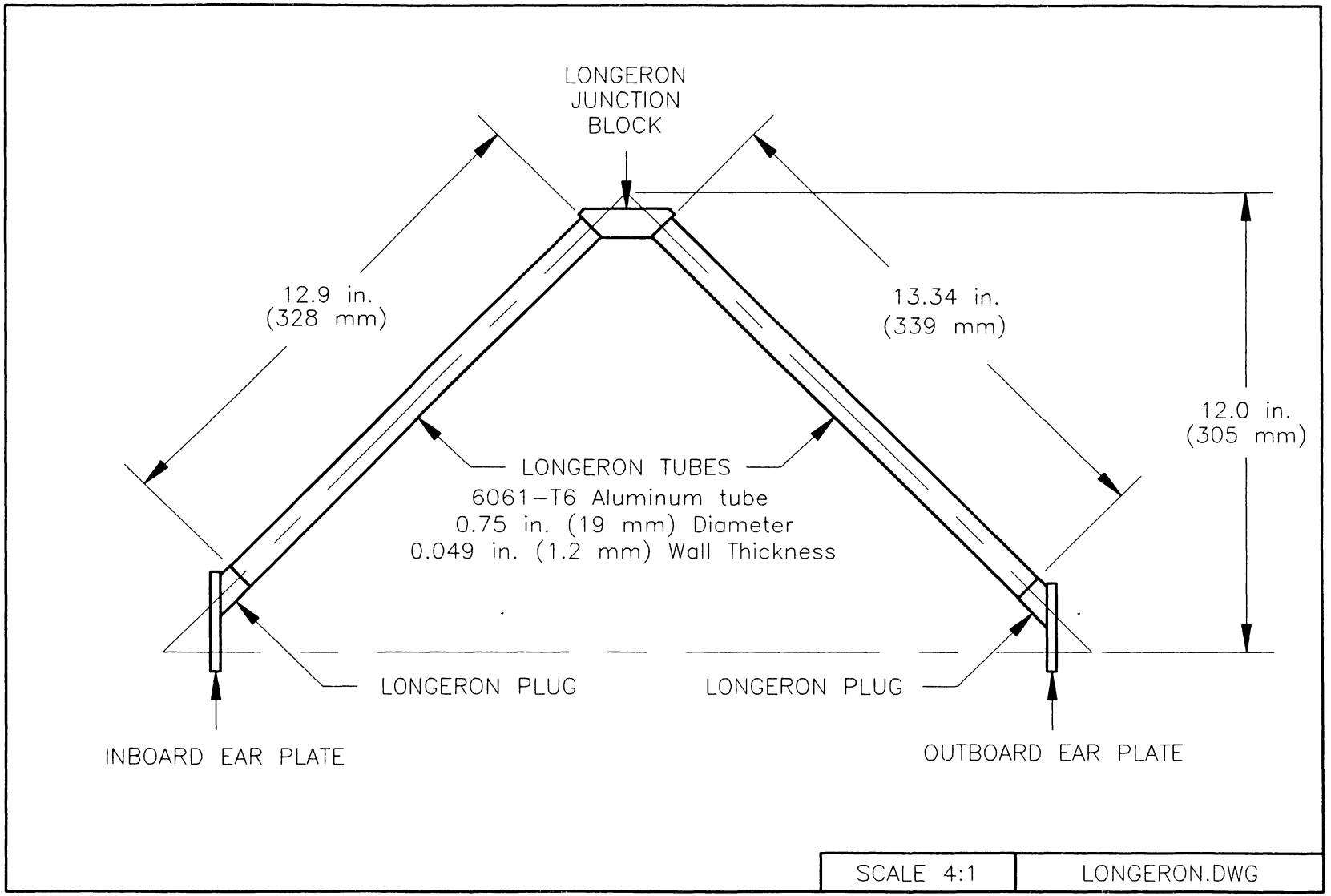

Figure A.15: Longeron Assembly

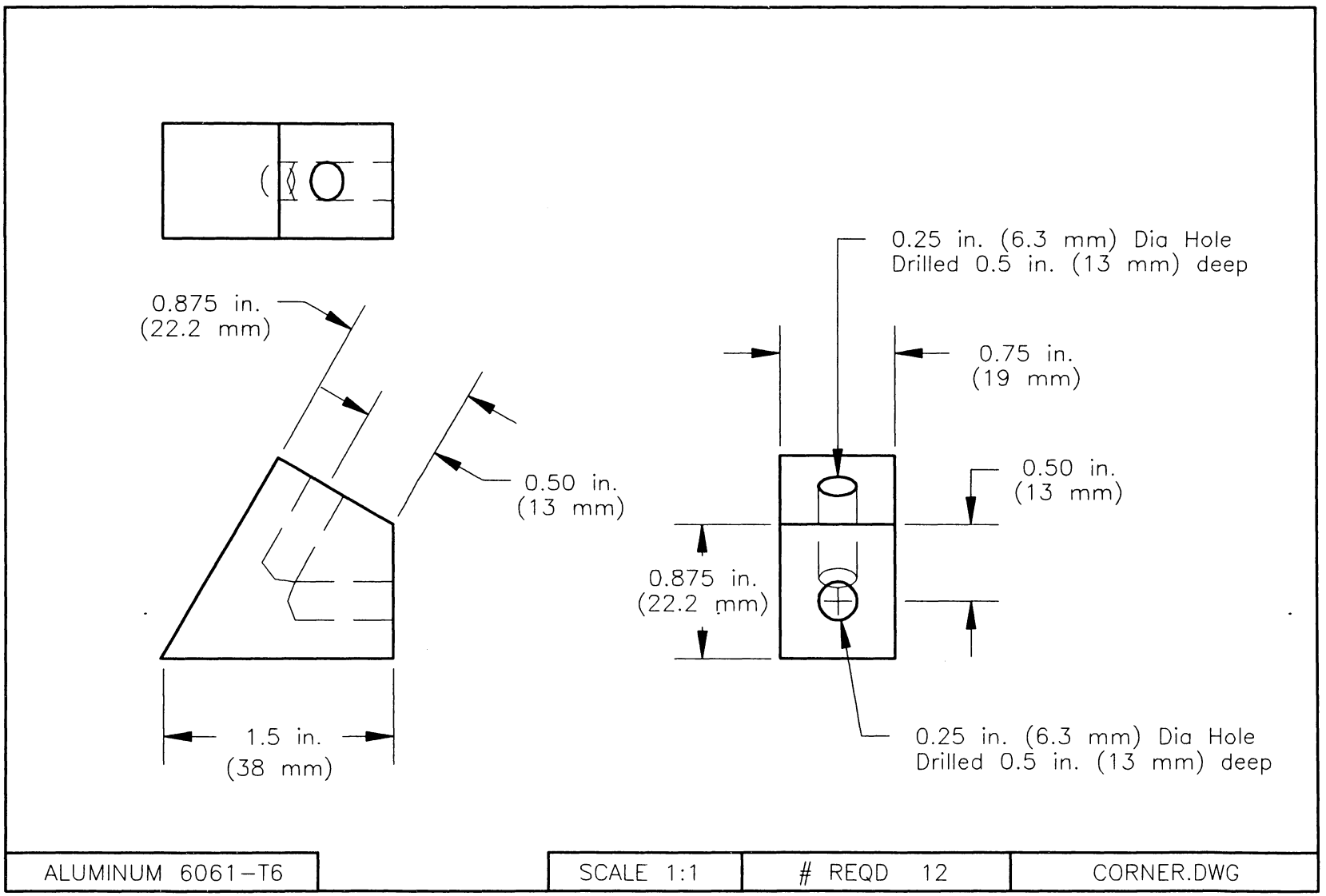

Figure A.16: Batten Corner – Connecting Batten Pins

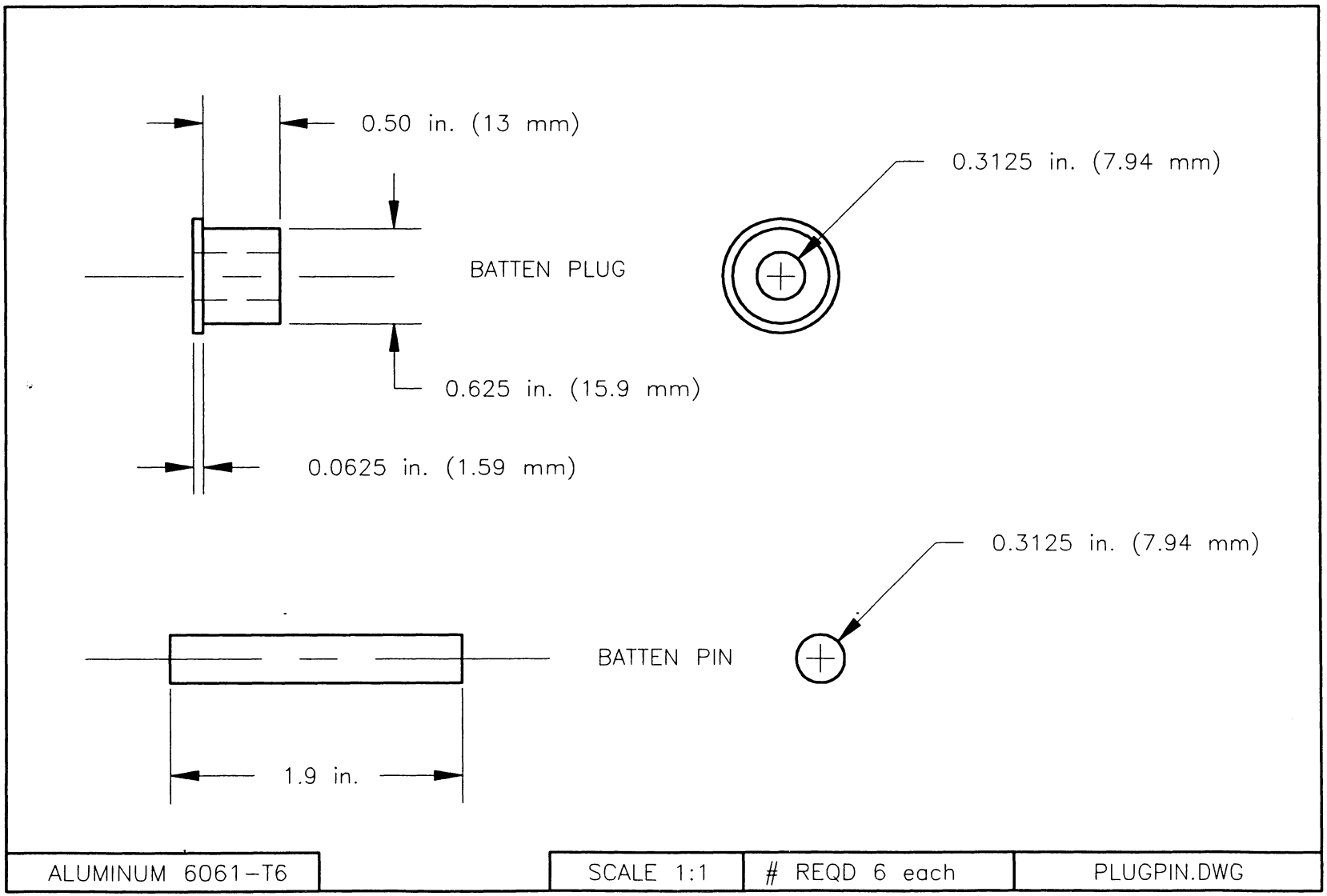

Figure A.17: Batten Plug & Pin – For Batten Frame Joint

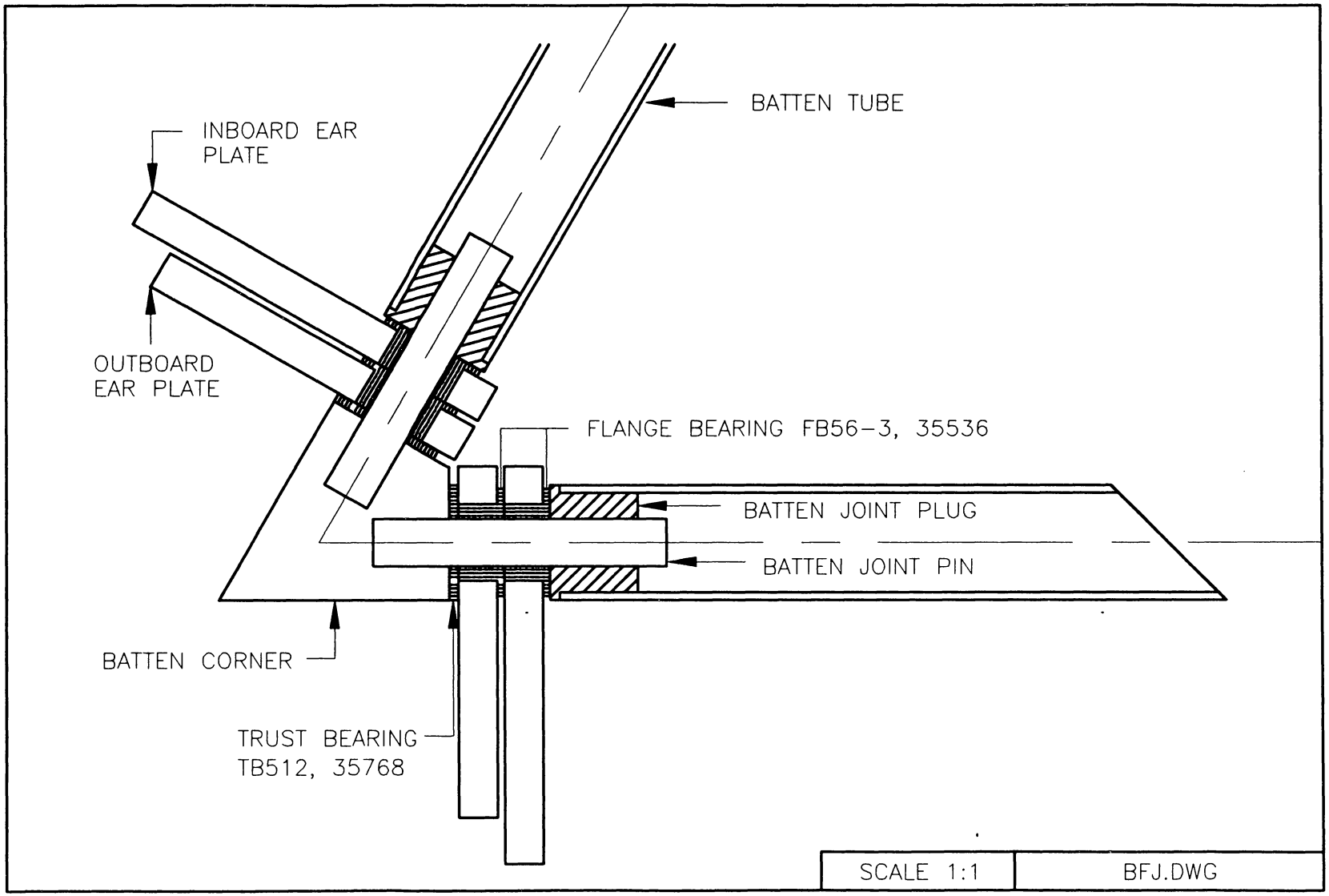

Figure A.18: Batten Frame Joint Section

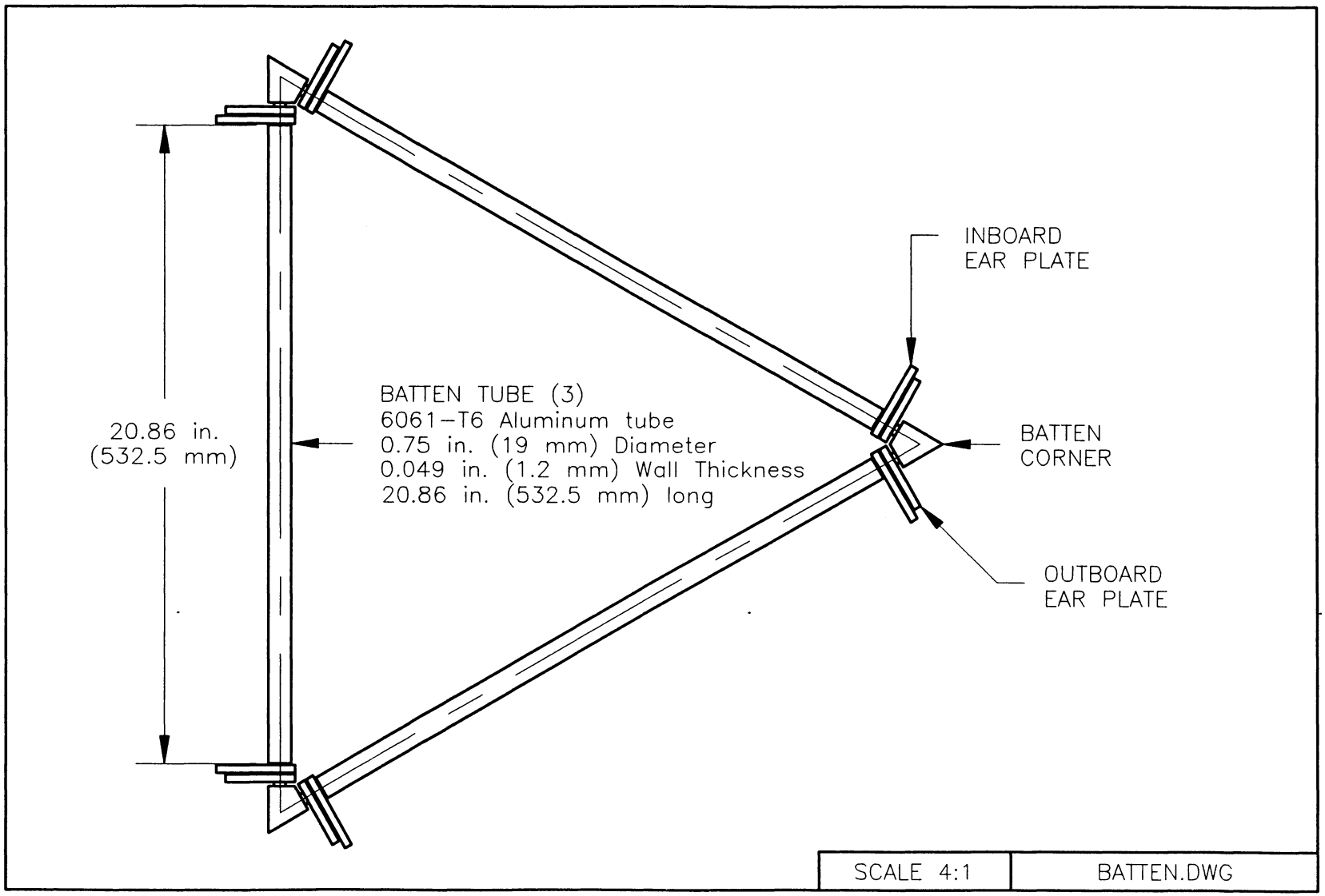

Figure A.19: Batten Frame Assembly

Appendix B

NC Milling Control Code

The joint instrument box was fabricated on a Tree NC milling machine using the following control code.

(JOINTBOX)	Program name.
N0005(9)M03T1S1200$	Spindle at 1200, tool 1: 3/4 end mill.
N0010(0)X.6Y-2.7Z.1$	Rapid move.
N0015(1)X.62Y-2.2F50C0$	Mill with comp off.
N0020(1)X.655C2$	Mill with comp on.
N0022(1)Y-1.8125$	Mill...
N0025(1)Z-0.575$	
N0028(1)Y-1.4375$	
N0030(1)X4.72F15$	
N0035(1)Y-1.5$	
N0040(1)X5.375$	
N0045(1)Y0$	
N0050(1)X4.72$	
N0055(1)Y-.0625F5$	
N0060(1)X1.03F15$	
N0065(1)Z.1F25$	
N0070(1)X.6Y-1$	
N0075(1)Y-1.5C0$	Mill with comp off.
N0080(0)X.6Y-2.7Z.1$	Rapid move.
N0085(1)X.62Y-2.2F25C0$	Mill with comp off.
N0090(1)X.655C2$	Mill with comp on.
N0095(1)Y-1.755$	Mill...
N0100(1)Z-0.575F5$	
N0105(1)Y-1.38$	
N0110(1)X4.72F15$	
N0115(1)Y-1.5$	
N0120(1)X5.375$	

```
N0125(1)Y0$
N0130(1)X4.72$
N0135(1)Y-.12F5$
N0140(1)X.655F15$
N0145(1)Y.6$
N0150(1)X.8Y.8F25C0$          Mill with comp off.
N0155(0)Z.1$                  Rapid move up.
N0215(1)X.62Y-2.2F25C0$       Mill with comp off.
N0220(1)X.655C2$              Mill with comp on.
N0222(1)Y-1.8125$             Mill...
N0225(1)Z-1.15$
N0228(1)Y-1.4375$
N0230(1)X4.72F15$
N0235(1)Y-1.5$
N0240(1)X5.375$
N0245(1)Y0$
N0250(1)X4.72$
N0255(1)Y-.0625F5$
N0260(1)X1.03F15$
N0265(1)Z.1F25$
N0270(1)X.6Y-1$
N0275(1)Y-1.5C0$              Mill with comp off.
N0280(0)X.6Y-2.7Z.1$          Rapid move.
N0285(1)X.62Y-2.2F50C0$       Mill with comp off.
N0290(1)X.655C2$              Mill with comp on.
N0295(1)Y-1.755$              Mill...
N0300(1)Z-1.15F5$
N0305(1)Y-1.38$
N0310(1)X4.72F15$
N0315(1)Y-1.5$
N0320(1)X5.375$
N0325(1)Y0$
N0330(1)X4.72$
N0335(1)Y-.12F5$
N0340(1)X.655F15$
N0345(1)Y.6$
N0350(1)X.8Y.8F25C0$          Mill with comp off.
N0355(0)Z.1$                  Rapid move to 100 above.
N0370(1)X.6Y-1$               Mill.
N0375(1)Y-1.5C0$              Mill with comp off.
N0380(0)X.6Y-2.7Z.1$          Rapid move to 100 above.
N0385(1)X.62Y-2.2F50C0$       Mill with comp off
```

```
N0390(1)X.655C2$                    Mill with comp on
N0395(1)Y-1.75$                     Mill...
N0400(1)Z-1.15F5$
N0405(1)Y-1.375$
N0410(1)X4.72F10$
N0415(1)Y-1.5F20$
N0420(1)X5.375$
N0425(1)Y0$
N0430(1)X4.72$
N0435(1)Y-.125F5$
N0440(1)X.655F10$
N0445(1)Y.6$
N0450(1)X.8Y.8F25C0$                Mill with comp off
N0455(0)Z.1$                        Rapid move up
N0460(0)X1.219Y-.75Z-1.15F2G3W.1K.1Q.05$
                                    Peck drill, feed 2,
N0465(0)X3.4625Y-.75Z-1F2G3W.1K.1Q.05$
                                    Peck drill, feed 2,
N0470(0)Z.1G0$                      Dummy move.
N0485(0)X.25Y-1.25$                 Reference position for pocket mill.
N0490(3)X1.938Y1Z-1.15W.1R.38D2C2G7K.1P5/F15L/.005/V10$
                                    Pocket mill.
N0495(0)X1.6Y-1.25$                 Reference position for pocket mill.
N0500(3)X3.525Y1Z-1W.1R.38D2C2G7K.1P5/F15L.005/V10$
                                    Pocket mill.
N0505(9)M6$                         Home, spindle off for tool change.
N0510(9)M3T3S1500$                  Spindle at 1500, tool 1: 1/4 end mill.
N0520(0)X.5Y-.35Z-1.15F5G1W.1$
                                    Drill (G cycle), feed 5, ref 100 above.
N0521(0)X.5Y-.3$                    Continue drilling...
N0522(0)X.5Y-.25$
N0523(0)X.375Y-.45$
N0524(0)X.375Y-.40$
N0525(0)X.375Y-.35$
N0526(0)X.375Y-.30$
N0527(0)X.375Y-.25$
N0530(0)X.5Y-1.15$
N0531(0)X.5Y-1.2$
N0533(0)X.375Y-1.05$
N0534(0)X.375Y-1.1$
N0535(0)X.375Y-1.15$
N0536(0)X.375Y-1.2$
```

```
N0537(0)X.375Y-1.25$
N0550(0)X.5Y-1.25Z.1G0$          Position move for end mill, G cycle off.
N0551(1)Z-1.15F5$                End mill down, feed 5.
N0552(1)X.375F8$                 Mill over, feed 8.
N0553(1)Y-.25$                   Mill back.
N0554(1)X.5$                     Mill over.
N0560(1)X.375$                   Repeat...
N0561(1)Y-1.25$
N0562(1)X.5$
N0563(1)Z.1F50$                  Rapid up to 100 above.
N0580(0)X4.875Y-.35Z-1F5G1W.1$ Drill (G cycle), feed 5, ref 100 above.
N0581(0)X4.875Y-.3$              Continue drilling.
N0582(0)X4.875Y-.25$
N0583(0)X5Y-.45$
N0584(0)X5Y-.40$
N0585(0)X5Y-.35$
N0586(0)X5Y-.30$
N0587(0)X5Y-.25$
N0590(0)X4.875Y-1.15$
N0591(0)X4.875Y-1.2$
N0593(0)X5Y-1.05$
N0594(0)X5Y-1.1$
N0595(0)X5Y-1.15$
N0596(0)X5Y-1.2$
N0597(0)X5Y-1.25$
N0600(0)X4.875Y-1.25Z.1G0$       Position move for end mill, G cycle off.
N0601(1)Z-1F5$                   End mill down, feed 5.
N0602(1)X5F8$                    Mill over, feed 8.
N0603(1)Y-.25$                   Mill...
N0604(1)X4.875$
N0610(1)X5$                      Repeat...
N0611(1)Y-1.25$
N0612(1)X4.875$
N0613(1)Z.1F50$                  Rapid up.
N0620(9)M30$                     Rapid home, spindle off, end program.
END                              End program.


(BOXHOLES)                       Program name.
N0005(9)M03T5S1800$              Spindle at 1800 rpm, Tool 5.
N0010(0)X.388Y.138Z-.03F4G1W.1$
                                 Spot Faces first bolt hole.
N0020(0)X0/Z-.5F4G1W.1$          Drills first bolt hole.
```

```
N0025(0)Y.862Z-.03F4G1W.1$      Spot Faces second bolt hole.
N0030(0)X0/Z-.5F4G1W.1$         Drills second bolt hole.
N0035(0)X1.112Z-.03F4G1W.1$     Spot Faces third bolt hole.
N0040(0)X0/Z-.5F4G1W.1$         Drills third bolt hole.
N0045(0)Y.138Z-.03F4G1W.1$      Spot Faces fourth bolt hole.
N0050(0)X0/Z-.5F4G1W.1$         Drills fourth bolt hole.
N0055(9)M06$                    Home, turn spindle off.
N0060(9)M03T6S1200$             Spindle at 1200 rpm, Tool 6.
N0070(0)X.75Y.5Z-.35F2G3W.1K.1Q.01$
                                Peck drills motor hole.
N0080(9)M30$                    Home, spindle off, end program.
END                             End program.


(FACEMILL)                      Program name.
N0005(9)M03T4S500$              Spindle at 500 rpm, Tool 4.
N0010(0)X-1.25Y-.75Z.25$        Rapid move.
N0015(1)X6.625F5$               Mill first pass.
N0020(0)Z.125$                  Rapid down.
N0025(1)X-1.25F5$               Mill second pass.
N0030(0)Z0$                     Rapid down.
N0035(1)X6.625F5$               Mill final pass.
N0040(9)M30$                    Home, spindle off, end program.
END                             End program.
```